FEDERAL UNIVERSITY OF RIO GRANDE DO SUL
PHYSICS INSTITUTE
PORTO ALEGRE, BRAZIL

A PROPER VELOCITY MEASURE FOR MESENCHYMAL CELLS MIGRATION

MASTERS DISSERTATION

GUILHERME S. Y. GIARDINI[a]

PORTO ALEGRE, RS
2022

FEDERAL UNIVERSITY OF RIO GRANDE DO SUL (UFRGS) - BRAZIL
PHYSICS INSTITUTE

A PROPER VELOCITY MEASURE FOR MESENCHYMAL CELLS MIGRATION

GUILHERME S. Y. GIARDINI[a]

Masters dissertation presented as a partial requirement for obtaining the title of Master.

Advisor:
Prof. Rita M. C. de Almeida[a,b,c]

[a] **Instituto de Física, Universidade Federal do Rio Grande do Sul, Porto Alegre, RS, Brazil**
[b] **Instituto Nacional de Ciência e Tecnologia, Sistemas Complexos, Universidade Federal do Rio Grande do Sul, Porto Alegre, RS, Brazil**
[c] **Programa de Pós Graduação em Bioinformática, Universidade Federal do Rio Grande do Norte, Natal, RN, Brazil**

PORTO ALEGRE, BRAZIL
2022

A Proper Velocity Measure for Mesenchymal Cells Migration / Guilherme S. Y. Giardini[a]. -- 2022.

118 pages. (including appendices)

Advisor: Rita M. C. de Almeida[a,b,c]

(Masters) dissertation – Federal University of Rio Grande do Sul– Porto Alegre, Brazil, 2022.

Keywords: Anisotropy, Velocity, Velocity Autocorrelation, Mean Square Displacement, Fürth, Active Matter, Cell Migration, Diffusion, Ornstein-Uhlenbeck, Polarity, Single-Cell, Vicsek

Abstract

Single cell migration experiments [Selmeczi et al., 2005, Dieterich et al., 2008] shows a short-time, diffusive behavior that precludes definition of instant velocity and puts in check some current cell migration theory [Thomas et al., 2020, Fortuna et al., 2020]. These experiments show a mostly ballistic motion for intermediate time intervals, followed by a diffusive (whose displacement evolves proportional to the square root of the elapsed time) migration for large time intervals, both already known, and a diffusive migration for short time intervals, a dynamics that makes the usual concept of instantaneous velocity, mathematically undefined (a diffusive displacement, that is proportional to the square root of the elapsed time goes to infinity when divided by an infinitesimal time interval). Consequently, any mathematical model that considers time derivatives for velocity is ill-defined. Recently, we proposed a two dimensional anisotropic migration model, which we analytically and numerically solved, that recreates this observed cellular dynamics [de Almeida et al., 2022]. We considered a polarization vector that defines a preferential migration orientation, along which velocity is well defined, described by a Langevin-like equation, and an orthogonal-to-polarization direction along which the cell describes a diffusive motion.The polarization direction is a further variable of the model, being continuously updated. The predicted values for mean square displacement are in agreement with experiments. However, the probability density function for the velocity along the polarization axis is symmetrical around zero, disagreeing with what is observed experimentally. Here we present analytic stochastic calculations where the noise term for the velocity along the polarization axis has a non-zero average value. The analytical results reproduce the experimentally observed behavior for the mean square displacement and probability density functions for the velocity along the polarization axis. The calculations are based on our analytical stochastic integration method presented in a previous work [de Almeida et al., 2022], and the results agree with experiments, numerical integration and the results from CompuCell3D simulation method.

Keywords: Anisotropy, Velocity, Velocity Autocorrelation, Mean Square Displacement, Fürth, Active Matter, Cell Migration, Diffusion, Ornstein-Uhlenbeck, Polarity, Single-Cell, Vicsek

Resumo

Experimentos de migração celular [Selmeczi et al., 2005, Dieterich et al., 2008] mostram para tempos curtos de observação, um comportamento difusivo que impede a definição de velocidade instantânea e põe em cheque algumas das teorias atuais de migração [Thomas et al., 2020, Fortuna et al., 2020]. Estes experimentos mostram um movimento de tipo balístico para intervalos intermediários de tempo, seguidos um novo regime difusivo (o deslocamento é proporcional à raiz quadrada do tempo decorrido) para longos intervalos de tempo, ambos previamente conhecidos. O regime de migração para intervalos curtos de observação é um regime que torna o conceito usual de velocidade instantânea, matematicamente mal definido (a razão entre um deslocamento proporcional à raiz do tempo pelo próprio tempo diverge quando o mesmo tende a zero). Consequentemente, qualquer modelo matemático que considera derivadas temporais da velocidade, fica mal definido. Recentemente, nós propusemos um modelo anisotrópico de migração (resolvido numérica e analiticamente) que recria essa nova dinâmica observada [de Almeida et al., 2022] ao considerar um vetor de polarização que define uma orientação preferencial de migração ao longo do qual a velocidade instantânea é bem definida, descrita por sua vez por uma equação de Langevin e uma direção ortogonal à polarização na qual a célula descreve um movimento difusivo. A orientação do vetor polarização é uma variável adicional do modelo e é continuamente atualizada. Os valores preditos para o deslocamento quadrático médio concordam com os experimentos. No entanto, a função de densidade de probabilidade da velocidade ao longo do eixo de polarização, assume uma curva simétrica em torno de zero, discordando com o que se é observado experimentalmente. Neste trabalho, nós mostramos um novo cálculo estocástico analítico no qual os termos de ruído para a velocidade definida ao longo do eixo de polarização apresentam um valor médio que não é centrado em zero. Os resultados analíticos reproduzem os comportamentos observados experimentalmente para o deslocamento quadrático médio e a função de densidade de probabilidade da velocidade ao longo do eixo de polarização. Os cálculos são baseados nos métodos estocásticos analíticos apresentados em nosso trabalho anterior, com algumas modificações e os resultados corcordam com as soluções numéricas, simulações produzidas no Compucell3D e experimentos de migração individual.

Keywords: Anisotropy, Velocity, Velocity Autocorrelation, Mean Square Displacement, Fürth, Active Matter, Cell Migration, Diffusion, Ornstein-Uhlenbeck, Polarity, Single-Cell, Vicsek

Contents

List of Figures

Nomenclature

$\beta_\perp$	White and Gaussian random noise responsible to changing the particle's polarization orientation.	$dimensionless$
$\Delta\vec{r}_\perp$	Variation of position perpendicular to the polarity axis.	$length$
δ	Time interval	$time$
γ	Coefficient of loss of memory	$1/time$
$\overline{\vec{v}}$	Average velocity.	$length/time$
$\sqrt{q}$	Proportionality constant between $\xi_\perp$ and β_{perp}	$length$
$\vec{n}$	Perpendicular vector to $\vec{p}$	$dimensionless$
$\vec{p}$	Vector representing the polarity orientation	$dimensionless$
$\vec{r}$	Position vector for the particle	$length$
$\xi_\parallel$	White and Gaussian random noise parallel to the polarization axis of the particle.	
$\xi_\perp$	White and Gaussian random noise perpendicular to the polarization axis of the particle.	
D	Coefficient of diffusion	$length^2/time$
D_{fast}	Coefficient of diffusion for small time intervals	$length^2/time$
D_{slow}	Coefficient of diffusion long time intervals	$length^2/time$
g	Variance of the white and Gaussian noise in the perpendicular orientation to the polarity axis.	$length^2/time^3$
k	Variance of the white and Gaussian noise responsible for changing the polarization orientation.	$1/time$
P	Coefficient of persistence	$time$
R	Relaxation time	$time$
S	Excess of diffusion	$dimensionless$

t	System's time variable	$time$

Chapter 1

Introduction

Cells are the units of life, being present in different kinds of environments forms and quantities. Some are able to exist on its own, while others form collectives of cells that are able to exist by cooperating with one another through the differentiation that allows tasks division, eventually forming multi-cellular beings as plants and animals as we know.

Surviving in a highly competitive environment is what propelled cells to evolve and develop different kinds of life maintenance mechanisms, like cilia for locomotion and chemical fields emission and sensing, enabling long distance cooperation between cells. Along with some other capacities, these favoured the emergence of multi-cellular beings.

Among the many existing processes exhibited by many cells, cellular migration is important for single cells to search for nourishment, flee from predators, find possible partners for sexual reproduction or a better environment to live. In case of multi-cellular organisms, migration presents itself as an organized and coordinated behavior necessary in tissue healing, embryo development, immunological defense and much more. Cell migration dynamics also plays a role in tumour evolution and spreading, meaning that a better understanding of cancerous cell migration could allow for better cancer therapies.

Cell migration has been the focus of scientific research since the beginning of the last century. Fürth and collaborators [Fürth, 1920] characterized cell migration by the mean square displacement (**MSD**). They concluded that cells' **MSD** was similar to that of Brownianan motion, whose equation is a solution for the Langevin´s problem of a point particle moving in a viscous fluid subject to thermal noise [Lemons and Gythiel, 1997]. For these

systems, the **MSD** presents two regimes, depending on the time interval used to measure displacements: for short-time intervals the movement is mostly ballistic and for long-time intervals the movement is diffusive. In this model, the short time predominantly ballistic movement implies that instantaneous velocity is well defined.

In the last decades single cell migration experiments [Selmeczi et al., 2005, Dieterich et al., 2008] showed that mesenchymal cells migrating on flat surfaces exhibit an additional very short-time diffusive regime i.e. $|\Delta\vec{r}| = |\vec{r}(T+\Delta T)-\vec{r}(T)| \sim \sqrt{\Delta T}$, where $\vec{r}(T)$ represents a cell position at time T. This short-time interval behavior precludes the definition of an instantaneous velocity as $|\vec{v}| = lim_{\Delta T\to 0}\frac{|\Delta\vec{r}|}{\Delta T} \sim \frac{\sqrt{\Delta T}}{\Delta T} \to \infty$. The concept of instantaneous velocity is frequently used to propose cell migration models and measurement procedures, overlooking the dependence on the time interval used to estimate cell velocity. Furthermore, a diverging instantaneous velocity puts in check some of the current single cell migration theory.

To account for the short-time diffusion observed in mesenchymal cell migration, we recently proposed a two-dimensional stochastic model. Whose analytical and numerical solutions present a three regime behavior observed in cell migration [de Almeida et al., 2022]: for short time intervals, the dynamics is diffusive, for intermediary intervals the dynamics is predominantly ballistic and for long time intervals, the dynamics is again diffusive. In this model, we considered a polarization vector that defines a preferential migration orientation, along which the velocity is well defined and is described by a Langevin-like equation. Orthogonal to the polarization vector, we introduced a diffusive dynamic described by a Wiener variable. The two different motions were then able to recreate the same mean square displacement behavior as seen experimentally, besides agreeing with the measured velocity auto-correlation function.

The model, however, is not perfect, the probability density distribution for the velocity along the polarization axis has a maximum at zero, meaning the cells could migrate with equal probability both forward or backward staying put on average. That disagrees with experiments: cells maintain a stable forward motion with respect of its polarization orientation. The importance of a forward biased cellular motion becomes apparent when we consider chemotaxis.

The effect of a chemical gradient is to make the cell change the direction of its internal organization such that they migrate following the gradient direction. However, aligning the cell's polarization with the chemical field gradient can only cause a preferential movement towards the chemical source if the probability density function for velocity is not symmetric around zero.

In this work adapt the anisotropic stochastic model by assuming a biased noise term acting on the parallel-to-polarization velocity. We obtain the analytical and numerical solutions and compare with experiments and simulations. We based our stochastic calculations on the methods of a previous work [de Almeida et al., 2022], while introducing new solutions such as the analytical velocity probability density function which agrees with experiments, numerical integration and the results from CompuCell3D simulation method.

In the chapters to come, we briefly present current biological background of single cell migration, focusing on the facts we used to create our model. Chapter three presents some useful mathematical tools we use in what follows. Chapter four presents the existing single cell migration models, the most common modelling approaches and discuss their advantages and disadvantages. Next, we present the anisotropic Ornstein-Uhlenbeck model [de Almeida et al., 2022], its analytical solutions and results and discuss why do we need a new biased model. Chapter five introduces the biased anisotropic Ornstein-Uhlenbeck model, and present its numerical and analytical solutions. In the last chapter we conclude and discuss future perspectives.

Chapter 2

Biological Background

In the eighteenth century the only known information was that cells were able to vary its rigidity by transitioning between states of solid and gel. Scientists didn't obtain new significant clues until mid 1970's were it was observed that under certain conditions the cell's lamellipodia (part of the cell that extends over the substrate and pulls the cells forwards and which at that time looked void of cellular organelles) could separate from the cell's main body and migrate on its own for several hours (without the energy provided by the mitochondria) while the cellular body stood mainly still. This observation showed that all the needed mechanisms for migration were present in the lamellipodium. During this same decade, Hatano and Oosawa [Pollard, 2017] and later, Thomas Pollard [Pollard and Korn, 1973], observed some proteins that are abundant in muscle tissue could be found inside diverse cells such as amoebas, platelets and white blood cells. These proteins localized more abundantly in the peripheral regions of these cells, which made scientists question their relation with migration.

Some years later, Pollard and Niederman [Niederman and Pollard, 1975] observed that inside each cell there were polymeric strands of actin that could provide rigidity for them. Even though the process of actin polymerization and depolymerisation was known from chemistry, there was no knowledge of it forming rigid structures inside biological cells. When it became possible, scientists observed through electron microscopy, that the actin strands could form a three-dimensional structure, an impossible feat if with actin was the only molecule in this process[Stossel, 1990]. Stossel and collaborators concluded that a second protein complex bound different actin strands in an orthogonal way and that they also

worked as hinges due to cells' variable flexibility. He coined these protein complexes as *actin binding proteins* (**ABP**).

In 1974, John Hartwind and Stossel isolated the first of these protein complexes from phagocytes, confirming the theory that the actin structures were very similar to polymer structures observed in gelatinous materials. Later on, Actin Related Proteins 2/3 (**Arp2/3**) complexes were also observed, they also connected different actin strands, but without flexibility and at an angle of $\sim 70°$.

The myosin complex was another very important protein complex that finally explained how cells could move its actin structure. They are very abundant in muscles and also bind to actin strands Using Adenosine Three-Phosphates (**ATP**s), the cells' chemical energy supply, myosin complexes are able to contract and generate movement, a phenomenon much similar to muscular contraction. The structure described previously is known today as the cytoskeleton. The capacity to extend and contract in a muscle-like way, was already hypothesised by [Pollard et al., 1974].

If we consider the protein interactions described above the cytoskeleton is able to extend itself, but it lacks directionality, as the polymerization occurs irrespective of orientation. And cells need an inherent polarization to move in one preferential direction. The steps required to achieve a stable polarization direction start when proteins from the Rho family (CDC42, Rho, Rac) translate mechano-chemical cues perceived by sensory organelles present in the cellular membrane into chemical gradients that end up creating a cytoskeletal asymmetry. The cytoskeleton asymmetry favors actin polymerizing at the farther ends of the cellular body, while favoring capping and actin depolymerising in regions that are near the cellular nucleus. This process creates a stable expansion of the cytoskeleton at the cell front effectively pushing the plasma membrane forwards [Stossel, 1990, Bugyi and Kellermayer, 2020, Mogilner, 2009, Callan-Jones and Voituriez, 2016, Maiuri et al., 2015, Hall, 1998] and a fast actin polymerizing depolymeryzing phenomena at other regions (this is very important to explain the short-time diffusion migration regimes).

Although this process pushes the plasma membrane forwards with a directional preference (we call it the polarization orientation), it is not enough to propel the whole cell for-

ward: cell movement requires traction, achieved by adhesion to the substrate. At the ends of each cytoskeletal protrusion, trans-membrane protein complexes (composed of integrins, talins, paxilins, vinculins and others) bind themselves to the external substrate at the cellular front, effectively creating an adhesion interface (that unbinds when needed) between the cellular cytoskeleton and the substrate. The translocation of the whole cellular body is accomplished when the myosins contract (process mediated by the Rho proteins). The cell body moves, but the adhesion point remains fixed in respect to the substrate, such that each adhesion point starts a retrograde movement with respect to the cell's body, and eventually breaks when they reach the cell's rear [Mogilner, 2009]. The sequence of steps described above is schematically represented in figure 2.1, a model that was schematically proposed by Abercrombie [Abercrombie et al., 1970] and that was confirmed in the following years.

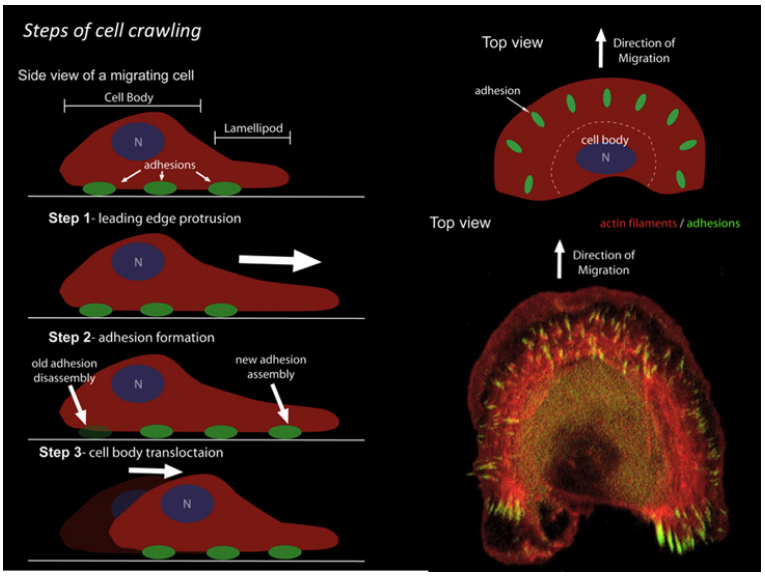

Figure 2.1: Simplified explanation of a single cell migration process adapted from reference [Schwartz, 2013]. Step 1: The cell starts to polymerize actin monomers at the cellular front, creating leading edge protrusions. Step 2: Formation of foci of new adhesion that adhere to the substrate at the leading edge, disassembly of old foci of adhesion located at the rear end of the cell due to the tension of the actin-myosin contraction. Step 3: With the contraction at the rear end and the creation of leading edge protrusions at the cellular front, the cell moves forwards.

Chapter 3

Useful Mathematical Concepts

The mechanisms that originate cellular migration are very complex and also depend on many external factors such as substrate irregularities, thermal fluctuations, protein diffusion, chemical and sometimes electrical fields. Due to the impossibility of taking all these factors into account, we consider the cellular migration as a stochastic phenomena and study the processes through mathematical modeling, computer simulations and statistical analyses. Here we define the quantities we will use in the following chapters.

Consider the trajectory of a particle given by $\vec{r}(T)$, in the time interval $0 \leq T \leq T_{final}$. The mean square displacement function **MSD**, is a function of the time interval Δt and is defined as

$$MSD(\Delta T) \;=\; \frac{1}{T_{final} - \Delta t} \int_0^{T_{final}} ds \; |\vec{r}(s + \Delta T) - \vec{r}(s)|^2 \quad , \tag{3.1}$$

Usually $MSD(\Delta T)$ is plotted as $log(MSD)$ versus $log(\Delta T)$, such that its slope indicate whether the particle is in a diffusive (slope = 1) or ballistic regime (slope = 2) or mixes of both regimes anomalous diffusive (1 ¡ slope ¡ 2). The mean square displacement obtained from the solution of an Ornstein-Uhlenbeck system was considered to describe single cell migration experiments. It is represented by a differential equation named after Langevin, who at the beginning of the twentieth century modelled the dynamics of microscopic particles immersed in a viscous fluid. The equation reads

$$\frac{d\vec{v}}{dT} = -\gamma \vec{v}(T) + \xi(T) \quad , \tag{3.2}$$

where $\vec{v}(T)$ is the particle's velocity at instant T with a friction constant γ and Wiener stochastic variable $\xi(T)$ with Gaussian distribution and zero average. It was believed that

the random expansion of the cytoskeleton through the diffusion of proteins inside the cells produced a behavior that could also be described by the Langevin equation and consequently exhibited the same mean square displacement solution, first applied in cell migration by Fürth [Fürth, 1920] and described as

$$MSD(\Delta T) \equiv \langle |\vec{r}(T+\Delta T) - \vec{r}(T)|^2 \rangle_T \tag{3.3}$$

$$= 4D\left(\Delta T - P(1 - e^{-\Delta T/P})\right) \quad , \tag{3.4}$$

where D is the diffusion constant for long time intervals and P the persistence coefficient (time scale for the particle to forget its initial trajectory, transiting from a anomalous diffusive movement to a diffusive one). Fürth equation shows us that the magnitude of the time interval we consider when analysing some trajectory influences on what is measured. If we observe time scales $\Delta T < P$, we will find a mostly ballistic regime (anomalous diffusion) $MSD(\Delta T) \sim \Delta T^2$ and for $\Delta T > P$ we observe a ballistic regime, where the particle has forgotten its initial trajectory.

The velocity auto-correlation function **VACF** measures the correlation between velocity measured at times separated by a time interval ΔT. It quantifies the time it takes for a particle to forget its previous velocity. The **VACF**'s definition is

$$VACF(\Delta T) = \frac{1}{T_{final} - \Delta t} \int_0^{T_{final}} ds\ \vec{v}(s+\Delta T) \cdot \vec{v}(s) \quad , \tag{3.5}$$

such that the **VACF** measures the correlation of velocity with itself in two different instants of time separated by ΔT.

Chapter 4

Single Cell Migration Mathematical Modelling

Mathematical and computational modeling is essential in studying many subjects, from biology to economy, as it allows for controlled environments, precisely varying every parameter of the system and non expensive *in-silico* experiments. It would not be different for the cell migration.

Models can describe a migrating particle in different ways, some, use a microscopic approach [Mogilner, 2009, Marée et al., 2006, Marée et al., 2012] with mathematical descriptions for the protein dynamics that are responsible for the cell movements, these models reproduce cellular behavior in a very accurate way, at the same time, they are computationally expensive and very hard to extend to a collective migration scenario.

Others have a more coarse-grained perspective such as the phase-field models [Shao et al., 2010, Ziebert and Aranson, 2013, Camley et al., 2013], who consist of differential field equations that represent each agent of the system through the values of multi dimensional functions, as function are continuously variable, they provide a very accurate representation of extensive bodies, being able to reproduce twists, expansion and contractions. However, this kind of representation presents the same difficulties from the previous approach, they are still very complex.

The cellular Potts models, adopts an even more coarse grained approach, they were adapted from solid state theory to model cellular segregation by [Graner and Glazier, 1992]

and are currently used for single and multi cellular migration [Albert and Schwarz, 2014, Goychuk et al., 2018, Fortuna et al., 2020]. They approximate continuum space to a grid, which reduces significantly the computational load and is versatile but may introduce artifacts to the system.

Lastly, there is the punctual particle perspective whose dynamics may be described in two ways, the probabilistic one, that considers stochastic differential equations whose solutions represent the probability of finding the particle with a given position and velocity at some time t (similar to the Fokker-Planck equation) [Szabó et al., 2006]. And the direct approach, which also uses stochastic differential equations, but with solutions that correspond directly to some particle's velocity and position [de Almeida et al., 2022, Vicsek et al., 1995, Szabó et al., 2006]. By considering punctual bodies, these models become computationally light, however this exact consideration makes it difficult to add interactions that depend on the extensiveness of objects (in a collective scenario, for example, where cell-cell interaction is present, the representation of a neighborhood of interaction is changeable and malleable, something difficult to create in the punctual particle scenario).

In this work, we consider punctual particle models, as we are dealing with single cells and are able to reproduce most of the phenomena that generate cell migration as the action of stochastic variables. The Ornstein-Uhlenbeck model is possibly one of the most used representations to recreate cell migration, adapting what was originally used to describe the dynamics of particles immersed in fluids to model cellular motion, it was able to reproduce experimental observations thus being a sound proposition. However, to account for the data provided by more recent experiments and computer simulations, the model required modifications.

Cell tracking experiments use intermittent photographs, where the time lapse between two frames is predefined by the experiment design and two successive points of the trajectories are actually not instantly successive, there are many fluctuations and movement between any two shots. Also the characteristic times of protein dynamics is on the molecular scale and impossible to observe when focusing on the whole cell. Both facts must be considered when comparing experiments and simulations with theory predictions.

Selmeczi and collaborators [Selmeczi et al., 2005] and Dieterich and collaborators [Dieterich et al., 2008] have observed a short-time diffusive behavior in the measured **MSD**. If we assume that correct (devoid of significant experimental errors [Thomas et al., 2020]), then, instantaneous velocities become ill defined since $v = \lim_{\Delta t \to 0} \Delta r / \Delta t = \infty$, in other words, instantaneous velocity measurements of diffusive particles, do not converge to a fixed value (A very nice account for this discussion on the beginning of the twentieth century is presented in reference [Genthon, 2020]). Consequently, models whose dynamics depend on a well defined instantaneous velocity and also present diffusive behaviors at short time scales must be modified to take into account divergent velocities.

Thomas and collaborators [Thomas et al., 2020] analyzed 12 experimental data sets regarding the **MSD**, concerning 5 different laboratories. All experiments showed a short-time diffusive regime, as presented in Fig. 4.1. The short-time diffusive regime is indicated by the higher values measured as compared to the **MSD** value predicted by the Fürth equation at short-time intervals. The same effect was observed in Potts Model simulations by Fortuna and collaborators [Fortuna et al., 2020].

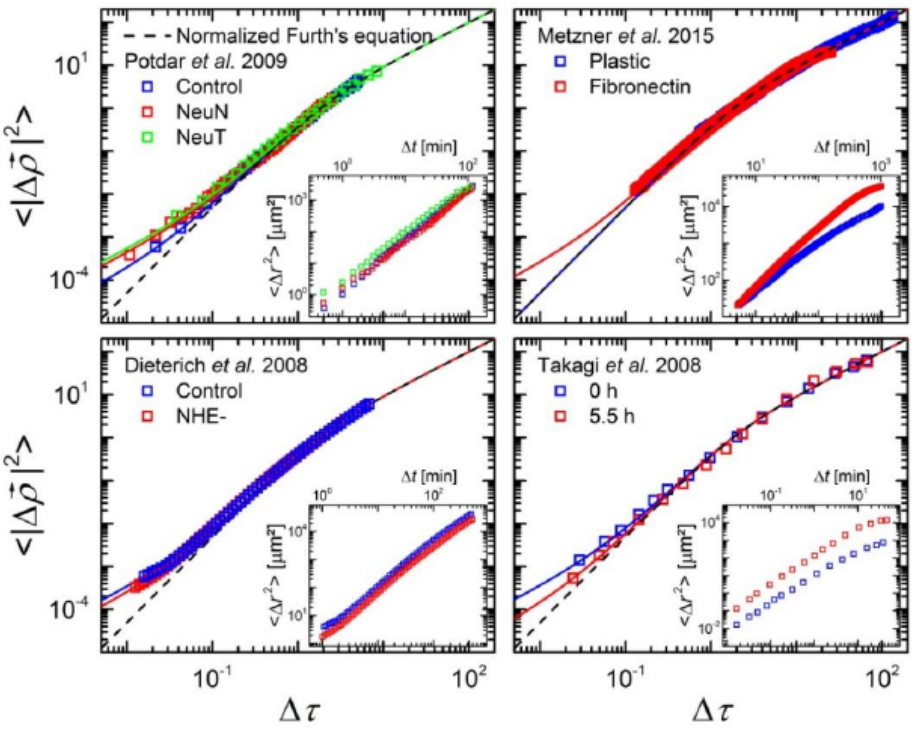

Figure 4.1: Comparison between the Fürth **MSD** (dashed lines) solution and experimental **MSD** curves from different articles [Dieterich et al., 2008, Takagi et al., 2008, Wu et al., 2014, Potdar et al., 2009]. Figure obtained from [Thomas et al., 2020].

The MSD curves presented in 4.1 also show a mostly ballistic regime for intermediate time intervals, followed by another diffusive migration regime for long time intervals. The last two regimes are predicted by Fürth equation, being the mostly ballistic or anomalous diffusive regime due to the stable polymerization of actin over the polarization axis and the long-time diffusive behavior due to changes in the orientation of the cellular front and consequently the preferential direction of migration (polarization direction). Thomas and collaborators [Thomas et al., 2020] explains the short-time diffusion as caused by the fast actin polymerization and depolymerization in the non preferential orientations of migration.

For punctual and/or rigid bodies, a short time interval diffusive regime poses a problem with the Newtonian description of such systems, a controversy that involved a stack of geniuses at the beginning of the twentieth century, such as Eisntein, Ornstein, Wiener, Langevin, among others [Genthon, 2020], whose work provided tools of how to study diffu-

sive processes. Extended bodies in contrast have centers of mass whose dynamics depend on a infinitely large number of events of mechanisms at the protein level, simultaneously acting in a time scale that is much shorter than those available to experiments. Their dynamics may be described by a mathematical model with diffusion at small time intervals. We tackle this short-time diffusion model in the next chapters.

Chapter 5

Anisotropic Ornstein-Uhlenbeck Model

5.1 The Model

The anisotropic Ornstein-Uhlenbeck (**AOU**) single cell migration model considers a particle exhibiting an internal degree of freedom, namely, a polarization orientation given by vector $\hat{p}(t) = \Big(cos\big(\theta(t)\big), sin\big(\theta(t)\big)\Big)$, which must exist, since cells spontaneously break their spacial symmetry through existing anisotropies in the distribution of proteins responsible for cell movement. We also define an orthogonal to polarization unit vector as $\hat{n}(t) = \Big(sin\big(\theta(t)\big), -cos\big(\theta(t)\big)\Big)$. We assume that **AOU** particle changes its polarization orientation at every step of time Δt obeying the equation

$$\theta(t + \Delta t) = \theta(t) + \int_t^{t+\Delta t} \beta(s)\, ds \quad , \tag{5.1}$$

where $\beta(t)$ is a Wiener variable. The polarity produces two different dynamics for the particle, one in the parallel-to-polarization orientation and another in the direction perpendicular to polarization.

The dynamics on the polarization direction is given by a modified Langevin equation

$$v_{\parallel}(t + \Delta t) \;\; = \;\; \left((1 - \gamma\Delta t)v_{\parallel}(t) + \int_t^{t+\Delta t} \xi_{\parallel}(s)\, ds\right) \big(\hat{p}(t) \cdot \hat{p}(t + \Delta t)\big) \quad , \tag{5.2}$$

where $v_{\parallel}(t)$ is the particle's parallel-to-polarization velocity (namely parallel velocity) at the instant of time t, γ is the dissipation constant, $\xi_{\parallel}(t)$ is a Wiener variable (Gaussian white noise) which is uncorrelated to β and replicates the acto-myosin mechanism that propels the particle forwards (because it is a zero centered distribution it also propels the particle backwards). The modification from the original Langevin equation is the product $\big(\hat{p}(t)\cdot\hat{p}(t+\Delta t)\big)$,

meaning that the particle's parallel velocity is projected onto the new polarization direction, effectively losing some velocity at each turn. Real cells also lose some of its velocity when turning due to the need of cytoskeletal reassembly.

The particle's dynamics in the orthogonal to polarization orientation is given by a Wiener process;

$$\vec{r}_{\perp}(t+\Delta t) = \vec{r}_{\perp}(t) + \int_{t}^{t+\Delta t} \xi_{\perp}(s)\, ds\, \hat{n}(t) \quad , \tag{5.3}$$

where $\xi_{\perp}$ is a Wiener variable directly proportional to β i.e. $\xi_{\perp} = \sqrt{q}\beta$ and $\hat{n}(t)$ is the unitary vector, orthogonal to $\hat{p}(t)$ direction. The sideways stochastic fluctuation of the particle's position is replicating the phenomena of rapid assembly and disassembly of the actin filaments on the lateral parts of the cellular body.

Each Wiener variable has zero mean and a scale given by its second momentum, that is

$$\langle \xi_{\parallel}(t) \rangle = 0 \quad \langle \xi_{\parallel}(t)\xi_{\parallel}(t') \rangle = g\delta(t-t') \tag{5.4}$$

$$\langle \beta(t) \rangle = 0 \quad \langle \beta(t)\beta(t') \rangle = 2k\delta(t-t') \tag{5.5}$$

$$\langle \xi_{\perp}(t) \rangle = 0 \quad \langle \xi_{\perp}(t)\xi_{\perp}(t') \rangle = 2qk\delta(t-t') \quad , \tag{5.6}$$

where g, k and qk have the units of [length^2]/[time^3], 1/[time] and [length^2]/[time] respectively.

In a succinct way, the **AOU** model consists of a particle with an inner degree of freedom represented by the polarization orientation that changes its direction at each instant of time (according to a Wiener process) and provides an asymmetric dynamics for the migrating particle. In the direction that is orthogonal to the polarization axis, the particle's position follows a Wiener process. The particle's dynamics on the polarization direction is ruled by a modified Langevin equation for the speed.

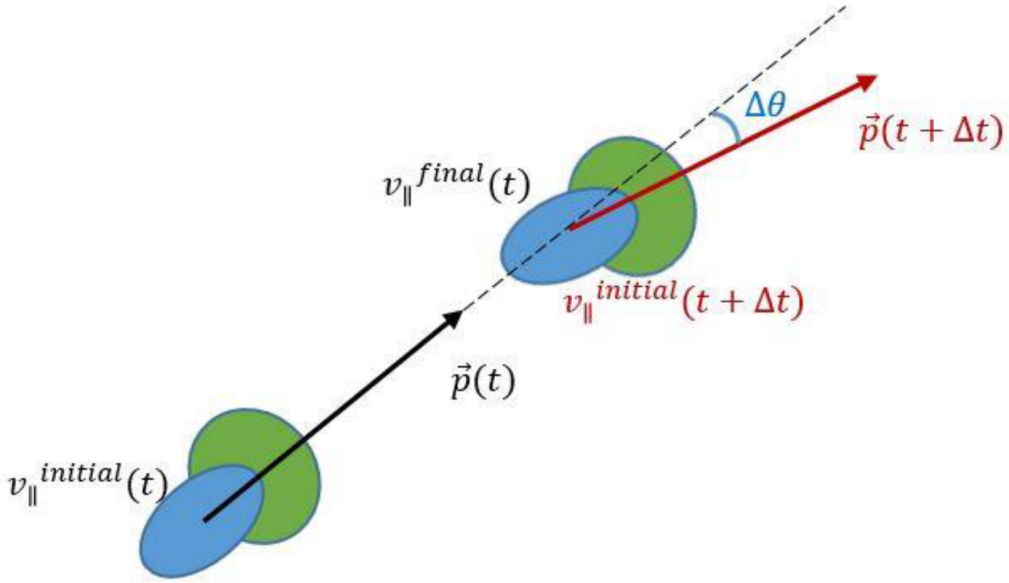

Figure 5.1: Diagrammatic representation of a particle that moves according to an Ornstein-Uhlenbeck process, where $v_{\parallel}(t)$ is its velocity in the polarity axis $\vec{p} = (cos(\theta(t)), sen(\theta(t)))$ and at each time-step its initial velocity is projected onto its new polarization axis, in other words, we model a cell's loss of velocity at each turn to the cytoskeletal reshaping.The figure was obtained from [de Almeida et al., 2022].

5.2 Analytical Solutions

Here we show the analytical solutions for the model's average velocity, parallel to polarization **VACF** and **MSD**.

In what follows, for brevity we shall call parallel velocity, the velocity parallel to the polarization and perpendicular (or orthogonal) displacement for the displacement on the direction perpendicular to the polarization. The solutions were obtained by iteration. We consider the trajectory in the time interval $0 \leq t \leq T$ where a partition of this time interval may be written as $\Delta t = T/n$ such that we have n partitions for this time interval. When we take the limit where $n \to \infty$ and $\Delta t \to 0$, such that $T = n\Delta t$ remains finite.

Average Square Parallel Velocities

The parallel velocity at the first time step is

$$v_{\parallel}(\Delta t)\hat{p}_1 = \left((1-\gamma\Delta t)v_{\parallel}(0) + \int_0^{\Delta t}\xi_{\parallel}(s)\,ds\right)(\hat{p}_0\cdot\hat{p}_1) \quad , \tag{5.7}$$

with $\hat{p}_i$ is the polarization vector at the instant of time $i\Delta t$. Then we found the parallel velocity equation corresponding to the second, third and fourth time steps and so on such that it was possible, after n iterations, to create a generalized parallel velocity equation for an arbitrary time step $T = n\Delta t$, it is written as

$$\begin{aligned} v_{\parallel}\hat{p}_n &= (1-\gamma\Delta t)^n v_{\parallel}(0)\prod_{i=0}^{n-1}(\hat{p}_i\cdot\hat{p}_{i+1})\,\hat{p}_n & (5.8)\\ &\quad + \sum_{j=0}^{n-1}(1-\gamma\Delta t)^{n-j+1}\int_{j\Delta t}^{(j+1)\Delta t}\xi_{\parallel}(s)\,ds\prod_{i=j}^{n-1}(\hat{p}_i\cdot\hat{p}_{i+1})\,\hat{p}_n \quad . & (5.9)\end{aligned}$$

We then squared equation (5.9) and averaged it reaching

$$\begin{aligned}\langle v_{\parallel}^2(n\Delta t)\rangle &= (1-\gamma\Delta t)^{2n}v_{\parallel}^2(0)\left\langle\prod_{i=0}^{n-1}(\hat{p}_i\cdot\hat{p}_{i+1})^2\right\rangle & (5.10)\\ &\quad + g\Delta t\sum_{j=0}^{n-1}(1-\gamma\Delta t)^{2(n-j+1)}\left\langle\prod_{i=0}^{n-1}(\hat{p}_i\cdot\hat{p}_{i+1})^2\right\rangle \quad , & (5.11)\end{aligned}$$

with $\left\langle\int_{l\Delta t}^{(l+1)\Delta t}\int_{j\Delta t}^{(j+1)\Delta t}\xi_{\parallel}(s)\xi_{\parallel}(s')ds\,ds'\right\rangle = g\Delta t\delta_{l,j}$, a result that is direct consequence of (5.4). We also employed the fact that $(\hat{p}_i\cdot\hat{p_{i+1}}) = cos\Big(\theta\big(j\Delta t\big) - \theta\big((j+1)\Delta t\big)\Big) = cos(\Delta\theta)$ where very small values of Δt allows us to write $cos(\Delta\theta)\sim 1-\frac{1}{2}(\Delta\theta)^2$ and $cos^2(\Delta\theta)\sim 1-(\Delta\theta)^2$. Considering the average values for $cos(\Delta t)$ over small time intervals Δt, we obtain from equation 5.5, $\langle(\Delta\theta)^2\rangle \overset{\Delta t\to 0}{=} 2k\Delta t$, which allows us to evaluate the product terms in equation 5.11, obtaining

$$\langle v_{\parallel}^2(n\Delta t)\rangle = v_{\parallel}^2(0)(1-\gamma\Delta t)^{2n}(1-k\Delta t)^{2(n-1)} + g\Delta t\sum_{j=0}^{n-1}(1-\gamma\Delta t)^{2(n-j-1)}(1-k\Delta t)^{2(n-j-1)} \tag{5.12}$$

Taking the limit $\Delta t\to 0$, with $n = \frac{T}{\Delta t}$, we obtain

$$\langle v_{\parallel}^2(T)\rangle = \frac{g}{2(\gamma+k)} + \left(v_{\parallel}^2(0) - \frac{g}{2(\gamma+k)}\right)e^{-2(\gamma+k)T} \quad . \tag{5.13}$$

If we assume an infinite time has passed ($T \to \infty$) such that the system has reached a stationary state, we find that $\langle v_\parallel^2 \rangle = \frac{g}{2(\gamma+k)}$. Notice that assuming $v_\parallel^2(0) = \frac{g}{2(\gamma+k)}$ forces the system into an initial stationary state. For detailed calculation, please see [de Almeida et al., 2022].

Equation 5.13 also allows us to find the rate at which the average squared velocity reaches its stationary value. We name it the relaxation time $R = (\gamma + k)^{-1}$.

Both experiments and simulation deal with discrete values of time. Also, instantaneous velocity is estimated from a means velocity, calculated for finite values of time intervals. When instantaneous velocity is a well defined quantity, an adequately small time interval gives the instantaneous velocity within a predefined precision. However, for diffusive movements this is not the case. To compare the theoretical predictions with the measured values in both experiments and simulations, we define a mean velocity, that depends on the time interval ε as follows

$$\left\langle v^2 \right\rangle_\varepsilon = \left\langle \frac{|\vec{r}(T+\varepsilon) - \vec{r}(T)|^2}{\varepsilon^2} \right\rangle \quad , \tag{5.14}$$

which can be decomposed into two components, one perpendicular ($\Delta\vec{r}_\perp$) to the polarization axis and one parallel ($\Delta\vec{r}_\parallel$)

$$\left\langle \frac{|\vec{r}(T+\varepsilon) - \vec{r}(T)|^2}{\varepsilon^2} \right\rangle = \left\langle \frac{|\vec{r}_\parallel(T+\varepsilon) - \vec{r}_\parallel(T)|^2}{\varepsilon^2} \right\rangle + \left\langle \frac{|\vec{r}_\perp(T+\varepsilon) - \vec{r}_\perp(T)|^2}{\varepsilon^2} \right\rangle \quad . \tag{5.15}$$

For small values of ε, equation 5.15 tends to

$$\left\langle \frac{|\vec{r}(T+\varepsilon) - \vec{r}(T)|^2}{\varepsilon^2} \right\rangle = \langle v_\parallel^2 \rangle + \left\langle \frac{|\vec{r}_\perp(T+\varepsilon) - \vec{r}_\perp(T)|^2}{\varepsilon^2} \right\rangle \quad , \tag{5.16}$$

Starting from a high velocity initial condition $\left\langle v_\parallel^2 \right\rangle$ tends to its stationary value $\frac{g}{2(\gamma+k)}$. Consequently, the difference $\left\langle \frac{|\vec{r}(T+\varepsilon)-\vec{r}(T)|^2}{\varepsilon^2} \right\rangle - \frac{g}{2(\gamma+k)}$ has two terms. The first is the excess in the parallel velocity in respect to its stationary value and the second component is due to the contribution from the stochastic displacement on the perpendicular direction that we expect to be constant in time. If the systems starts with a high parallel velocity, the plot of this difference against T should decrease from the initial value and stabilize at $\frac{2qk}{\varepsilon}$, the value of the contribution from the perpendicular displacement. Figure 5.2 shows a semi-log plot of The

difference $\left\langle \frac{|\vec{r}(T+\varepsilon)-\vec{r}(T)|^2}{\varepsilon^2} \right\rangle - \left\langle v_\parallel^2 \right\rangle$ versus time for $v_\parallel(0) = 10^3$ in arbitrary units and 4 values of k.

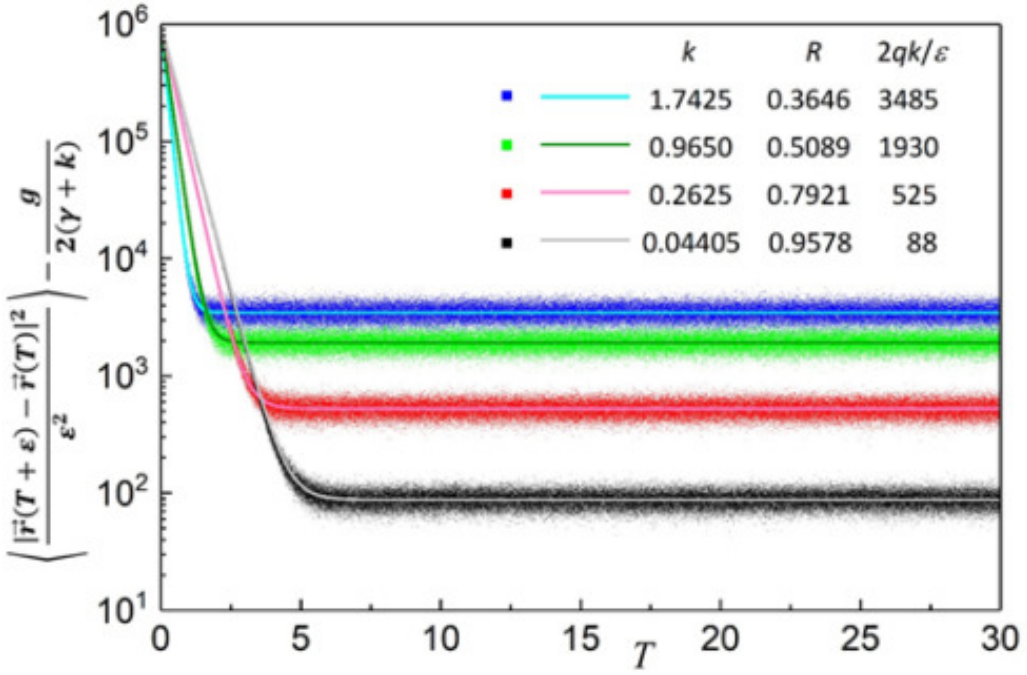

Figure 5.2: Semi-log plots of the average square displacement over ε^2 subtracted by $\frac{g}{2(\gamma+k)}$ versus T, with arbitrary (values selected for best display of the model's possible dynamics) $\varepsilon = 10^{-4}$, $q = 0.1$, $g = 10$, $\gamma = 1$ and k indicated in the figure's superior right-side corner. The dots consists of the numerical estimations made of over 10 particles and 10^6 steps.

Mean Square Displacement (MSD)

The **MSD** was obtained by partitioning the time interval $0 \leq t \leq \Delta T$ in N time intervals Δt such that $\Delta T = N\Delta T$. We iterate the evolution equations to obtain a general equations for the quantity of interest, then we take the average over the stochastic noise terms and finally take the limit for $n \to \infty$ and $\Delta t \to 0$, such that ΔT remains finite. See [de Almeida et al., 2022] and C for more information.

For $N > 0$ steps, the particle's position is described as

$$\begin{aligned}\vec{r}(n\Delta t) &= \vec{r}(0) + v_{\parallel}(0)\Delta t \sum_{n=0}^{N}(1-\gamma\Delta t)^n \prod_{i=0}^{n-1}(\hat{p}_i \cdot \hat{p}_{i+1})\,\hat{p}_n \\ &+\Delta t \sum_{n=0}^{N}\sum_{j=0}^{n-1}(1-\gamma\Delta t)^{n-1-j}\int_{j\Delta t}^{(j+1)\Delta t}\xi_{\parallel}(s)\,ds \prod_{i=j}^{n-1}(\hat{p}_i \cdot \hat{p}_{i+1})\,\hat{p}_n \\ &+\Delta t \sum_{n=0}^{N}\int_{n\Delta t}^{(n+1)\Delta t}[(n+1)\Delta t - s]\,\xi_{\parallel} ds \hat{p}_n \\ &+\sum_{n=0}^{N}\int_{n\Delta t}^{(n+1)\Delta t}\xi_{\perp}(s) ds\,\hat{n}_n \quad . \end{aligned} \tag{5.17}$$

Squaring the particle's position and averaging over the noise terms, we find

$$\mathbf{MSD}(\Delta T) = \langle \vec{r}(T+\Delta T) - \vec{r}(T)\rangle \tag{5.18}$$

$$= \frac{g}{(\gamma+2k)(\gamma+k)}\left[\Delta T - \frac{1}{\gamma+2k}(1-e^{-(\gamma+2k)\Delta T})\right] + 2qk\Delta T \quad , \tag{5.19}$$

which has the same form as the Fürth equation [Fürth, 1920] added to a diffusive term $(2qk\Delta T)$:

$$\mathbf{MSD}_{\text{Fürth}}(\Delta T) = 2D\left(\Delta T - P(1-e^{-\Delta T/P})\right) \quad , \tag{5.20}$$

that can be rewritten as

$$\mathbf{MSD}_{\text{Modified Fürth}}(\Delta T) = 2D\left(\frac{\Delta T}{1-S} - P(1-e^{-\Delta T/P})\right) \quad , \tag{5.21}$$

that has been used as fitting equation, called the modified Fürth equation [Thomas et al., 2020], that could account for the observed short-time diffusive regime.

By comparing the modified Fürth equation and the **MSD** equation we found for the **AOU** model, we obtain the fitting parameters as functions of the theoretical model parameter, as follows:

$$D = \frac{g}{2(\gamma+2k)(\gamma+k)} \tag{5.22}$$

$$P = \frac{1}{\gamma+2k} \quad \text{and} \tag{5.23}$$

$$S = \frac{2qk(\gamma+2k)(\gamma+k)}{g+2qk(\gamma+2k)(\gamma+k)} \quad . \tag{5.24}$$

Varying the constants g, q, k and γ allows us to obtain different dynamics, for $k = 0$ the **AOU** model presents a one dimensional Ornstein-Uhlenbeck particle, with a normal Fürth equation for its **MSD** and $S = 0$, $P = \frac{1}{\gamma}$ and $D = \frac{g}{2\gamma^2}$. When $k > 0$ and $q = 0$ we obtain a Vicsek-like model [Vicsek et al., 1995] but with a variable speed ruled by a Langevin equation in the $\hat{p}(t)$ direction, in this case, our **MSD** curve is still the same as Fürth one, but with different $\langle v_{\parallel}^2 \rangle$ and relaxation time R from that of the usual Ornstein-Uhlenbeck process. For $q, k > 0$, we observe the **AOU** model with the three regime **MSD** and $\langle v_{\parallel}^2 \rangle = \frac{g}{2(\gamma+k)}$.

We also find important the study of the limit cases for the **MSD** from the **AOU** model, for small ΔT, 5.21 yields

$$\lim_{\Delta T \to 0} MSD_{\text{Modified Fürth}} \sim \frac{2DS}{1-S}\Delta T \quad , \tag{5.25}$$

indicating that for small time intervals of observation, the system exhibits a diffusive regime with diffusion constant $D_{\text{fast}} = \frac{DS}{1-S} = qk$. For $\Delta T >> P$, we find that

$$\lim_{\Delta T \to \infty} MSD_{\text{Modified Fürth}} \sim \frac{2D}{1-S}\Delta T \quad , \tag{5.26}$$

reproducing a long diffusive dynamic with diffusion constant $D_{\text{slow}} = \frac{D}{1-S}$. This way, it is possible to attribute a meaning to the S constant, as a ratio, $S = \frac{D_{\text{fast}}}{D_{\text{slow}}}$, from [Fortuna et al., 2020], we name it the *excess diffusion coefficient*. The four variables S, P, D and R then define a three regime **MSD** with a short diffusive interval for $\Delta T < SP$, a medium anomalous diffusive or partially ballistic regime for $SP < \Delta T < P$ and a long diffusive regime for $\Delta T > P$, which reproduces the three regime **MSD** found experimentally [Thomas et al., 2020].

An important aspect from the **AOU** model is the possibility of defining natural units for time and space, which rescales any system obeying an anisotropic Ornstein-Uhlenbeck process and allows quantitatively comparing theory, simulations, and experiments. We follow the rescaling done in [Thomas et al., 2020] where $\frac{2DP}{1-S}$ is used as a length scale and P as a time scale. The reescaled **MSD** is

$$\left\langle |\Delta\vec{\rho}|^2 \right\rangle = \frac{\langle |\Delta\vec{r}|^2 \rangle}{2DP/(1-S)} \tag{5.27}$$

$$= \Delta\tau - (1-S)(1-e^{-\Delta\tau}) \quad , \tag{5.28}$$

where $\Delta\tau = \frac{\Delta T}{P}$ and $\langle |\Delta\vec{\rho}|^2 \rangle$ are dimensionless variables.

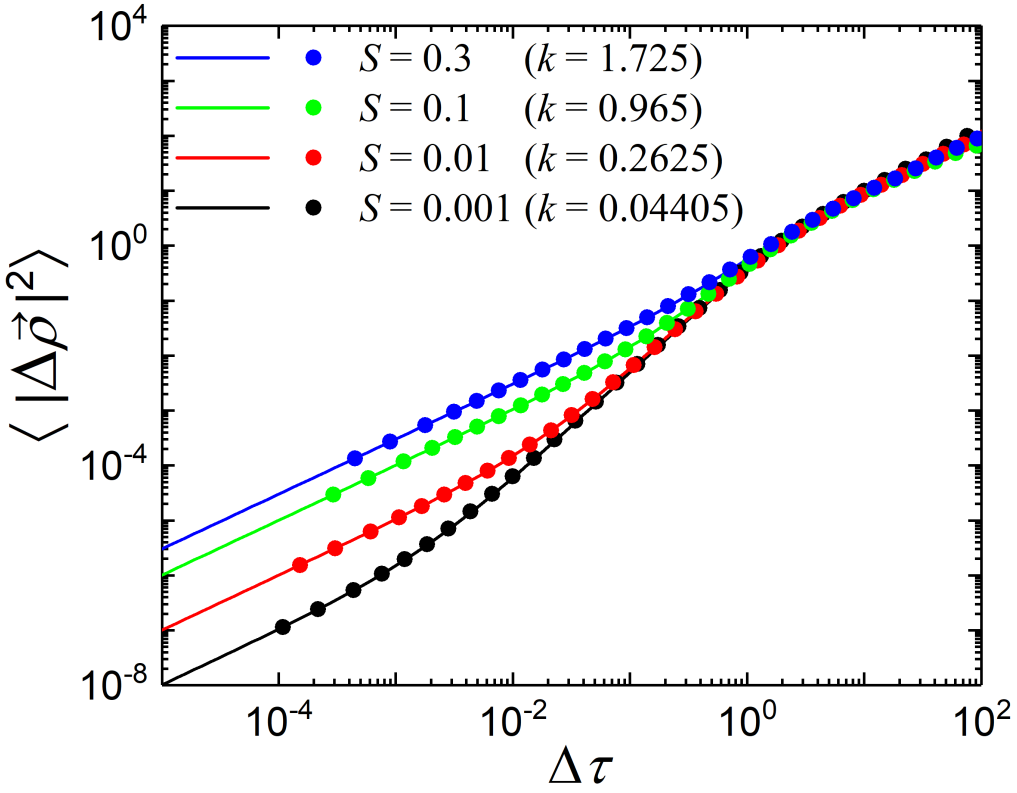

Figure 5.3: Log-log plot comparing the analytical **MSD** curve in natural units from equation 5.28 (continuous lines) with the numerical **MSD** solutions (dots) for $q = 0.1$, $g = 10$, $\gamma = 1$ and four values of k, they are $k \in \{0.04405, 0.2625, 0.965, 1.7425\}$ corresponding to four values of S, they are $S \in \{0.001, 0.01, 0.1, 0.3\}$. The numerical solutions are the results of 100 independent trajectories.

Velocity Auto-Correlation Functions

The anisotropy of the **AOU** model, allows us to establish two different displacements with respect to the polarization axis, one parallel and the other perpendicular to the cell polarization . In natural units this displacement is written as

$$\begin{aligned} \Delta\vec{\rho} &= \vec{\rho}(\tau + \delta) - \vec{\rho}(\tau) \\ &= \Delta\vec{\rho}_{\parallel} + \Delta\vec{\rho}_{\perp} \quad , \end{aligned} \tag{5.29}$$

where $\Delta\vec{\rho}_{\parallel}$ is the dimensionless displacement parallel to the polarization axis and $\Delta\vec{\rho}_{\perp}$ the perpendicular one. With the displacements in hand, we hypothetically calculate the instan-

taneous velocity as

$$\vec{u}(\tau) = \lim_{\delta\to 0} \frac{\Delta\vec{\rho}_{\parallel} + \Delta\vec{\rho}_{\perp}}{\delta} = u_{\parallel}(\tau)\hat{p}(\tau) + \lim_{\delta\to 0} \frac{\Delta\vec{\rho}_{\perp}}{\delta}\hat{n}(\tau) \quad , \tag{5.30}$$

when $k > 0$ and $q > 0$ the ratio $\lim_{\delta\to 0} \frac{\Delta\vec{\rho}_{\perp}}{\delta}$ goes to infinity as $\Delta\vec{\rho}_{\perp} \sim \sqrt{\delta}$, a fact that originates from the perpendicular Wiener process whose nature is always diffusive. The other component of displacement $\Delta\vec{\rho}_{\parallel}$ originates from an Ornstein-Uhlenbeck process, which is ballistic for $\delta \to 0$ and thus, finite.

To better illustrate how an **AOU** particle's speed diverges for small values of δ, we plotted the the average mean speed versus δ and show that it is mostly constant for the time intervals corresponding to the partially ballistic regime and it gets larger as δ gets smaller.

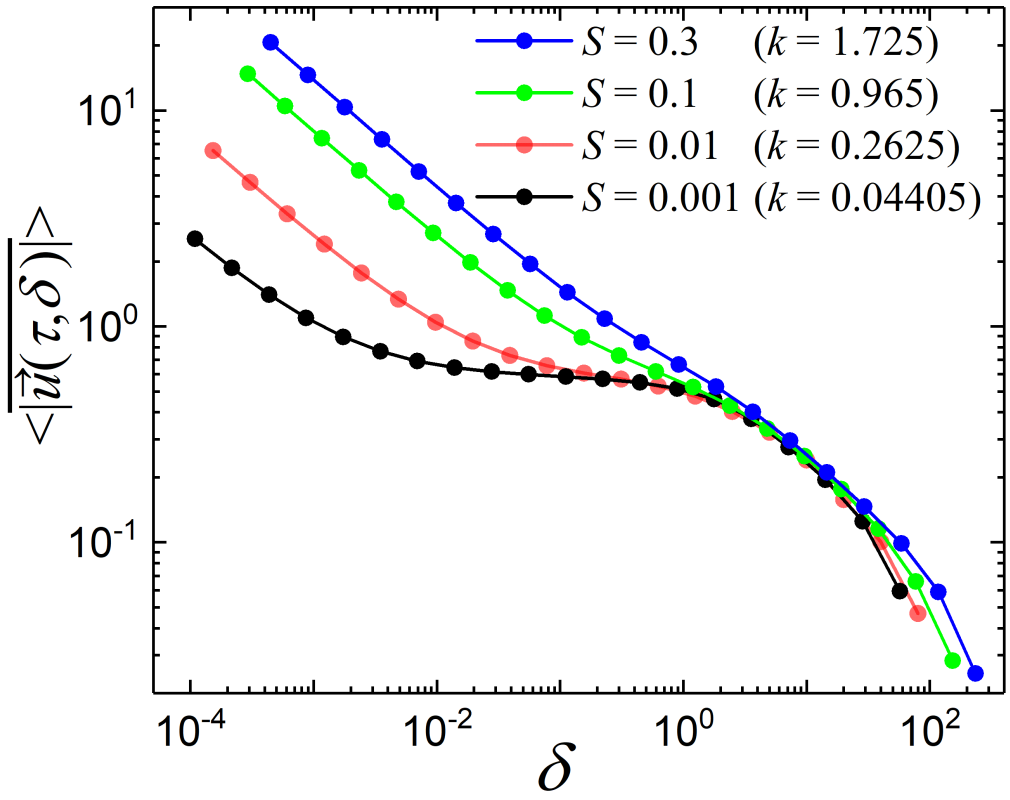

Figure 5.4: Log-log plot of the average mean speed reescaled in natural units of velocity $\sqrt{\frac{2D}{P(1-S)}}$ and time P, whose numerical solutions are the result of 100 independent trajectories, with $q = 0.1$, $g = 10$, $\gamma = 1$ and four values of $k\,k \in \{0.04405, 0.2625, 0.965, 1.7425\}$ corresponding to four values of S $S \in \{0.001, 0.01, 0.1, 0.3\}$. The speeds are mostly convergent when δ values correspond to that of mostly ballistic regimes and diverge when $\delta \to 0$.

In the laboeratory, it is not always possible to separate the perpendicular and parallel displacement components. However, a profile of the mean speed against the time intervals δ provides us some clues. Defining the mean velocity as

$$\overline{\vec{u}(\tau,\delta)} \equiv \frac{\vec{\rho}(\tau+\delta)-\vec{\rho}(\tau)}{\delta} \quad , \tag{5.31}$$

we know that for $\delta \to 0$, the mean speed value $\langle\overline{\vec{u}(\tau,\delta)}\rangle$ should diverge, but for some specific value of δ, we observe that $\Delta\vec{\rho}_{\parallel}$ becomes much more significant than $\Delta\vec{\rho}_{\perp}$ such that the mean velocity may be characterize by this value, as we see in what follows.

Velocity Auto-Correlation Function **VACF**

We observe that, although $\vec{v}(\tau) = \frac{\Delta\vec{\rho}}{\delta}$ diverges as $\delta \to 0$, velocity auto-correlation function does not. The reason for that is that the only term that does not vanish for finite values of δ is the parallel velocity, as shown below:

$$\begin{aligned} VACF(\Delta T) &= \lim_{\delta\to 0}\left\langle\left(v_{\parallel}(T)\hat{p}(T)+\frac{\Delta r_{\perp}(T)}{\delta}\hat{n}(T)\right)\cdot\left(v_{\parallel}(T+\Delta T)\hat{p}(T+\Delta T)+\frac{\Delta r_{\perp}(T+\Delta T)}{\delta}\hat{n}(T+\Delta T)\right)\right\rangle \\ &= \left\langle v_{\parallel}(T)\hat{p}(T)\cdot v_{\parallel}(T+\Delta T)\hat{p}(T+\Delta T)\right\rangle \quad , \end{aligned} \tag{5.32}$$

since $\Delta r_{\perp}(T)$ and $\Delta r_{\perp}(T+\Delta T)$ both obey a Wiener process with zero average and zero auto-correlation when considering two different instants of time (T and $T+\Delta T$).

The analytical velocity auto-correlation function may be obtained by iteration method used in obtaining MSD, and is

$$VACF(\Delta T) = \left\langle v_{\parallel}^2(T)e^{-(\gamma+2k)\Delta T}\right\rangle = \left\langle v_{\parallel\ \text{stationary}}^2\right\rangle e^{-\Delta T/P} \quad , \tag{5.33}$$

which corresponds to the second derivative of the **MSD** curve, as it should. Because both the Fürth **MSD** curve and the **AOU** modified Fürth one have the same second derivative, both models have equivalent **VACF** curves: an exponential decay given by the constant $P = (\gamma+2k)^{-1}$.

Mean Velocity Auto-Correlation Function $\Psi(\delta, \Delta T)$

We conclude through equation 5.33 that when in the stationary state we have $VACF(\Delta T \to 0) = \langle v_{\parallel\ \text{stationary}}^2\rangle$, however, this result usually does not agree with what is observed ex-

perimentally. There are two different factors that play an important role in experimental measuring, as we discuss below.

Velocities are defined as the ratio of a displacement and the time interval in which the displacement occurred and instantaneous velocities consider the case where $\delta \to 0$ such that

$$\vec{u} = \lim_{\delta \to 0} \frac{\Delta\vec{\rho}(\delta)}{\delta} = \lim_{\delta \to 0} \left[\frac{\Delta\rho_{\parallel}(\delta)}{\delta}\hat{p} + \frac{\Delta\rho_{\perp}(\delta)}{\delta}\hat{n} \right] \quad . \tag{5.34}$$

However, for a Wiener process dynamics the ratio $\frac{\Delta\rho_{\perp}(\delta)}{\delta}$ diverges, making the instantaneous velocity to diverge.

In the experimental cell migration scenario, it is not possible to obtain truly instantaneous velocities and their values are estimated using finite values for δ. Separating the displacement into two components, it becomes clear that for $S < \delta < 1$ (in natural units of time, $P = 1$) the predominant component for the total displacement is $\Delta\vec{\rho}_{\parallel}$. This case will result in the experimental measurements of the **VACF** agreeing with the theoretical results, as the ballistic behavior dominates.

On the other hand, if $\delta < S$, we observe that $\Delta\vec{\rho}_{\perp} >> \Delta\vec{\rho}_{\parallel}$, in other words, the predominant component of the velocity becomes $\vec{u}(\tau) \approx \frac{\Delta\rho_{\perp}(\tau)}{\delta}\hat{n}(\tau)$, which results into decreasing values for the velocity auto-correlation as $\Delta\rho_{\perp}(\tau)$ obeys a Wiener process.

Using the average velocity concept for a finite time interval δ we define *mean velocity auto-correlation function* **MVACF** as

$$\psi(\delta, \Delta\tau) \equiv \left\langle \overline{\vec{u}(\tau, \delta)} \cdot \overline{\vec{u}(\tau + \Delta\tau, \delta)} \right\rangle \quad , \tag{5.35}$$

where $\overline{\vec{u}(\tau, \delta)} = \frac{\Delta\rho_{\parallel}(\delta)}{\delta}\hat{p}(\tau) + \frac{\Delta\rho_{\perp}(\delta)}{\delta}\hat{n}(\tau)$. For displacement measurements for finite time intervals δ, we find an analytical **MVACF** (with the system represented in natural units) as

$$\psi(\delta, \Delta\tau) = \frac{\gamma + 2k}{\gamma} \frac{\left(1 - e^{-\gamma\delta/(\gamma+2k)}\right)\left(1 - e^{-\gamma\delta}\right)}{\delta^2} e^{-\Delta\tau} \left\langle u_{\parallel}^2 \right\rangle_{\text{stationary}} \quad . \tag{5.36}$$

The detailed calculations may be found in Ref. [de Almeida et al., 2022].

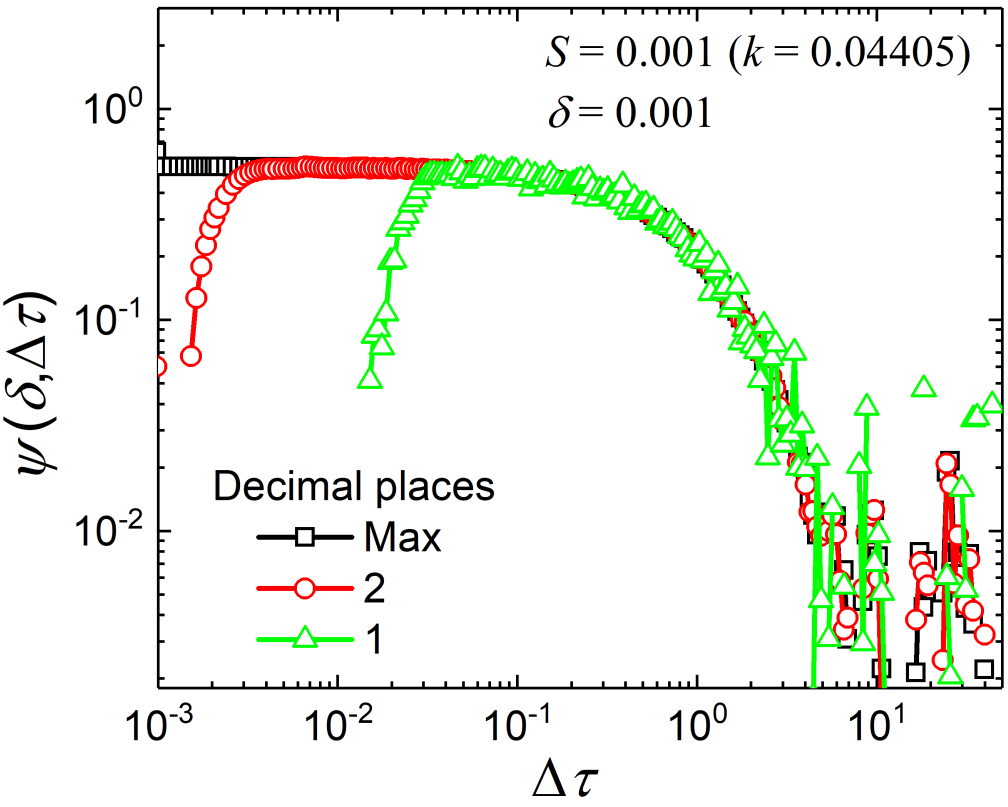

Figure 5.5: Log-log plot of numerical **MVACF** solutions (in natural units) versus $\Delta\tau$ for $q = 0.1$, $g = 10$, $\gamma = 1$, $k = 0.04405$ and $\delta = 0.001$. To emulate low precision measurements, we truncated the position and velocities estimates. From Ref.[de Almeida et al., 2022].

For experimental measurements with a finite precision, it may happen that the measurement only detects the perpendicular displacement, that is much larger than the parallel one for small values of δ. In this case, we expect that the measured velocity auto-correlation goes to zero, since perpendicular displacements are not auto-correlated. In Fig. 5.5 we present the results where we have mimicked a loss of precision by artificially cutting the number of digits of speed in our numeric solutions.

Since in real experiments we do not have infinitesimal δ values, we have to be careful to keep $\Delta\tau > \delta$. $\delta > \Delta\tau$ introduces an artificial velocity auto-correlation due to the overlapping of the time intervals δ used to calculate the average $\overline{\vec{u}(\tau,\delta)}$ and $\overline{\vec{u}(\tau+\Delta\tau,\delta)}$. This phenomenon happens even for high precision measurements. Figure 5.6 shows the mean velocity auto-correlation function for different values of δ. When $\Delta\tau < \delta$ the MVACF curve

separates from the theoretically calculated VACF.

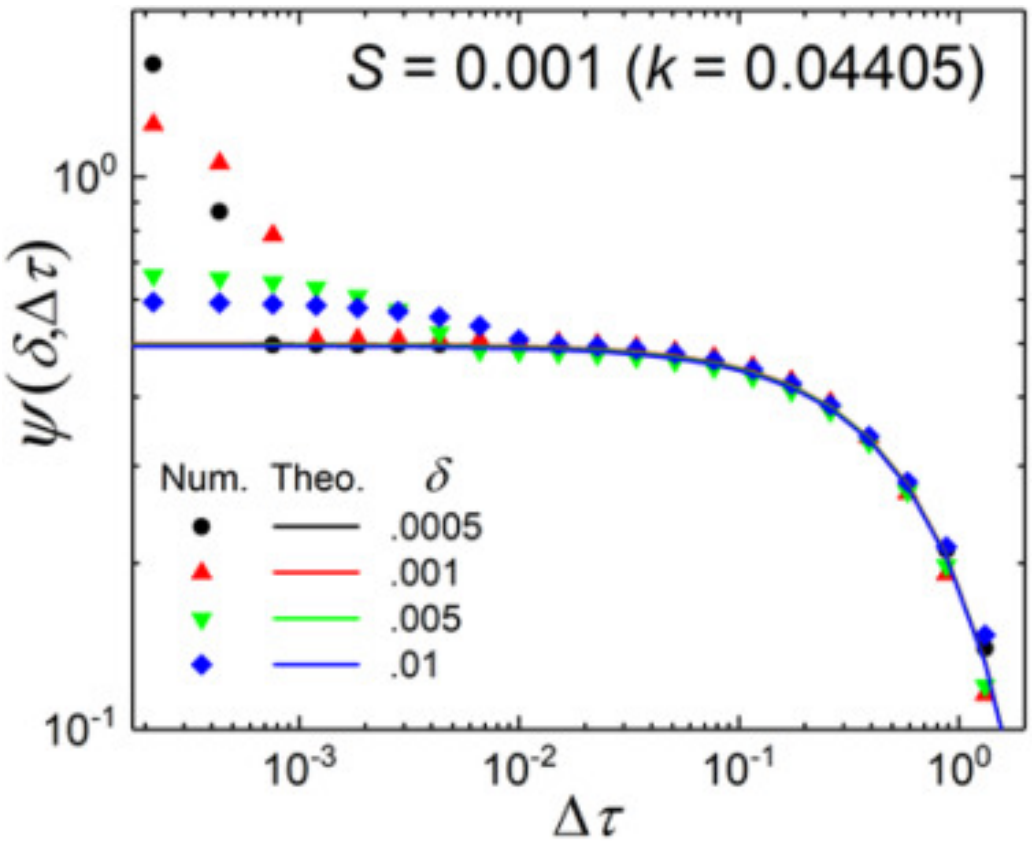

Figure 5.6: Log-log plot of numerical **MVACF** solutions (in natural units) versus $\Delta\tau$ for $q = 0.1$, $g = 10$, $\gamma = 1$, $k = 0.04405$ with four values of δ in which we measure the average velocity auto-correlation for $\Delta\tau < \delta$, effectively introducing an artificial correlation. The lines correspond to the **VACF** solution and the symbols to the numerical solutions from 10 trajectories. From Ref. [de Almeida et al., 2022]

There is also the possibility of both the low precision measurements (big values of δ) and the overlapping quantities being present in some migration experiment, which may cause erroneous measurements and conclusions.

The Anisotropic-Ornstein Uhlenbeck is successful in reproducing the three regime **MSD** observed experimentally and in simulations, we introduced natural units of length and time, which allows for comparisons between different cells, simulations and any system whose dynamics is a composition two perpendicular processes, one of them a Ornstein-Uhlenbeck and the other a Wiener process. We were also able to explain the shortcoming

of **VACF** measurements in the laboratories whose measuring apparatus present finite precision, which end up diminishing the auto-correlation for short time intervals between successive shots.

Although the **AOU** model was able to reproduce various cell behaviors, it considers an Ornstein-Uhlenbeck process in the direction of polarization, with a parallel velocity distribution centered around zero something that is not observed experimentally. Real cells maintain a stable actin polymerization activity at their frontal region and they exhibit velocity distributions centered around a positive velocity value. This is clearly shown by Nousi and colleagues [Nousi et al., 2021]. They first measured brain cancer cells **MSD** obtaining what we see in figure 5.7.

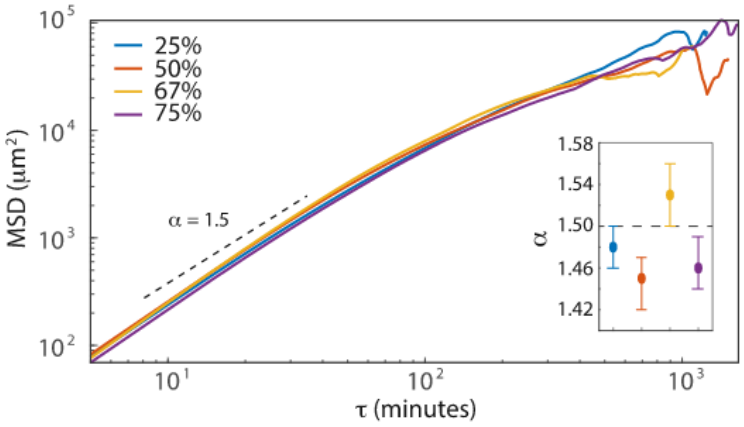

Figure 5.7: Experimental log-log plot of mean square displacements of brain cancer cells. The values 25%, 50%, 67% and 75% represent the quantity of adhering substrate (extra cellular matrix or **ECM**) used in each experiment. Fig. from [Nousi et al., 2021]

Figure 5.7 shows four **MSD** curves with no short-time diffusive behavior, meaning that subsequent displacements should be mostly ballistic, consequently calculated average velocities should converge to what we defined as the parallel velocity $v_{\parallel}$ i.e.

$$\overline{\vec{v}(T,\varepsilon)} \overset{SP<\varepsilon<P}{\approx} \vec{v}_{\parallel}(T) \quad . \tag{5.37}$$

Knowing that the average velocity converges to the parallel one when considering time-intervals corresponding to mostly ballistic regimes, we may compare our model's parallel velocity distribution $F(u_{\parallel x}, 0)$ shown in figure 5.8 with the displacement distributions

obtained by Nousi et. al. shown in fig. 5.9 (both distributions are comparable because in a mostly ballistic regime, the parallel velocity is proportional to the particles' displacement i.e. $\frac{\Delta \vec{r}_{\parallel}}{\delta} \overset{SP<\varepsilon<P}{\approx} v_{\parallel}$).

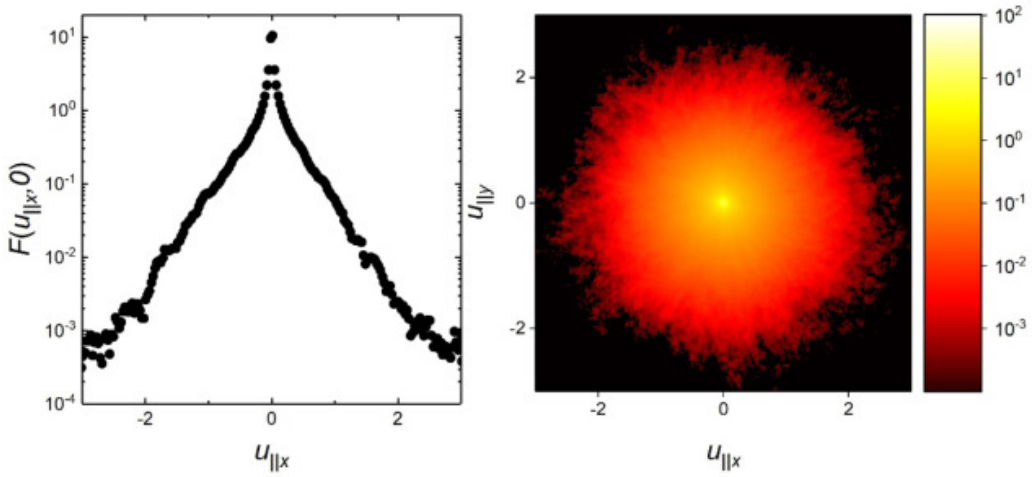

Figure 5.8: Parallel velocity histogram plots in natural units. The left figure is a cross section of the average velocity histogram $F(u_{\parallel x}, u_{\parallel y})$ for $u_{\parallel y} = 0$, i.e. $F(u_{\parallel x}, 0)$. The right figure is the superior view of a two dimensional histogram $F(u_{\parallel x}, u_{\parallel y})$ versus $(u_{\parallel x}, u_{\parallel y})$), for $q = 0.1$, $g = 10$, $\gamma = 1$ and $k = 0.04405$.

Figure 5.8 shows the numerical solutions for the velocity probability density function $F(u_{\parallel x}, u_{\parallel y})$ with $\vec{u}_{\parallel} = \left(u_{\parallel x}, u_{\parallel y}\right)$ the parallel velocity written in natural units of velocity for the parameters $q = 0.1$, $g = 10$, $\gamma = 1$ and $k = 0.04405$. The right panel shows a heat-map of both velocity axes, while the left map shows a cross section of the **PDF** at $u_{\parallel y} = 0$ i.e. $F(u_{\parallel x}, 0)$. Both panels show velocity **PDF**s whose peaks are localized at the origin ($u_{\parallel x} = 0, u_{\parallel y} = 0$).

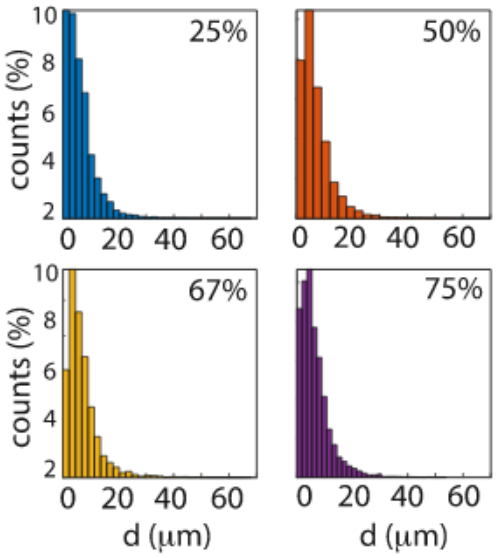

Figure 5.9: Distribution of experimental cells displacements d given in micrometers. Where 25%, 50%, 67% and 75% represent the quantity of adhering substrate (extra cellular matrix or **ECM**) used in each experiment. Fig. from [Nousi et al., 2021]

Figure 5.9 shows experimentally obtained displacements distributions in counts versus displacement d in micrometers where each of the four figures show the distribution for different quantities of the cellular substrate known as extracellular matrix **ECM**. With exception of the first figure with 25% of **ECM** concentration, all of the other distributions present peaks displaced from the origin. thus in the least, the **AOU** model should have a parameter that controls said displacement.

With evidence that cells exhibit forwards biased migration, we introduced a bias in the parallel-to-polarization axis Ornstein-Uhlenbeck dynamics, shifting the parallel velocity's average from zero to a positive value. We explain this model in the following chapters.

Chapter 6

Biased Anisotropic Ornstein-Uhlenbeck

6.1 The Model

As in the previous chapter, we consider a particle with a preferential direction of motion described by a polarization vector $\hat{p} = (cos(\theta), sin(\theta))$ whose orientation varies according to a Wiener variable

$$\theta(t + \Delta t) - \theta(t) = \int_t^{t+\Delta t} \beta(s) ds \quad , \tag{6.1}$$

where

$$\langle \beta(t) \rangle = 0 \quad \text{and} \tag{6.2}$$

$$\langle \beta(t)\beta(t') \rangle = 2k\delta(t - t') \quad , \tag{6.3}$$

with zero average and variance $2k$. The polarization introduces a spacial asymmetry, which allows the existence of two different dynamics, one for each direction. Parallel to the polarization direction, the particle moves according to a biased Ornstein-Uhlenbeck process that loses speed after every infinitesimal reorientation through the projection of the current parallel velocity onto the new polarization direction:

$$v_{\parallel}(t + \Delta t) = \left((1 - \gamma \Delta t) v_{\parallel}(t) + \int_t^{t+\Delta t} \left(\xi_{\parallel}(s) + b \right) ds \right) \left(\hat{p}(t) \cdot \hat{p}(t + \Delta t) \right) \quad ,$$

where γ is the velocity dissipation due to the cells' internal cytoskeleton dynamics, $\xi_{\parallel}$ is a Wiener variable with zero average and variance g and b is the bias constant, responsible for emulating a cell's higher probability of moving forwards in the polarization direction

instead of backwards. In short, this is the main difference between the **AOU** and the biased **AOU** model.

The second dynamics, on the orthogonal-to-polarization direction, evolves due to the same Wiener process that dictates the turnover fluctuation of the polarization (both processes are consequences of the actin-myosin fluctuations [Mogilner, 2009]). This is why we define the relation

$$\xi_{\perp}(t) = \sqrt{q}\beta(t) \quad , \tag{6.4}$$

where the perpendicular Wiener variable $\xi_{\perp}(t)$ is proportional to $\beta(t)$. The dynamics originated by $\xi_{\perp}(t)$ is then written as

$$\Delta r_{\perp} = \int_{t}^{t+\Delta t} \xi_{\perp}(s)ds \quad , \tag{6.5}$$

where $\langle \xi_{\perp} \rangle = 0$ and the variance of the Wiener variable is considered $\langle \xi_{\perp}(t)\xi_{\perp}(t') \rangle = 2qk\delta(t-t')$. The variables g, k, qk and b have the units of [length^2]/[time^3], 1/[time], [length^2]/[time] and [length]/[time$^{3/2}$] respectively.

To fully represent the perpendicular-to-polarization direction we need a second vector $\hat{n} = (sin(\theta), -cos(\theta))$ that is orthogonal to $\hat{p}(t)$, consequently $\hat{p} \cdot \hat{n} = 0$. Figure **6.1** schematically represents the dynamics of our model.

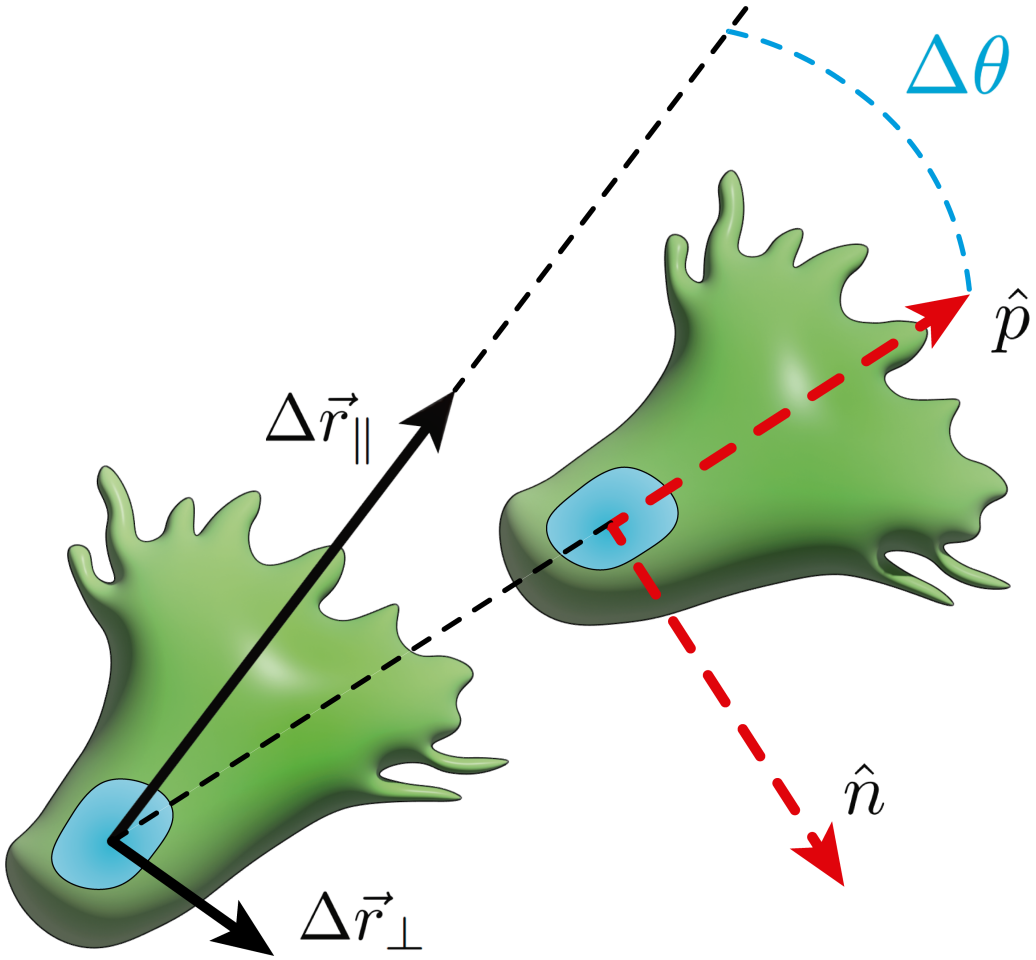

Figure 6.1: Diagrammatic representation of a particle of our model, where its total displacement is decomposed into two components, $\Delta\vec{r}_{\parallel}$ given by a biased Ornstein-Uhlenbeck process and $\Delta\vec{r}_{\perp}$, a Brownian process. The components are decomposed according to the polarity axis $\hat{p} = (cos(\theta(t)), sen(\theta(t)))$ and its perpendicular counterpart $\hat{n}$.

6.2 Analytical Solutions

Analytical Solutions for $\langle v_{\parallel}(T)\rangle$ and $\langle v_{\parallel}^2(T)\rangle$

We start by considering a particle whose parallel velocity is described during the time interval $0 \geq t \geq T$, where T may be separated by n partitions of infinitesimal size Δt. To obtain

a generalized formula for said velocity, we consider it at the first time partition $t = \Delta t$:

$$v_{\parallel}(\Delta t) = \left((1-\gamma\Delta t)v_{\parallel}(0) + \int_0^{\Delta t}\left(\xi_{\parallel}(s)+b\right)ds\right)\left(\hat{p}(0)\cdot\hat{p}(\Delta t)\right) \quad \text{and}$$

We iterate this equation over n partitions and generalize it for $n \to \infty$, such that in the limit of $\Delta t \to 0$, the product $n\Delta t$ remains finite. We then find an equation for the particle's parallel velocity

$$\begin{aligned} v_{\parallel}(n\Delta t) &= (1-\gamma\Delta t)^n v_{\parallel}(0)\prod_{i=0}^{n-1}(\hat{p}_i\cdot\hat{p}_{i+1}) \\ &\quad + \sum_{i=1}^{n}(1-\gamma\Delta t)^{n-i}\left(\int_{(i-1)\Delta t}^{i\Delta t}(\xi_{\parallel}(s)+b)ds\right)\prod_{j=i-1}^{n-1}(\hat{p}_j\cdot\hat{p}_{j+1}) \quad , \end{aligned}$$

where we used the sub-index notation $\hat{p}(n\Delta t) = \hat{p}_n$ for simplicity. Every integral with respect to the Wiener's variables are fully integrable via stochastic Ito's integral [Klebaner, 2005]. For more details, please see the appendix (B).

From equation (6.6) we take the average over noise terms and obtain

$$\langle v_{\parallel}(T)\rangle = \frac{b}{\gamma+k} + \left(v_{\parallel}(0) - \frac{b}{\gamma+k}\right)e^{-(\gamma+k)T} \quad . \tag{6.6}$$

The stationary value is taken as the limit $T \to \infty$ such that $\langle v_{\parallel}\rangle_{St} = \frac{b}{\gamma+k}$. Observe that the system exhibits a non zero average velocity. The non-biased **AOU** model presents $\langle v_{\parallel}\rangle = 0$ [de Almeida et al., 2022].

Following the same procedure to obtain 6.6, we found the squared parallel velocity, as follows

$$\begin{aligned} \langle v_{\parallel}^2(T)\rangle &= e^{-(\gamma+k)T}\left[-\frac{2b^2}{(\gamma+k)^2} + \frac{2bv_{\parallel}(0)}{\gamma+k}\right] \\ &\quad + e^{-2(\gamma+k)T}\left[v_{\parallel}^2(0) + \frac{b^2}{(\gamma+k)^2}\right] \\ &\quad + e^{-2(\gamma+k)T}\left[-\frac{g}{2(\gamma+k)} - \frac{2bv_{\parallel}(0)}{\gamma+k}\right] \\ &\quad + \frac{g}{2(\gamma+k)} + \frac{b^2}{(\gamma+k)^2} \quad , \end{aligned} \tag{6.7}$$

and hence we obtain the second moment for the parallel velocity, as

$$\langle v_{\parallel}^2(T)\rangle - \langle v_{\parallel}(T)\rangle^2 = \frac{g}{2(\gamma+k)} - \frac{g}{2(\gamma+k)}e^{-2(\gamma+k)T} \quad , \tag{6.8}$$

what shows that the dispersion around $\langle v_\parallel(T)\rangle$ behaves the same as in the non biased AOU, that is

$$\langle v_\parallel^2\rangle_{St} - \langle v_\parallel\rangle_{St}^2 = \frac{g}{2(\gamma+k)} \quad . \tag{6.9}$$

Mean Square Displacement

We then proceed to obtain a general formula for the particle's position $\vec{r}(t)$, by considering that $\vec{v}_\parallel(t)\Delta t = \big[\vec{r}_\parallel\big((n+1)\Delta t\big) - \vec{r}_\parallel\big(n\Delta t\big)\big]$. We find

$$\begin{aligned}
\vec{r_\parallel}\big((N+1)\Delta t\big) - \vec{r}_\parallel(0) &= u_\parallel(0)\Delta t\sum_{n=0}^{N}(1-\gamma\Delta t)^n\prod_{j=0}^{n-1}(\hat{p}_j\cdot\hat{p}_{j+1})\hat{p}_n \\
&+\frac{b}{\gamma+k}\,\Delta t\sum_{n=0}^{N}(1-\gamma\Delta t)^n\prod_{j=0}^{n-1}(\hat{p}_j\cdot\hat{p}_{j+1})\hat{p}_n \\
&+b\Delta t^2\sum_{n=0}^{N}\sum_{i=0}^{n-1}(1-\gamma\Delta t)^{n-1-i}\prod_{j=i}^{n-1}(\hat{p}_j\cdot\hat{p}_{j+1})\hat{p}_n \\
&+\Delta t\sum_{n=0}^{N}\sum_{i=0}^{n-1}(1-\gamma\Delta t)^{n-1-i}\prod_{j=i}^{n-1}(\hat{p}_j\cdot\hat{p}_{j+1})\int_{i\Delta t}^{(i+1)\Delta t}\xi_\parallel(s)ds\;\hat{p}_n \\
&+\Delta t\;\sum_{n=0}^{N}\int_{n\Delta t}^{(n+1)\Delta t}[(n+1)\Delta t - s]\xi_\parallel(s)ds\,\hat{p}_n \quad .
\end{aligned} \tag{6.10}$$

Equation (6.10) represents only the parallel-to-polarization displacement. The complete displacement is obtained by adding the perpendicular displacement $\Delta\vec{r}_\perp(t) = \int \xi_\perp(s)\,ds\;\hat{n}(t)$ at every time step. The final position depends on integrals of stochastic variables, whose averages are always zero because the polarity direction distribution (θ distribution) is isotropic.

The mean square displacement (MSD), is obtained by squaring equation (6.10) and taking its average, a long, but straightforward procedure found on appendix (C). The result

is

$$
\begin{aligned}
MSD \;=\; & \frac{g\,\Delta T}{(\gamma+k)(\gamma+2k)} + 2qk\Delta T \\
& - \frac{g}{(\gamma+k)(\gamma+2k)^2}\left[1 - e^{-(\gamma+2k)\Delta T}\right] \\
& - \frac{2b^2}{\gamma(\gamma+k)^2}\left[\frac{1 - e^{-2(\gamma+k)\Delta T}}{2(\gamma+k)}\right] \\
& + \frac{2b^2}{\gamma k(\gamma+k)}\left[\frac{1 - e^{-(\gamma+2k)\Delta T}}{\gamma+2k}\right] \\
& + \frac{2b^2}{k(\gamma+k)^2}\left[\Delta T - \frac{1 - e^{-k\Delta T}}{k}\right] \\
& - \frac{2b^2}{k(\gamma+k)^2}\left[\frac{1 - e^{-(\gamma+k)\Delta T}}{\gamma+k}\right] \quad .
\end{aligned}
\tag{6.11}
$$

We have numerically solved this model equations and the result agrees with the theoretical prediction. Also, for adequate parameter values, the **MSD** equation has the same shape as the modified Fürth equation 5.21 introduced by [Fortuna et al., 2020], presenting all three migration regimes shown by real cells, indicating that we may be able to define a set of effective parameters $S_{\text{eff.}}$, $P_{\text{eff.}}$, $D_{\text{eff.}}$ and $R_{\text{eff.}}$ that map onto the Biased Ornstein-Uhlenbeck model's parameters g, q, γ, b and k.

Since equation 6.11 is composed of more than one exponential term with different decay rates, however, the mapping of g, q, γ, b and k onto the effective Fürth variables $S_{\text{eff.}}$, $P_{\text{eff.}}$, $D_{\text{eff.}}$ and $R_{\text{eff.}}$, becomes a hard task which has not been completed. Without the aforementioned mapping, the definition of proper natural units for the system is not yet possible. Consequently, our future work will focus on these tasks. In what follows we show figures and calculations with the standard units of time and length instead of the dimensionless ones introduced in chapter 5.

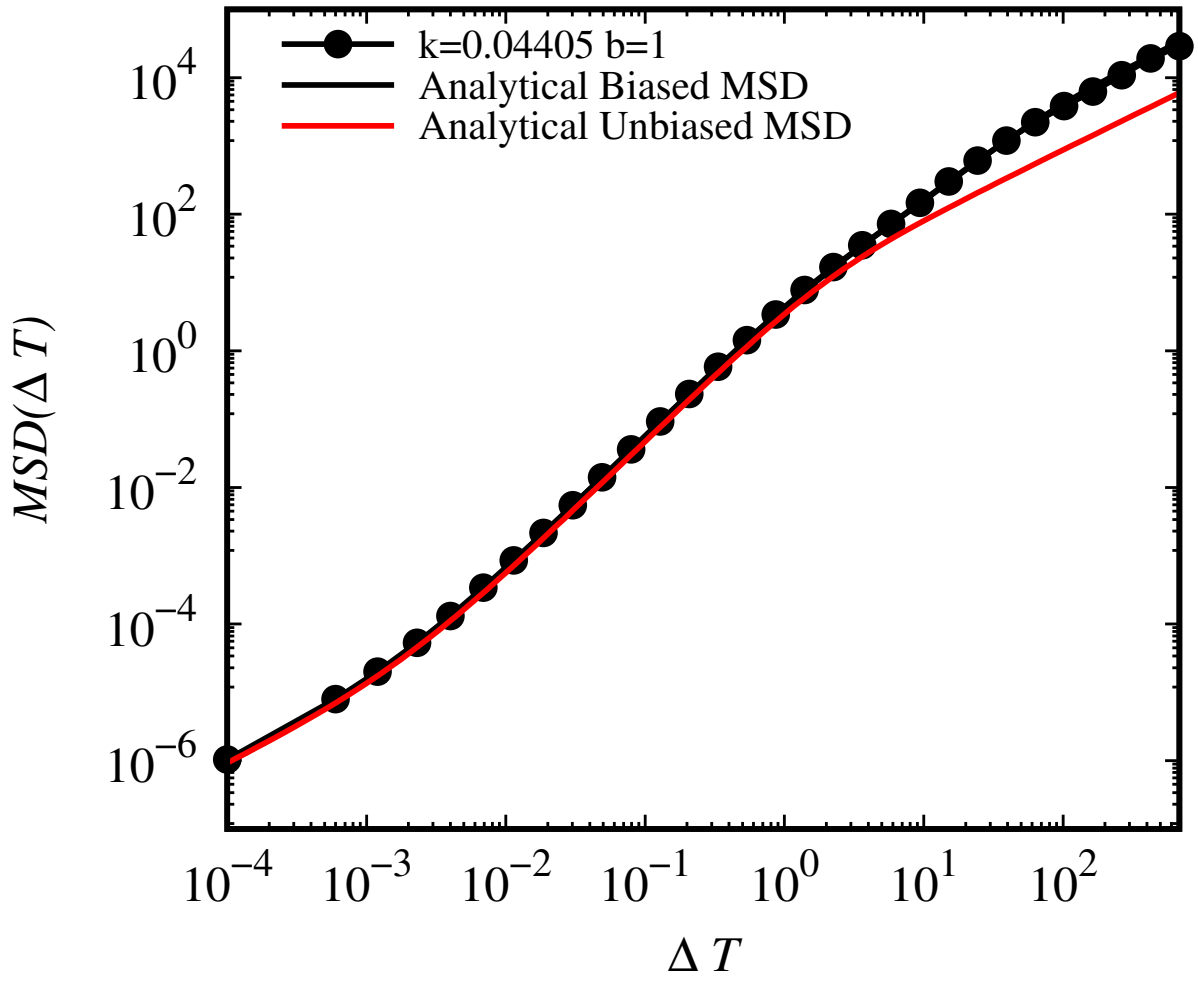

Figure 6.2: Comparison between the **mean square displacement** (MSD) measured from the numerical solution of our model for 10 particles and with constants $g = 10$, $q = 0.1$, $\gamma = 1$, $k = 0.04405$ and $b = 1$ (black dots) with the analytical solutions of our current biased model (black line) and our previous model [de Almeida et al., 2022] (red line), whose velocity PDF did not agree with experimental results.

Figure 6.2 shows the three-regime behavior: the movement is diffusive for $\Delta T \to 0$, mostly ballistic or anomalous diffusive for $0 < \Delta T < \infty$ and diffusive for $\Delta T \to \infty$, as observed in real cells [Thomas et al., 2020]. In comparison to the **AOU** model, the bias extends the particle's persistence. Observe that the diffusive motion when $\Delta T \to 0$ precludes the definition of instant velocity, the same for the non-biased case.

Parallel Velocity Probability Density Function

Since this model has a non zero average for the stationary parallel velocity, we may conclude that this model produces a particle more prone to move forwards than backwards on its polarization direction. However, these results are not enough to fully characterize cell motion. Cell migration experiments also measure probability distributions. Our previous model [de Almeida et al., 2022] presents a parallel velocity probability density function (**PDF**) peaked at zero, a result that does not agree with cell migration experiments.

In this section we analytically obtain the velocity probability density function. We assume an infinitesimal variation in the **PDF**, denoted as $\Delta\rho\big(v_\parallel(T)\big) = \rho\big(v_\parallel(T+\Delta t)\big) - \rho\big(v_\parallel(T)\big)$ at time $T = n\Delta t$, which may be partitioned in n infinitesimal time intervals Δt. Then we expand $\rho\big(v_\parallel(T+\Delta t)\big)$ in a Taylor series where $v_\parallel$ is given by equation (6.6). Because we only consider an infinitesimal variation in the **PDF** and consequently on $v_\parallel$, the higher than second order terms can be neglected.

Taking $\Delta t \to 0$, we obtain a differential equation for the **PDF**, known as the Fokker-Planck equation

$$\frac{\partial P(v_\parallel, T)}{\partial T} = [\gamma + k]\frac{\partial}{\partial v_\parallel}\left(P(v_\parallel, T)\left(v_\parallel - \frac{b}{\gamma + k}\right)\right) + \frac{g}{2}\frac{\partial^2 P(v_\parallel, T)}{\partial v_\parallel^2} \quad ,$$

where a possible stationary solution $\frac{\partial P(v_\parallel, t)}{\partial t} = 0$ is a gaussian function, written as

$$P(v_\parallel) = \sqrt{\frac{\gamma + k}{\pi\, g}}\exp\left(-[\gamma + k]\frac{\left(v_\parallel - \frac{b}{\gamma+k}\right)^2}{g}\right) \quad , \tag{6.12}$$

a result that implies that in the stationary limit, the velocity probability density function becomes a gaussian centered at $v_\parallel = \frac{b}{\gamma+k}$. Hence, the particle has the highest probability of moving with velocity $v_\parallel = \frac{b}{\gamma+k}$ along the polarization direction, as is observed for single cell migration, where a cell maintains its actin polymerization at its frontal region. A full explanation in how to obtain the Fokker-Planck equation (6.12) can be found in appendix (A). If we compare the analytical results and the numerical ones we see that they agree, as shown in Fig. 6.3.

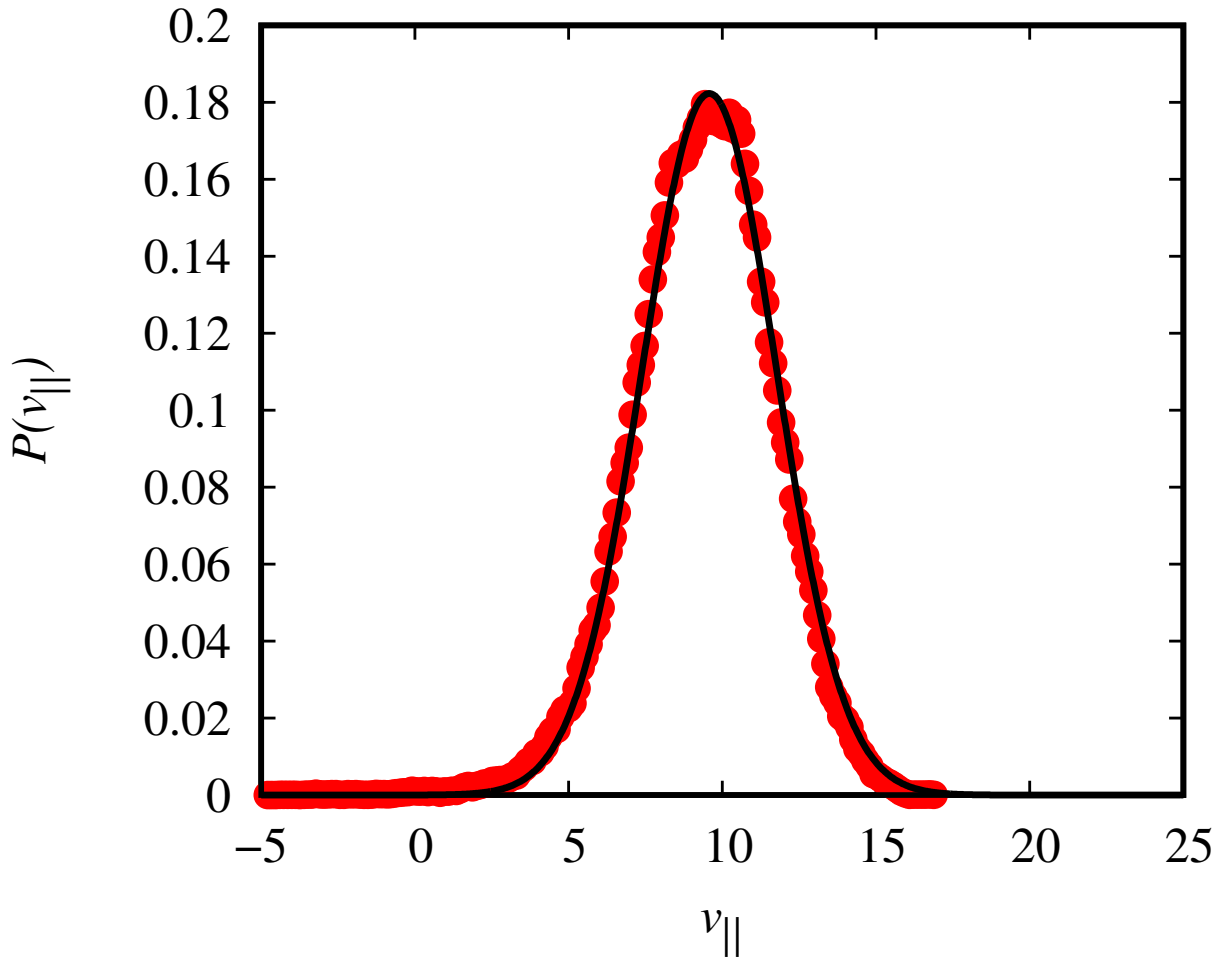

Figure 6.3: Comparison between the analytical (black line) parallel velocity probability density function with the numerical results (red dots), for 20 particles and with constants $g = 10$, $q = 0.1$, $\gamma = 1$, $k = 0.04405$ and $b = 10$.

In figure 6.3 we see indeed that the probability density function for the parallel-to-polarity velocity has a non zero average and assumes a Gaussian form similar to experimental results. The Gaussian form in our model is due to the uncorrelated impulses originated from the Wiener variable.

We also measured the velocity **PDF** along the velocity x and y axes, forming an axially symmetrical velocity distribution, easily seen that is not centered on zero

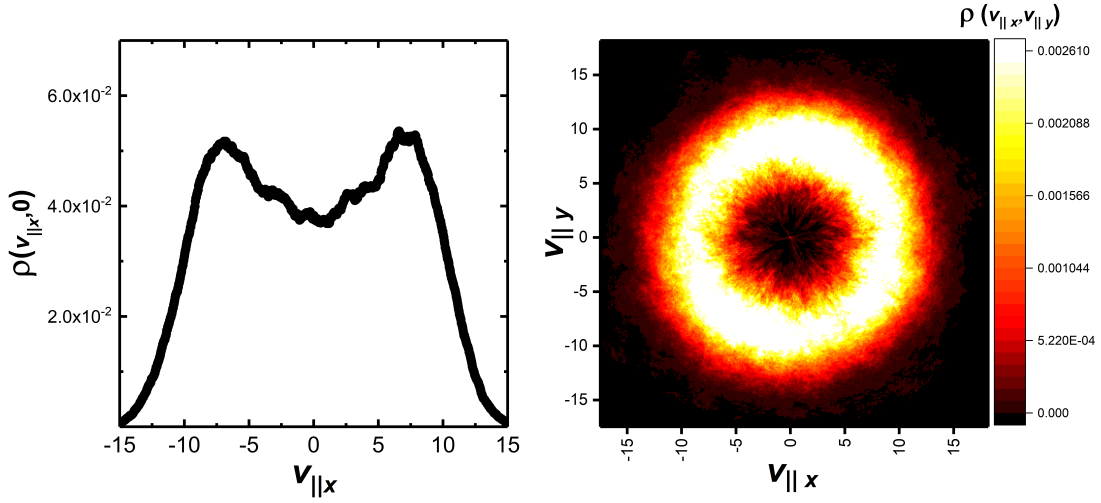

Figure 6.4: Parallel velocity probability density function obtained from the numerical solution of our model for 10 particles and with constants $g = 10$, $q = 0.1$, $\gamma = 1$, $k = 0.04405$ and $b = 10$. Left: cross section of the parallel velocity's x axis versus the velocity probability density function (VPDF). Right: upper view of the VPDF where the coloring present the probability of each point in the $v_{\parallel x}$ vs $v_{\parallel y}$.

In experiments, the parallel and perpendicular displacements may not always be separated. In these cases, displacements are measured together and the ill-definition for instantaneous velocity has its effect. That can be by-passed by choosing an adequate time interval for estimating the mean velocities as $\vec{v}_{\text{avg}} = \frac{\vec{r}(t+\varepsilon)-\vec{r}(T)}{\varepsilon}$. This is showcased in figure 6.5, as we plotted six heat-maps of mean velocity distributions for varying values of ε.

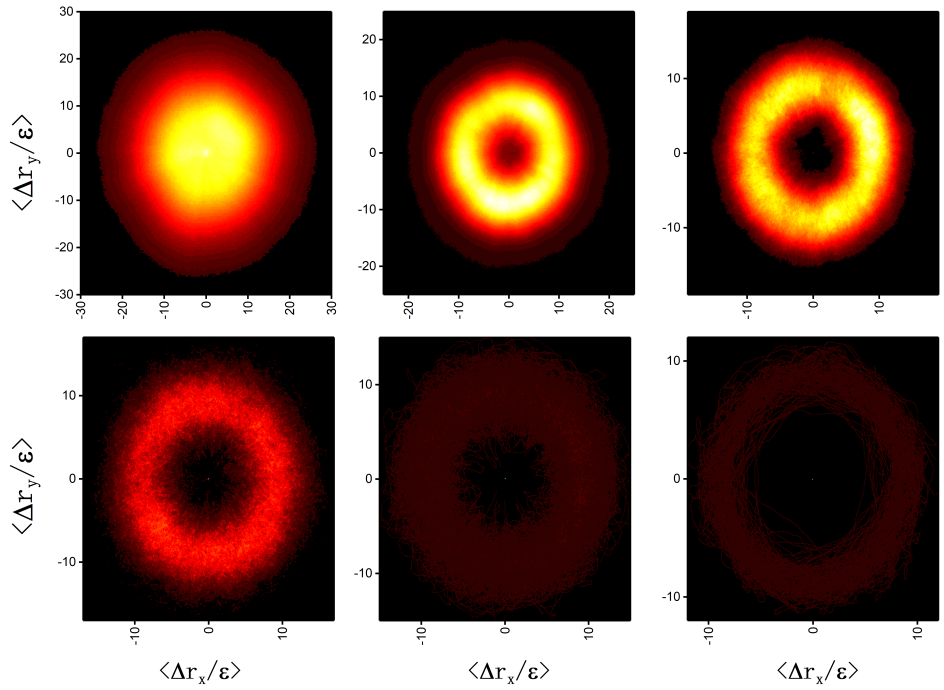

Figure 6.5: Upper view of the mean velocity probability density function obtained from the numerical solutions, for varying ε values ($\varepsilon = 0.0001,\ 0.001,\ 0.01,\ 0.1,\ 1$ and 10 from left to right and top to bottom). The data considers 10 particles and parameter values $g = 10$, $q = 0.1$, $\gamma = 1$, $k = 0.04405$ and $b = 10$. The brighter the color, the greater the number of occurrences.

We see in figure 6.5 that the time interval in which the average velocity is measured changes the velocity probability density function. It is also visible that when $\varepsilon = 0.01$ computational units, the distribution is mostly similar to the parallel-to-polarization distribution, indicating an approximately ideal time interval of measurement for the mean velocities.

An ideal experimental procedure for robust velocity measurements is to film the trajectories of some cells, obtain its mean square displacement and through the analysis of the exponents of the mean square displacement curve, find the ideal time interval (when the trajectory is mostly ballistic) [Fortuna et al., 2020, Thomas et al., 2020].

Velocity Auto-Correlation Function

Similar to what is found in chapter 5, the biased **AOU** model also exhibits a exponentially decaying velocity auto-correlation function. Here, we also define an instantaneous velocity as

$$\begin{aligned} \vec{v}(T) &= \lim_{\varepsilon\to 0}\frac{\Delta\vec{r}(T)}{\varepsilon} \\ &= \lim_{\varepsilon\to 0}\frac{\Delta\vec{r}_{\parallel}(T)}{\varepsilon}+\frac{\Delta\vec{r}_{\perp}(T)}{\varepsilon} \\ &= \vec{v}_{\parallel}(T)+\lim_{\varepsilon\to 0}\frac{\Delta\vec{r}_{\perp}(T)}{\varepsilon} \quad , \end{aligned} \tag{6.13}$$

a value that diverges as $\varepsilon \to 0$ due to the diffusive nature of the particle's perpendicular dynamics i.e. $\lim_{\varepsilon\to 0}\frac{\Delta\vec{r}_{\perp}}{\varepsilon} \sim \frac{\sqrt{\sqrt{\varepsilon}}}{\varepsilon} \to \infty$. This does not happen for the **VACF** solution, as the perpendicular displacements do not correlate with each other (the perpendicular displacements are both Wiener processes at different instants of time)

$$\begin{aligned} VACF(\Delta T) &\equiv \left\langle \left(\vec{v}_{\parallel}(T)+\lim_{\varepsilon\to 0}\frac{\Delta\vec{r}_{\perp}(T)}{\varepsilon}\right)\cdot\left(\vec{v}_{\parallel}(T+\Delta T)+\lim_{\varepsilon\to 0}\frac{\Delta\vec{r}_{\perp}(T+\Delta T)}{\varepsilon}\right)\right\rangle \\ &\equiv \left\langle \left(\vec{v}_{\parallel}(T)\right)\cdot\left(\vec{v}_{\parallel}(T+\Delta T)\right)\right\rangle \quad . \end{aligned} \tag{6.14}$$

From the parallel velocity equation for the biased **AOU** model for an arbitrary time T and equation 6.14, we find

$$VACF(\Delta T) = \frac{g}{2(\gamma+k)}e^{-(\gamma+2k)\Delta T}+\frac{b^2}{(\gamma+k)^2}e^{-k\Delta T} \quad , \tag{6.15}$$

which is an expected result since for $\Delta T \to 0$, the correlation is maximum and equal to the average square velocity $VACF(\Delta T) = \langle \vec{v}_{\parallel}(T)\cdot\vec{v}_{\parallel}(T+\Delta T)\rangle \overset{\Delta T\to 0}{=} \langle v_{\parallel}^2\rangle$ and when $\Delta T \to \infty$, the correlation becomes zero, as the particle forgets its past velocities.

Mean Velocity Auto-Correlation Function $\Psi(\varepsilon, \Delta T)$

In the previous section, we have shown the parallel velocity auto-correlation solution is at its maximum when the observation time interval ΔT goes to zero, however experimental measurements present finite precision, meaning that when the perpendicular displacement

is much larger than the parallel displacement, the measurement may keep information only from the perpendicular component. That is

$$\overline{\vec{v}(\varepsilon,T)} = \frac{\Delta\vec{r}_{\parallel}}{\varepsilon} + \frac{\Delta\vec{r}_{\perp}}{\varepsilon} \sim \frac{\Delta\vec{r}_{\perp}}{\varepsilon} \quad . \tag{6.16}$$

The finite precision effect is more important for smaller ε, like in the **AOU** model. Using such measurements to obtain the **MVACF** implies that only the non-correlated, perpendicular displacements are taken into account, thus decreasesing the auto-correlation for small time-intervals $\Delta\varepsilon$.

However, if ε was exactly zero (infinite precision measurements), all of the information regarding both $\vec{v}_{\parallel} = \frac{\Delta\vec{r}_{\parallel}}{\varepsilon}$ and $\frac{\Delta\vec{r}_{\perp}}{\varepsilon}$ would be known, meaning that when the correlations were calculated, the only remaining value would be that of $\langle\vec{v}_{\parallel}(T)\cdot\vec{v}_{\parallel}(T+\Delta T)\rangle$ as the self-correlation $\langle\Delta\vec{r}_{\perp}(T)\cdot\vec{r}_{\perp}(T+\Delta T)\rangle$ is zero. The consequence is that the theoretical value for the **MVACF** may be different when compared to experiments.

To obtain a mean velocity auto-correlation function, we considered two average velocities separated by a time interval ΔT given as $\overline{\vec{v}(\varepsilon,T)} = \frac{\vec{r}(T+\varepsilon)-\vec{r}(T)}{\varepsilon}$ and $\overline{\vec{v}(\varepsilon,T+\Delta T)} = \frac{\vec{r}(T+\Delta T+\varepsilon)-\vec{r}(T+\Delta T)}{\varepsilon}$ and using equation (6.10) found their respective values. Then we found their correlation function by calculating the average dot product $\psi(\varepsilon,\Delta T) = \langle\overline{\vec{v}(\varepsilon,T)}\cdot\overline{\vec{v}(\varepsilon,T+\Delta T)}\rangle$, which is the mean velocity auto-correlation function.

We got

$$\begin{aligned}\psi(\varepsilon,\Delta T) &= \frac{g}{2(\gamma+k)\varepsilon^2}\left(\frac{e^{-(\gamma+2k)\Delta T}}{(\gamma+2k)^2}(1-e^{-(\gamma+2k)\varepsilon})(e^{(\gamma+2k)\varepsilon}-1)\right)\\ &\quad+\frac{b^2}{\varepsilon^2(\gamma+k)^2}\left(\frac{e^{-k\Delta T}}{k^2}(1-e^{-k\varepsilon})(e^{k\varepsilon}-1)\right) \quad ,\end{aligned} \tag{6.17}$$

which makes sense as we assume the limit $\varepsilon \to 0$, as

$$\begin{aligned}\psi(\varepsilon\to 0,\Delta T) &= \frac{g}{2(\gamma+k)\varepsilon^2}\left(\frac{e^{-(\gamma+2k)\Delta T}}{(\gamma+2k)^2}\big(1-(1-(\gamma+2k)\varepsilon)\big)\big((1+(\gamma+2k)\varepsilon)-1\big)\right)\\ &\quad+\frac{b^2}{\varepsilon^2(\gamma+k)^2}\left(\frac{e^{-k\Delta T}}{k^2}\big(1-(1-k\varepsilon)\big)\big((1+k\varepsilon)-1\big)\right) \qquad (6.18)\\ &= \frac{g}{2(\gamma+k)}e^{-(\gamma+2k)\Delta T}+\frac{b^2}{(\gamma+k)^2}e^{-k\Delta T} \quad , \qquad (6.19)\end{aligned}$$

which is precisely the **VACF** solution, when the perpendicular displacement component is disregarded. We also note that there is no problem concerning eventual values of $e^{k\varepsilon}$ and $e^{(\gamma+2k)\varepsilon}$ for $\varepsilon \to \infty$.

If $\Delta T < \varepsilon$ we artificially introduce a correlation originated from overlapping average velocities intervals, meaning that T must be always bigger than ε, as we concluded from chapter 5 section 5.2. Thus if $\varepsilon \to \infty$ then $\Delta T \to \infty$ which makes $\psi(\varepsilon, \Delta T) \to 0$.

To emulate the lack of instrumental precision in the numerical solutions, we forcibly reduced the significant figures for the particle's position, which in turn produced **MVACF** solutions with lower correlations for small time intervals ΔT. The numerical solutions were

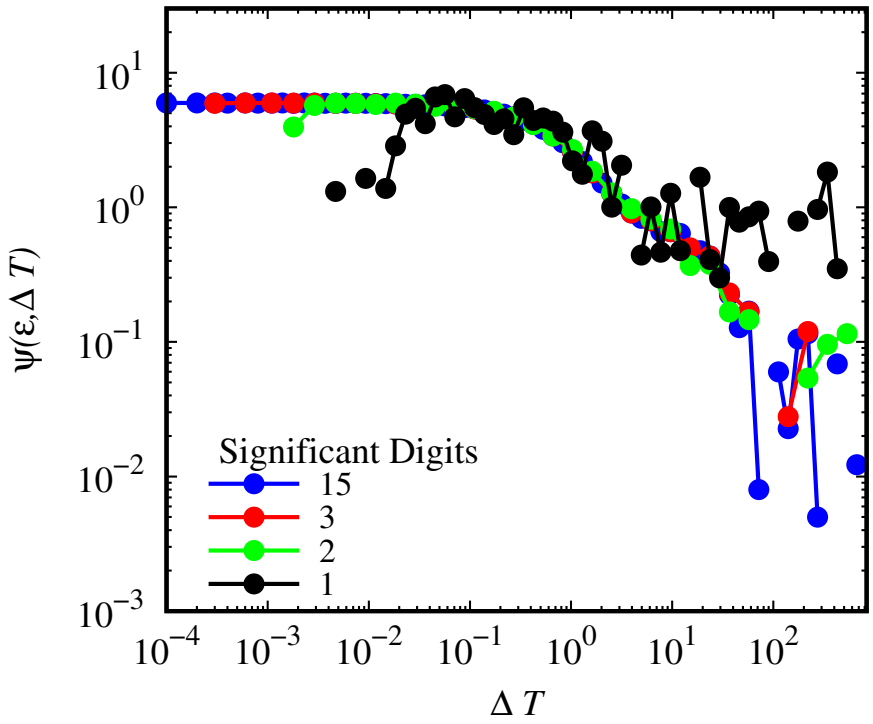

Figure 6.6: Log-log plot of $\psi(\varepsilon, \Delta T)$ versus ΔT considering the numerical solution of our model for 10 particles and with constants $g = 10$, $q = 0.1$, $\gamma = 1$, $k = 0.04405$ and $b = 1$ with. Where significant places were reduced as a way to reproduce a reduction of experimental precision.

As expected, by artificially reducing the significant digits in calculating MVACF we successfully reproduced experimental velocity auto-correlation graphs [Thomas et al., 2020].

Also note that the results in figure 6.6 are very similar to the **MVACF** results from chapter 5 as expected from the analytical results of equations (6.19) and (6.15).

Chapter 7

Conclusion and Perspectives

In this work we show that to model single cell dynamics focusing on its kinetics properties we must consider both asymmetry in the dynamics equations and a bias in the stochastic term responsible to provide kinetic energy to the parallel-to-polarization degree of freedom. In this way, we could explain the short time interval diffusive regime and still consider a Langevin-like dynamics for the parallel velocity. The result is a properly described kinetics, that evinces a century-old problem in measuring single cell speed, that yields theoretical predictions for **MSD**, **VACF**, and velocity density functions that describe well the experimental findings.

For the non-biased model, it was possible to obtain natural units to the system based on the theoretical parameters. These natural units provided a straightforward way to quantitatively compare theory, simulations, and experiments. For example, simulation units as Monte Carlo Steps and the lattice constants may be translated into seconds and micrometers. The biased model revealed to be more complicated and requires further work to understand the limits for the theory parameters where natural units of length and time may be adequately defined. The resulting plots for **MSD** and **VACF**, however, show the same behavior as the experiments and the non-biased model, indicating that at least approximately these natural units may be defined.

Adding anisotropy to both models is important to separate the dynamics and by introducing the Wiener dynamics for the perpendicular displacement we could explain the short-time interval diffusive regime. For point particles, that could be a conceptual problem, regarding on how to assign Newton's law to a particle for which it is not possible to

define velocity. However, cells are not point particles nor they are rigid body. The lamellipodium in mensechymal migrating cells are constantly protruding and receding at many different time and size scales. At a given moment more than one membrane fluctuation may occur at different locations of the lamellipodium. The cell's center of mass will change due to a sum of these fluctuations. Furthermore, there is a favored direction in the lamellipodium protrusions due to an organized mesh of fibers that carry the necessary molecules to the cell front. Directions perpendicular to the preferred orientation of these fibers are less favored and it may be a sound hypothesis that they sum up as a Gaussian source of stochastic displacements. As a by-product, the model we proposed basis a robust procedure for experimental cell speed measurement as well as its correlation and probability density functions, by pointing to the important role played by the choice of the adequate time intervals to estimate speed and velocity.

A further remark regards to chemotaxis, an important process in cell migration, present in many *in-vivo* phenomena. A cell is guided by chemical gradients, but not in the same way as a charged particle is attracted or repelled by an electric field. The cell is not pulled by the chemical gradient, in the sense that the cell machinery is responsible for the cell motion with or without a chemical field. A cell always migrate due to its internal machinery and in the direction that its lamellipodium is pulling. Due to the lamellipodium dynamics, in the absence of a chemical field, the cell movement changes direction with a a persistence that is characteristic of the experimental set-up. When a chemical gradient is present, the lamellipodium direction changes are affected, such that the motion direction persistence may be infinite. Increasing the chemical gradient, for example, may not change the cell speed, this is determined by the internal cell machinery. However, the cell velocity in the direction of the chemical gradient is enhanced, due to the increased directional persistence.

Forcing an alignment of cell polarization with the chemical gradient in the non-biased **AOU** model cannot increase the average cell velocity in this direction since its average is zero. On the other hand, in the biased **AOU** model may explain the cell kinetics under the action of a chemical gradient. This is part of my future work.

Finally, the Fokker Planck equation for migrating cells, presented as a way to calculated velocity probability density function, opens the possibility of describing cells dynamics

as probability equations and extending it to a system made of many cells, where the interaction terms between each cell may be added. Naturally in this case, we must focus on numerical solutions. This will be contemplated in future works.

Bibliography

[Abercrombie et al., 1970] Abercrombie, M., Heaysman, J. E., and Pegrum, S. M. (1970). The locomotion of fibroblasts in culture i. movements of the leading edge. *Experimental Cell Research*, 59:393–398.

[Albert and Schwarz, 2014] Albert, P. J. and Schwarz, U. S. (2014). Dynamics of cell shape and forces on micropatterned substrates predicted by a cellular potts model. *Biophysical Journal*, 106:2340–2352.

[Bugyi and Kellermayer, 2020] Bugyi, B. and Kellermayer, M. (2020). The discovery of actin: "to see what everyone else has seen, and to think what nobody has thought"*. *Journal of Muscle Research and Cell Motility*, 41:3–9.

[Callan-Jones and Voituriez, 2016] Callan-Jones, A. C. and Voituriez, R. (2016). Actin flows in cell migration: From locomotion and polarity to trajectories. *Current Opinion in Cell Biology*, 38:12–17.

[Camley et al., 2013] Camley, B. A., Zhao, Y., Li, B., Levine, H., and Rappel, W. J. (2013). Periodic migration in a physical model of cells on micropatterns. *Physical Review Letters*, 111:158102.

[de Almeida et al., 2022] de Almeida, R. M., Giardini, G. S., Vainstein, M., Glazier, J. A., and Thomas, G. L. (2022). Exact solution for the anisotropic ornstein–uhlenbeck process. *Physica A: Statistical Mechanics and its Applications*, 587:126526.

[Dieterich et al., 2008] Dieterich, P., Klages, R., Preuss, R., and Schwab, A. (2008). Anomalous dynamics of cell migration. *Proceedings of the National Academy of Sciences of the United States of America*, 105:459–463.

[Fortuna et al., 2020] Fortuna, I., Perrone, G. C., Krug, M. S., Susin, E., Belmonte, J. M., Thomas, G. L., Glazier, J. A., and de Almeida, R. M. (2020). Compucell3d simulations reproduce mesenchymal cell migration on flat substrates. *Biophysical Journal*, 118:2801–2815.

[Fürth, 1920] Fürth, R. (1920). Die brownsche bewegung bei berücksichtigung einer persistenz der bewegungsrichtung. mit anwendungen auf die bewegung lebender infusorien. *Zeitschrift für Physik*, 2:244–256.

[Genthon, 2020] Genthon, A. (2020). The concept of velocity in the history of brownian motion – from physics to mathematics and vice versa. *European Physical Journal H*, 45:49–105.

[Goychuk et al., 2018] Goychuk, A., Brückner, D. B., Holle, A. W., Spatz, J. P., Broedersz, C. P., and Frey, E. (2018). Morphology and motility of cells on soft substrates. *arXiv*.

[Graner and Glazier, 1992] Graner, F. and Glazier, J. A. (1992). Simulation of biological cell sorting using a two-dimensional extended potts model. *Physical Review Letters*, 69:2013–2016.

[Hall, 1998] Hall, A. (1998). Rho gtpases and the actin cytoskeleton. *Science*, 279:509–514.

[Klebaner, 2005] Klebaner, F. C. (2005). *Introduction to Stochastic Calculus with Applications*. PUBLISHED BY IMPERIAL COLLEGE PRESS AND DISTRIBUTED BY WORLD SCIENTIFIC PUBLISHING CO.

[Lemons and Gythiel, 1997] Lemons, D. S. and Gythiel, A. (1997). Paul langevin's 1908 paper "on the theory of brownian motion" ["sur la théorie du mouvement brownien," c. r. acad. sci. (paris) 146 , 530–533 (1908)]. *American Journal of Physics*, 65:1079–1081.

[Maiuri et al., 2015] Maiuri, P., Rupprecht, J. F., Wieser, S., Ruprecht, V., Bénichou, O., Carpi, N., Coppey, M., Beco, S. D., Gov, N., Heisenberg, C. P., Crespo, C. L., Lautenschlaeger, F., Berre, M. L., Lennon-Dumenil, A. M., Raab, M., Thiam, H. R., Piel, M., Sixt, M., and Voituriez, R. (2015). Actin flows mediate a universal coupling between cell speed and cell persistence. *Cell*, 161:374–386.

[Marée et al., 2012] Marée, A. F., Grieneisen, V. A., and Edelstein-Keshet, L. (2012). How cells integrate complex stimuli: The effect of feedback from phosphoinositides and cell shape on cell polarization and motility. *PLoS Computational Biology*, 8:e1002402.

[Marée et al., 2006] Marée, A. F., Jilkine, A., Dawes, A., Grieneisen, V. A., and Edelstein-Keshet, L. (2006). Polarization and movement of keratocytes: A multiscale modelling approach. *Bulletin of Mathematical Biology*, 68:1169–1211.

[Mogilner, 2009] Mogilner, A. (2009). Mathematics of cell motility: Have we got its number? *Journal of Mathematical Biology*, 58:105–134.

[Niederman and Pollard, 1975] Niederman, R. and Pollard, T. D. (1975). Human platelet myosin: Ii. in vitro assembly and structure of myosin filaments. *Journal of Cell Biology*, 67:72–92.

[Nousi et al., 2021] Nousi, A., Søgaard, M. T., Audoin, M., and Jauffred, L. (2021). Single-cell tracking reveals super-spreading brain cancer cells with high persistence. *Biochemistry and Biophysics Reports*, 28:101120.

[Pollard, 2017] Pollard, T. D. (2017). Tribute to fumio oosawa the pioneer in actin biophysics. *Cytoskeleton (Hoboken, N.J.)*, 74:446–449.

[Pollard and Korn, 1973] Pollard, T. D. and Korn, E. D. (1973). Acanthamoeba myosin. *Journal of Biological Chemistry*, 248:4682–4690.

[Pollard et al., 1974] Pollard, T. D., Weihing, R. R., and Adelman, M. R. (1974). Actin and myosin and cell movemen. *Critical Reviews in Biochemistry and Molecular Biology*, 2:1–65.

[Potdar et al., 2009] Potdar, A. A., Lu, J., Jeon, J., Weaver, A. M., and Cummings, P. T. (2009). Bimodal analysis of mammary epithelial cell migration in two dimensions. *Annals of Biomedical Engineering*, 37:230–245.

[Schwartz, 2013] Schwartz, J. L. (2013). How cells crawl — nih intramural research program.

[Selmeczi et al., 2005] Selmeczi, D., Mosler, S., Hagedorn, P. H., Larsen, N. B., and Flyvbjerg, H. (2005). Cell motility as persistent random motion: Theories from experiments. *Biophysical Journal*, 89:912–931.

[Shao et al., 2010] Shao, D., Rappel, W. J., and Levine, H. (2010). Computational model for cell morphodynamics. *Physical Review Letters*, 105:108104.

[Stossel, 1990] Stossel, T. P. (1990). How cells crawl. *American Scientist*, 78(5):408–423.

[Szabó et al., 2006] Szabó, B., Szöllösi, G. J., Gönci, B., Jurányi, Z., Selmeczi, D., and Vicsek, T. (2006). Phase transition in the collective migration of tissue cells: Experiment and model. *Physical Review E - Statistical, Nonlinear, and Soft Matter Physics*, 74:061908.

[Takagi et al., 2008] Takagi, H., Sato, M. J., Yanagida, T., and Ueda, M. (2008). Functional analysis of spontaneous cell movement under different physiological conditions. *PLoS ONE*, 3:e2648.

[Thomas et al., 2020] Thomas, G. L., Fortuna, I., Perrone, G. C., Glazier, J. A., Belmonte, J. M., and de Almeida, R. M. (2020). Parameterizing cell movement when the instantaneous cell migration velocity is ill-defined. *Physica A: Statistical Mechanics and its Applications*, 550:124493.

[Vicsek et al., 1995] Vicsek, T., Czirk, A., Ben-Jacob, E., Cohen, I., and Shochet, O. (1995). Novel type of phase transition in a system of self-driven particles. *Physical Review Letters*, 75:1226–1229.

[Wu et al., 2014] Wu, P. H., Giri, A., Sun, S. X., and Wirtz, D. (2014). Three-dimensional cell migration does not follow a random walk. *Proceedings of the National Academy of Sciences of the United States of America*, 111:3949–3954.

[Ziebert and Aranson, 2013] Ziebert, F. and Aranson, I. S. (2013). Effects of adhesion dynamics and substrate compliance on the shape and motility of crawling cells. *PLoS ONE*, 8:64511.

Appendix A

Parallel Velocity Density of Probability Function

Considering the parallel velocity equation 6.4 at time $t = n\Delta t$, with n being an arbitrary integer

$$v_{\parallel}(t+\Delta t) = \left[(1-\gamma\Delta t)v_{\parallel}(t) + \int_t^{t+\Delta t}(\xi_{\parallel}+b)ds\right]\hat{p}_n\cdot\hat{p}_{n+1} \quad , \tag{A.1}$$

we may write a probability density function $\rho(v_{\parallel})$ as

$$\rho(v_{\parallel}(t+\Delta t)) = \rho\left(\left[(1-\gamma\Delta t)v_{\parallel}(t) + \int_t^{t+\Delta t}(\xi_{\parallel}+b)ds\right]\hat{p}_n\cdot\hat{p}_{n+1}\right) \quad \text{then,} \tag{A.2}$$

we can write a finite time difference of the aforementioned probability density as

$$\begin{aligned}\Delta\rho &= \rho\left(v_{\parallel}(t+\Delta t)\right) - \rho\left(v_{\parallel}(t)\right) \\ &= \rho\left(\left[(1-\gamma\Delta t)v_{\parallel}(t) + \int_t^{t+\Delta t}(\xi_{\parallel}+b)ds\right]\hat{p}_n\cdot\hat{p}_{n+1}\right) - \rho\left(v_{\parallel}(t)\right) \quad .\end{aligned} \tag{A.3}$$

To obtain a differential equation that depends directly on the parallel velocity equation, we consider that the difference of $v_{\parallel}$ will be infinitesimal when considering an infinitesimal time interval Δt i.e. $v_{\parallel}(t+\Delta t) - v_{\parallel}(t) = \Delta v_{\parallel} \sim \Delta t$. For an infinitesimal variation in $v_{\parallel}$, we may expand the probability density function in Taylor series centered around t

$$\begin{aligned}\Delta\rho &= \rho(v_{\parallel}(t)) + \rho'(v_{\parallel}(t))\left(\left[(1-\gamma\Delta t)v_{\parallel}(t) + \int_t^{t+\Delta t}(\xi_{\parallel}+b)ds\right]\hat{p}_n\cdot\hat{p}_{n+1} - v_{\parallel}(t)\right) \\ &\quad + \frac{1}{2}\rho''(v_{\parallel}(t))\left(\left[(1-\gamma\Delta t)v_{\parallel}(t) + \int_t^{t+\Delta t}(\xi_{\parallel}+b)ds\right]\hat{p}_n\cdot\hat{p}_{n+1} - v_{\parallel}(t)\right)^2 - \rho\big(v_{\parallel}(t)\big) + \mathcal{O}(\Delta t^2) \quad .\end{aligned} \tag{A.4}$$

Here we prove that higher than second order terms can be left out. To do this, we first note that $\langle \hat{p}_n \cdot \hat{p}_{n+1} \rangle = \langle cos(\Delta\theta) \rangle \approx (1 - k\Delta t)$, a conclusion from appendix F. Allowing us to rewrite equation (A.4) as

$$\begin{aligned}
\Delta\rho &= \rho'(v_\parallel(t)) \left(\left[(1-\gamma\Delta t) v_\parallel(t) + \int_t^{t+\Delta t} (\xi_\parallel + b) ds \right] cos(\Delta\theta) - v_\parallel(t) \right) \\
&\quad + \frac{1}{2}\rho''(v_\parallel(t)) \left(\left[(1-\gamma\Delta t) v_\parallel(t) + \int_t^{t+\Delta t} (\xi_\parallel + b) ds \right] cos(\Delta\theta) - v_\parallel(t) \right)^2 - \rho\big(v_\parallel(t)\big) + \mathcal{O}(\Delta t^2) \\
&= \rho'(v_\parallel(t)) \left(\left[\left(1 - \frac{1}{cos(\Delta\theta)} - \gamma\Delta t \right) v_\parallel(t) + \int_t^{t+\Delta t} (\xi_\parallel + b) ds \right] cos(\Delta\theta) \right) \\
&\quad + \frac{1}{2}\rho''(v_\parallel(t)) \left(\left[\left(1 - \frac{1}{cos(\Delta\theta)} - \gamma\Delta t \right) v_\parallel(t) + \int_t^{t+\Delta t} (\xi_\parallel + b) ds \right] cos(\Delta\theta) \right)^2 + \mathcal{O}(\Delta t^2)
\end{aligned} \quad , \tag{A.5}$$

here, the series will be proportional to powers of (the parallel velocity equation)

$$v_\parallel(t+\Delta t) = \left(\left[\left(1 - \frac{1}{cos(\Delta\theta)} - \gamma\Delta t \right) v_\parallel(t) + \int_t^{t+\Delta t} (\xi_\parallel + b) ds \right] cos(\Delta\theta) \right) \quad . \tag{A.6}$$

The second power of (A.6) is

$$\begin{aligned}
(A.6)^2 &= \left[\left(1 - \frac{1}{cos(\Delta\theta)} - \gamma\Delta t \right)^2 v_\parallel^2(t) + \left(\int_t^{t+\Delta t} (\xi_\parallel + b) ds \right)^2 \right. \\
&\quad \left. + 2 \left\{ \left(1 - \frac{1}{cos(\Delta\theta)} - \gamma\Delta t \right) v_\parallel(t) \right\} \int_t^{t+\Delta t} (\xi_\parallel + b) ds \right] cos^2(\Delta\theta) \quad ,
\end{aligned} \tag{A.7}$$

after averaging, we have

$$\begin{aligned}
\langle (A.6)^2 \rangle &= \left\langle \left[\left(1 - \frac{1}{cos(\Delta\theta)} - \gamma\Delta t\right)^2 v_\parallel^2(t) + \left(\int_t^{t+\Delta t} (\xi_\parallel + b) ds\right)^2 \right.\right. \\
&\quad \left.\left. +2\left\{\left(1 - \frac{1}{cos(\Delta\theta)} - \gamma\Delta t\right) v_\parallel(t)\right\} \int_t^{t+\Delta t} (\xi_\parallel + b) ds \right] cos^2(\Delta\theta) \right\rangle \\
&= \left(1 - \frac{1}{1-k\Delta t} - \gamma\Delta t\right)^2 \langle v_\parallel^2(t)\rangle \langle cos^2(\Delta\theta)\rangle + \left(\int_t^{t+\Delta t} (\xi_\parallel + b) ds\right)^2 cos^2(\Delta\theta) \\
&\quad +2\left(1 - \frac{1}{1-k\Delta t} - \gamma\Delta t\right) \langle v_\parallel(t)\rangle \int_t^{t+\Delta t} (\xi_\parallel + b) ds \langle cos^2(\Delta\theta)\rangle \\
&\approx \Big(1 - k\Delta t - 1 - \gamma\Delta t(1-k\Delta t)\Big)^2 \langle v_\parallel^2(t)\rangle + \left\langle \left(\int_t^{t+\Delta t} (\xi_\parallel + b) ds\right)^2 \right\rangle (1-k\Delta t)^2 \\
&\quad +2\Big((1-k\Delta t)^2 - (1-k\Delta t) - \gamma(1-k\Delta t)^2\Delta t\Big) \langle v_\parallel(t)\rangle \left\langle \int_t^{t+\Delta t} (\xi_\parallel + b) ds \right\rangle \\
&\approx \cancelto{0}{\Big(-k\Delta t - \gamma\Delta t\Big)^2} \langle v_\parallel^2(t)\rangle + \Big(g\Delta t + b^2\Delta t^2\Big)(1-2k\Delta t) \\
&\quad +2\Big(1 - 2k\Delta t - 1 + k\Delta t - \gamma(1-2k\Delta t)\Delta t\Big) \langle v_\parallel(t)\rangle b\Delta t \\
&\approx g\Delta t + 2\Big(-k\Delta t - \gamma(1-2k\Delta t)\Delta t\Big) \langle v_\parallel(t)\rangle b\Delta t \\
&\approx g\Delta t \quad . \qquad \text{(A.8)}
\end{aligned}$$

Because $(A.6)^2 \approx g\Delta t$, we know that every other higher power of $(A.6)$ will result in terms proportional to $\Delta t^n\ n > 3/2$, which can be ruled out. Considering $(A.6)^3 \sim 0$, we have

$$\begin{aligned}
\langle \Delta\rho \rangle &= \left\langle \rho'(v_\parallel(t)) \left(\left[\left(1 - \frac{1}{cos(\Delta\theta)} - \gamma\Delta t\right) v_\parallel(t) + \int_t^{t+\Delta t} (\xi_\parallel + b) ds \right] cos(\Delta\theta) \right) \right\rangle \\
&\quad + \frac{1}{2} \langle \rho''(v_\parallel(t))\rangle g\Delta t + \mathcal{O}(\Delta t^2) \\
&= \left\langle \rho'(v_\parallel(t)) \left(\left[1 - k\Delta t - 1 - \gamma\Delta t\,(1-k\Delta t)\right] v_\parallel \right) \right\rangle + \left\langle \rho'(v_\parallel(t)) b\Delta t(1-k\Delta t)\right) \right\rangle \\
&\quad + \frac{1}{2} \langle \rho''(v_\parallel(t))\rangle g\Delta t + \mathcal{O}(\Delta t^2) \\
&= \left\langle \rho'(v_\parallel(t)) \left([-k\Delta t - \gamma\Delta t]\, v_\parallel + b\Delta t \right) \right\rangle \\
&\quad + \frac{1}{2} \langle \rho''(v_\parallel(t))\rangle g\Delta t + \mathcal{O}(\Delta t^2) \quad . \qquad \text{(A.9)}
\end{aligned}$$

Now, we divide both sides of equation (A.9) by Δt, wee have a time variation of the

parallel velocity probability density

$$\frac{\langle \Delta\rho \rangle}{\Delta t} = -\left\langle \rho'(v_\parallel(t)) \left([\gamma + k]\, v_\parallel - b \right) \right\rangle + \frac{1}{2} \langle \rho''(v_\parallel(t)) \rangle g + \mathcal{O}(\Delta t^2) \quad , \tag{A.10}$$

here, we have obtained an equation that is similar to a Fokker-Planck however we must remove the averaging brackets to obtain a full Fokker-Planck equation, to do it, we assume that

$$\langle F\big(x(t)\big) \rangle = \int P(z,t)\, F(z)\, dz \quad \text{thus,} \tag{A.11}$$

we rewrite the left side of equation (A.10) as

$$\frac{\langle \Delta\rho \rangle}{\Delta t} \overset{\Delta t \to 0}{=} \frac{\partial}{\partial t} \int P(z,t) \rho(z)\, dz \quad \text{whereas,}$$

the right side terms of (A.10) may be rewritten as

$$\langle \rho'(v_\parallel) \left([\gamma + k]\, v_\parallel - b \right) \rangle = \int P(z,t) \left([\gamma + k]\, v_\parallel - b \right) \rho'(z)\, dz \quad \text{and} \tag{A.12}$$

$$\frac{\langle \rho''(v_\parallel) g \rangle}{2} = \int P(z,t) g \rho''(z)\, dz \quad \text{now,} \tag{A.13}$$

considering the special case where $\rho(v_\parallel) = \delta(v_\parallel(t) - V_\parallel)$ (the velocities all start from the same point at $t = 0$), we have

$$\begin{aligned} \frac{\langle \Delta\rho \rangle}{\Delta t} &\overset{\Delta t \to 0}{=} \frac{\partial}{\partial t} \int P(z,t) \delta(z - V_\parallel)\, dz \\ &\overset{\Delta t \to 0}{=} \frac{\partial}{\partial t} P(V_\parallel, t) \quad , \end{aligned} \tag{A.14}$$

to simplify the other terms, we recall that the Dirac's delta function has the property of "transferring" a derivative applied to itself to a function that it is multiplied by inside an integral (this is actually a case of the integration by parts),

$$\begin{aligned} \langle \rho'(v_\parallel) \left([\gamma + k]\, v_\parallel - b \right) \rangle &= \int P(z,t) \left([\gamma + k]\, z - b \right) \frac{d}{dz} \delta \left(z - V_\parallel \right)\, dz \\ &= -\int \frac{d}{dz} \left(P(z,t) \left([\gamma + k]\, z - b \right) \right) \delta \left(z - V_\parallel \right)\, dz \\ &= -\frac{\partial}{\partial V_\parallel} \Big(P(V_\parallel, t) \left([\gamma + k] V_\parallel - b \right) \Big) \quad , \end{aligned} \tag{A.15}$$

the second term is

$$\begin{aligned} \langle \rho''(v_\parallel(t)) \rangle g &= \int P(z,t)\, g\, \frac{d^2}{dz^2} \delta(z - V_\parallel) dz \\ &= \int \delta(z - V_\parallel) \frac{d^2}{dz^2} \Big(P(z,t)\, g \Big) dz \\ &= g \frac{d^2}{dV_\parallel^2} P(V_\parallel, t) \quad , \end{aligned} \tag{A.16}$$

after grouping the three separate terms, the final simplified equation has the form of

$$\begin{aligned}\frac{\partial P(V_\parallel,t)}{\partial t} &= \frac{\partial}{\partial V_\parallel}\Big(P(V_\parallel,t)\big([\gamma+k]V_\parallel-b\big)\Big)+\frac{g}{2}\frac{\partial^2 P(V_\parallel,t)}{\partial V_\parallel^2}\\ &= [\gamma+k]\frac{\partial}{\partial V_\parallel}\left(P(V_\parallel,t)\left(V_\parallel-\frac{b}{\gamma+k}\right)\right)+\frac{g}{2}\frac{\partial^2 P(V_\parallel,t)}{\partial V_\parallel^2} \quad , \end{aligned} \tag{A.17}$$

here, $V_\parallel$ is an arbitrary variable, we can write it as the old parallel to polarization velocity $v_\parallel$, in other words,

$$\frac{\partial P(v_\parallel,t)}{\partial t} = [\gamma+k]\frac{\partial}{\partial v_\parallel}\left(P(v_\parallel,t)\left(v_\parallel-\frac{b}{\gamma+k}\right)\right)+\frac{g}{2}\frac{\partial^2 P(v_\parallel,t)}{\partial v_\parallel^2} \quad . \tag{A.18}$$

The known solution of a Fokker-Planck equation for the Ornstein-Uhlenbeck process is a Gaussian function, to find a stationary result, we impose $\frac{\partial P(v_\parallel,t)}{\partial t}=0$, thus obtaining

$$P(v_\parallel)=\sqrt{\frac{\gamma+k}{\pi\, g}}\exp\left(-[\gamma+k]\frac{\left(v_\parallel-\frac{b}{\gamma+k}\right)^2}{g}\right) \quad , \tag{A.19}$$

a result that implies that in the stationary limit, the velocity probability density function becomes a Gaussian curve centered at $v_\parallel=\frac{b}{\gamma+k}$, in other words, the particle has the highest probability of moving with velocity $v_\parallel=\frac{b}{\gamma+k}$ in the polarity axis, as is observed in individual cellular migration, where a cell maintains a stable actin polymerization in its frontal region.

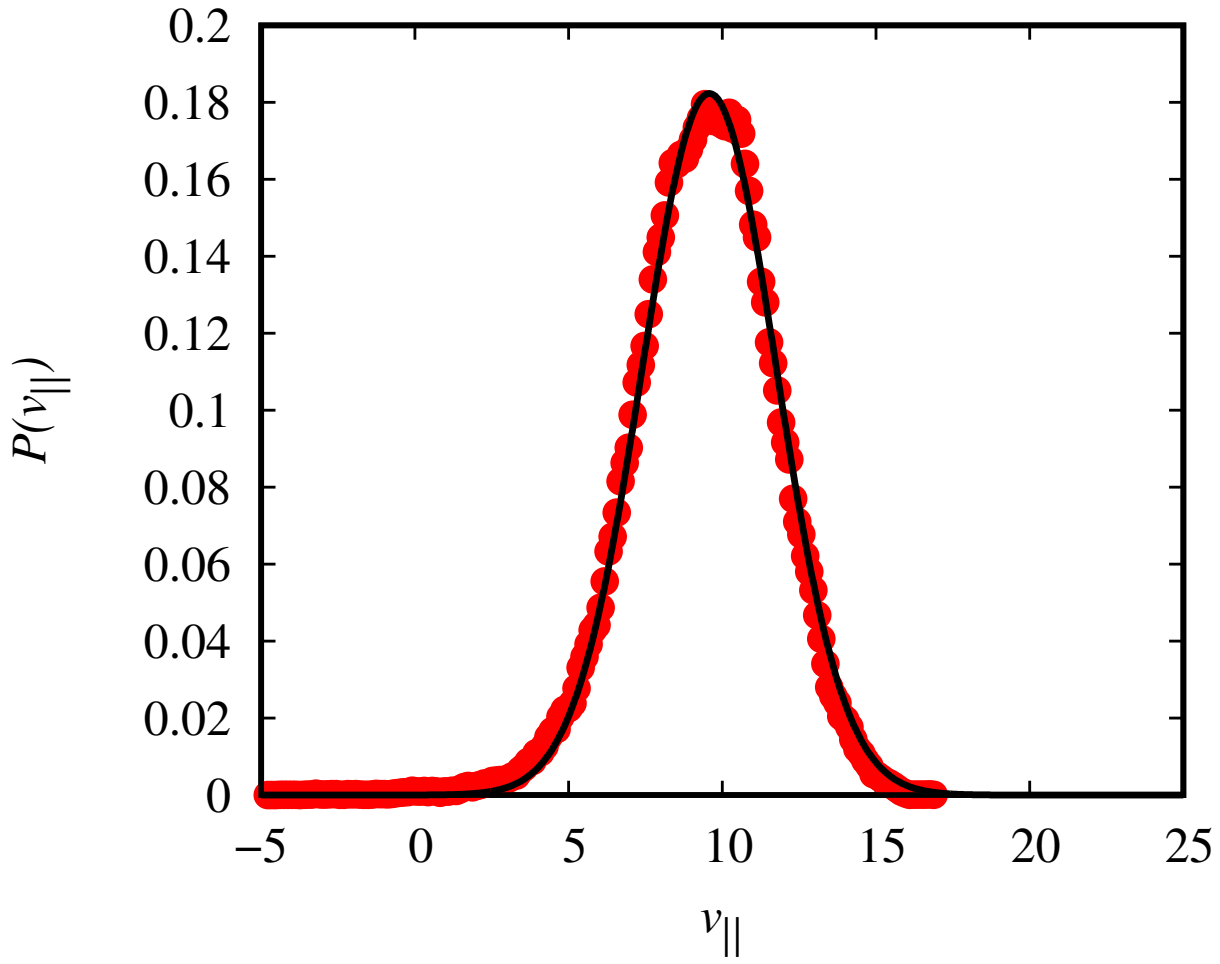

Figure A.1: Comparing between the analytical parallel-to-polarity vector velocity probability density function with the numerical results, for 20 particles and with constants $g = 10$, $q = 0.1$, $\gamma = 1$, $k = 0.04405$ and $b = 10$.

Appendix B

Parallel Velocity Solution

B.1 Average Parallel Velocity

We start at $t = 0$ with the speed $v_{\parallel 0}$ (which can be either positive or negative) in the direction of the cell polarization $\hat{p}_0$. The velocity in the direction of cell polarization $\hat{p}_1$ at the beginning of the subsequent small time interval $[\Delta t, 2\Delta t]$ is:

$$v_{\parallel}(\Delta t)\hat{p}_1 = \left[(1-\gamma\Delta t)v_{\parallel}(0) + \int_0^{\Delta t}(\xi_{\parallel}(s)+b)ds\right](\hat{p}_0\cdot\hat{p}_1)\hat{p}_1 \quad , \tag{B.1}$$

where $\hat{p}_i$ is the polarization vector at time interval $[i\Delta t, (i+1)\Delta t]$, b is the constant of biased motion and $\xi_{\parallel}$ is a Gaussian white noise with variation g ($\langle\xi_{\parallel}(t)\xi_{\parallel}(t')\rangle = g\delta(t-t')$). By iterating the velocity equation (B.1) once, we obtain $v_{\parallel}$ at the beginning of the subsequent time interval $[2\Delta t, 3\Delta t]$

$$\begin{aligned} v_{\parallel}(2\Delta t)\hat{p}_2 &= \left[\chi\, v_{\parallel}(\Delta t) + \int_{\Delta t}^{2\Delta t}(\xi_{\parallel}(s)+b)ds\right](\hat{p}_1\cdot\hat{p}_2)\hat{p}_2 \\ &= \left[\left(\chi^2\, v_{\parallel}(0) + \chi\int_0^{\Delta t}(\xi_{\parallel}(s)+b)ds\right)(\hat{p}_0\cdot\hat{p}_1) + \int_{\Delta t}^{2\Delta t}(\xi_{\parallel}(s)+b)ds\right](\hat{p}_1\cdot\hat{p}_2)\hat{p}_2 \quad , \end{aligned} \tag{B.2}$$

where we have used $(1-\gamma t) = \chi(t)$. For the next time interval $[3\Delta t, 4\Delta t]$, $v_{\parallel}$ is

$$\begin{aligned} v_{\parallel}(3\Delta t)\hat{p}_3 &= \left[\chi\, v_{\parallel}(2\Delta t) + \int_{2\Delta t}^{3\Delta t}(\xi_{\parallel}(s)+b)ds\right](\hat{p}_2\cdot\hat{p}_3)\hat{p}_3 \\ &= \left[\left(\chi^3 v_{\parallel}(0) + \chi^2\int_0^{\Delta t}(\xi_{\parallel}(s)+b)ds\right)(\hat{p}_0\cdot\hat{p}_1) + \left(\chi\int_{\Delta t}^{2\Delta t}(\xi_{\parallel}(s)+b)ds\right)\right](\hat{p}_1\cdot\hat{p}_2)(\hat{p}_2\cdot\hat{p}_3)\hat{p}_2 \\ &+ \int_{2\Delta t}^{3\Delta t}(\xi_{\parallel}(s)+b)ds\;(\hat{p}_2\cdot\hat{p}_3)\hat{p}_3 \quad . \end{aligned} \tag{B.3}$$

We iterate the formula once more:

$$\begin{aligned} v_{\parallel}(4\Delta t)\hat{p}_4 &= \chi^4 v_{\parallel}(0)(\hat{p}_0\cdot\hat{p}_1)(\hat{p}_1\cdot\hat{p}_2)(\hat{p}_2\cdot\hat{p}_3)(\hat{p}_3\cdot\hat{p}_4)\hat{p}_4 \\ &+\chi^3\left(\int_0^{\Delta t}(\xi_{\parallel}(s)+b)ds\right)(\hat{p}_0\cdot\hat{p}_1)(\hat{p}_1\cdot\hat{p}_2)(\hat{p}_2\cdot\hat{p}_3)(\hat{p}_3\cdot\hat{p}_4)\hat{p}_4 \\ &+\chi^2\left(\int_{\Delta t}^{2\Delta t}(\xi_{\parallel}(s)+b)ds\right)(\hat{p}_1\cdot\hat{p}_2)(\hat{p}_2\cdot\hat{p}_3)(\hat{p}_3\cdot\hat{p}_4)\hat{p}_4 \\ &+\chi\left(\int_{2\Delta t}^{3\Delta t}(\xi_{\parallel}(s)+b)ds\right)(\hat{p}_3\cdot\hat{p}_4)\hat{p}_4 \\ &+\int_{3\Delta t}^{4\Delta t}(\xi_{\parallel}(s)+b)ds\ \hat{p}_4 \quad . \end{aligned} \tag{B.4}$$

With the results above, we can create a generalized formula for the n^{th} step

$$v_{\parallel}(n\Delta t)\hat{p}_n = \chi^n v_{\parallel}(0)\prod_{i=0}^{n-1}(\hat{p}_i\cdot\hat{p}_{i+1})\hat{p}_n + \sum_{i=1}^{n}\chi^{n-i}\left(\int_{(i-1)\Delta t}^{i\Delta t}(\xi_{\parallel}(s)+b)ds\right)\prod_{j=i-1}^{n-1}(\hat{p}_j\cdot\hat{p}_{j+1})\hat{p}_n\,. \tag{B.5}$$

With a generalized equation for the parallel velocity in hands, we must characterize this stochastic function by taking its average and squared average. The first step is to take an average over the noise realizations of the parallel velocity's noise $\xi_{\parallel}$

$$\begin{aligned} \langle v_{\parallel}(n\Delta t)\rangle &= \left\langle \chi^n v_{\parallel}(0)\prod_{i=0}^{n-1}(\hat{p}_i\cdot\hat{p}_{i+1})\right\rangle + \left\langle \sum_{i=1}^{n}\chi^{N-i}\left(\int_{(i-1)\Delta t}^{i\Delta t}(\xi_{\parallel}(s)+b)ds\right)\prod_{j=i-1}^{n-1}(\hat{p}_j\cdot\hat{p}_{j+1})\right\rangle \\ &= \chi^n v_{\parallel}(0)(1-k\Delta t)^n + \Delta t b\sum_{i=1}^{n}\chi^{n-i}(1-k\Delta t)^{n-i} \\ &= v_{\parallel}(0)\chi^n\alpha^n + b\Delta t\sum_{i=1}^{n}\chi^{n-i}\alpha^{n-i} \quad , \end{aligned} \tag{B.6}$$

where we call $\alpha = (1-k\Delta t)$. To obtain a solution for the geometric summation, we will invert the order of the powers of χ and α such that

$$X = \sum_{i=1}^{n}x^{n-i} = \sum_{i=0}^{n-1}x^i \quad , \tag{B.7}$$

this is always true, as we may consider the terms in a increasing or decreasing order of powers.

By applying the same identity to the parallel velocity formula, we get

$$\begin{aligned}\langle v_{\parallel}(n\Delta t)\rangle &= v_{\parallel}(0)\chi^n\alpha^n + b\Delta t\sum_{i=0}^{n-1}\chi^i\alpha^i \\ &= v_{\parallel}(0)\chi^n\alpha^n + b\Delta t\left(\frac{1-(\chi\alpha)^{n-1}}{1-\chi\alpha}\right) \quad . \end{aligned} \tag{B.8}$$

In the equation above (B.8), we used the definition for a geometric sum

$$\sum_{i=j}^{n} x^i = \frac{x^j - x^{n+1}}{1-x} \quad . \tag{B.9}$$

The next step is to assume that $n \to \infty$ and $n\Delta t \to T < \infty$. If $n \to \infty$, we can use

$$(1-x\Delta t)^n = \left(1 - x\frac{T}{n}\right)^n \overset{n\to\infty}{=} e^{-xT} \quad , \tag{B.10}$$

we also consider that the product of χ and α is

$$\begin{aligned}\chi\alpha &= (1-\gamma\Delta t)(1-k\Delta t) = 1-(\gamma+k)\Delta t + \gamma k\Delta t^2 \\ &= 1-(\gamma+k)\Delta t + \mathcal{O}(\Delta t^2) \\ &\overset{\Delta t^2 << \Delta t}{\approx} 1-(\gamma+k)\Delta t \quad , \end{aligned} \tag{B.11}$$

where we assumed that $\Delta t^2 << \Delta t$, allowing us to rule out the term $\gamma k\Delta t^2$. Using identities B.10 and B.10 onto B.8, we find

$$\begin{aligned}\langle v_{\parallel}(n\Delta t)\rangle &\approx v_{\parallel}(0)(1-(\gamma+k)\Delta t)^N + b\Delta t\left(\frac{1-(1-(\gamma+k)\Delta t)^N}{(\gamma+k)\Delta t}\right) \\ &\approx v_{\parallel}(0)e^{-(\gamma+k)T} + b\left(\frac{1-e^{-(\gamma+k)T}}{\gamma+k}\right) \quad , \end{aligned} \tag{B.12}$$

which may be rewritten as

$$\langle v_{\parallel}(n\Delta t)\rangle = \frac{b}{\gamma+k} + \left(v_{\parallel}(0) - \frac{b}{\gamma+k}\right)e^{-(\gamma+k)T} \tag{B.13}$$

So if we start from an initial distribution of $v_{\parallel}(0)$ whose average is $\frac{b}{\gamma+k}$, the average parallel speed becomes assumes its stationary value. Consequently,

$$\langle v_{\parallel}(N\Delta t)\rangle_{stationary} = \frac{b}{\gamma+k} \tag{B.14}$$

We can also define $u_\parallel$ as

$$u_\parallel = v_\parallel - \frac{b}{\gamma + k}. \tag{B.15}$$

Using Eq.B.15 in Eq.B.1, after we have projected to the new polarization direction, but at the beginning of interval $[\Delta t, 2\Delta t)$,

$$\begin{aligned}\left[u_\parallel(\Delta t) + \frac{b}{\gamma+k}\right]\hat{p}_1 &= \left\{(1-\gamma\Delta t)\left[u_\parallel(0) + \frac{b}{\gamma+k}\right] + \int_0^{\Delta t}(\xi_\parallel(s)+b)ds\right\}(\hat{p}_0\cdot\hat{p}_1)\hat{p}_1 \\ &= \left\{(1-\gamma\Delta t)\left[u_\parallel(0) + \frac{b}{\gamma+k}\right] + b\Delta t + \int_0^{\Delta t}\xi_\parallel(s)ds\right\}(\hat{p}_0\cdot\hat{p}_1)\hat{p}_1 \quad ,\end{aligned} \tag{B.16}$$

Iterating, we get the expression for $\left[u_\parallel(2\Delta t) - \frac{b}{\gamma+k}\right]$ as

$$\begin{aligned}\left[u_\parallel(2\Delta t) + \frac{b}{\gamma+k}\right]\hat{p}_2 &= \left\{(1-\gamma\Delta t)\left[u_\parallel(\Delta t) + \frac{b}{\gamma+k}\right] + \int_{\Delta t}^{2\Delta t}(\xi_\parallel(s)+b)ds\right\}(\hat{p}_1\cdot\hat{p}_2)\hat{p}_2 \\ &= (1-\gamma\Delta t)^2\left[u_\parallel(0) + \frac{b}{\gamma+k}\right](\hat{p}_0\cdot\hat{p}_1)(\hat{p}_1\cdot\hat{p}_2)\hat{p}_2 \\ &\quad + b\Delta t\left[(1-\gamma\Delta t)(\hat{p}_0\cdot\hat{p}_1)+1\right](\hat{p}_1\cdot\hat{p}_2)\hat{p}_2 \\ &\quad + (1-\gamma\Delta t)\int_0^{\Delta t}\xi_\parallel(s)ds\,(\hat{p}_0\cdot\hat{p}_1)(\hat{p}_1\cdot\hat{p}_2)\hat{p}_2 \\ &\quad + \int_{\Delta t}^{2\Delta t}\xi_\parallel(s)ds\,(\hat{p}_1\cdot\hat{p}_2)\hat{p}_2 \ \ldots\end{aligned} \tag{B.17}$$

and for the next time interval

$$\begin{aligned}\left[u_\parallel(3\Delta t) + \frac{b}{\gamma+k}\right]\hat{p}_3 &= \left\{(1-\gamma\Delta t)\left[u_\parallel(2\Delta t) + \frac{b}{\gamma+k}\right] + \int_{2\Delta t}^{3\Delta t}(\xi_\parallel(s)+b)ds\right\}(\hat{p}_2\cdot\hat{p}_3)\hat{p}_3 \\ &= (1-\gamma\Delta t)^3\left[u_\parallel(0) + \frac{b}{\gamma+k}\right](\hat{p}_0\cdot\hat{p}_1)(\hat{p}_1\cdot\hat{p}_2)(\hat{p}_2\cdot\hat{p}_3)\hat{p}_3 \\ &\quad + b\Delta t\left[(1-\gamma\Delta t)^2(\hat{p}_0\cdot\hat{p}_1)(\hat{p}_1\cdot\hat{p}_2) + (1-\gamma\Delta t)(\hat{p}_1\cdot\hat{p}_2)+1\right](\hat{p}_2\cdot\hat{p}_3)\hat{p}_3 \\ &\quad + (1-\gamma\Delta t)^2\int_0^{\Delta t}\xi_\parallel(s)ds\,(\hat{p}_0\cdot\hat{p}_1)(\hat{p}_1\cdot\hat{p}_2)(\hat{p}_2\cdot\hat{p}_3)\hat{p}_3 \\ &\quad + (1-\gamma\Delta t)\int_{\Delta t}^{2\Delta t}\xi_\parallel(s)ds\,(\hat{p}_1\cdot\hat{p}_2)(\hat{p}_2\cdot\hat{p}_3)\hat{p}_3 \\ &\quad + \int_{2\Delta t}^{3\Delta t}\xi_\parallel(s)ds\,(\hat{p}_2\cdot\hat{p}_3)\hat{p}_3 \ .\end{aligned} \tag{B.18}$$

Generalizing,

$$\begin{aligned}
\left[u_{\parallel}(n\Delta t)+\frac{b}{\gamma+k}\right]\hat{p}_n &= \left\{(1-\gamma\Delta t)\left[u_{\parallel}((n-1)\Delta t)+\frac{b}{\gamma+k}\right]+\int_{(n-1)\Delta t}^{n\Delta t}(\xi_{\parallel}(s)+b)ds\right\}(\hat{p}_{n-1}\cdot\hat{p}_n)\hat{p}_n \\
&= (1-\gamma\Delta t)^n\left[u_{\parallel}(0)+\frac{b}{\gamma+k}\right]\prod_{i=0}^{n-1}(\hat{p}_i\cdot\hat{p}_{i+1})\,\hat{p}_n \\
&\quad +b\Delta t\Big[(1-\gamma\Delta t)^{n-1}\prod_{i=0}^{n-1}(\hat{p}_i\cdot\hat{p}_{i+1})+(1-\gamma\Delta t)^{n-2}\prod_{i=1}^{n-2}(\hat{p}_i\cdot\hat{p}_{i+1})+\cdots+1\Big]\hat{p}_{n-1} \\
&\quad +(1-\gamma\Delta t)^{n-1}\int_0^{\Delta t}\xi_{\parallel}(s)ds\prod_{i=0}^{n-1}(\hat{p}_i\cdot\hat{p}_{i+1})\,\hat{p}_n \\
&\quad +(1-\gamma\Delta t)^{n-2}\int_{\Delta t}^{2\Delta t}\xi_{\parallel}(s)ds\prod_{i=1}^{n-1}(\hat{p}_i\cdot\hat{p}_{i+1})\,\hat{p}_n \\
&\quad +\cdots \\
&\quad +\int_{(n-1)\Delta t}^{n\Delta t}\xi_{\parallel}(s)ds\,(\hat{p}_{n-1}\cdot\hat{p}_n)\hat{p}_n
\end{aligned} \tag{B.19}$$

or in the summation notation

$$\begin{aligned}
\left[u_{\parallel}(n\Delta t)+\frac{b}{\gamma+k}\right]\hat{p}_n &= u_{\parallel}(0)\chi^n\prod_{j=0}^{n-1}(\hat{p}_j\cdot\hat{p}_{j+1})\hat{p}_n \\
&\quad +\left(\frac{b}{\gamma+k}\right)\chi^n\prod_{j=0}^{n-1}(\hat{p}_j\cdot\hat{p}_{j+1})\hat{p}_n \\
&\quad +b\Delta t\left(\sum_{i=0}^{n-1}\chi^{n-1-i}\prod_{j=i}^{n-1}(\hat{p}_j\cdot\hat{p}_{j+1})\right)\hat{p}_n \\
&\quad +\left(\sum_{i=0}^{n-1}\chi^{n-1-i}\prod_{j=i}^{n-1}((\hat{p}_j\cdot\hat{p}_{j+1}))\int_{i\Delta t}^{(i+1)\Delta t}\xi_{\parallel}(s)ds\right)\hat{p}_n
\end{aligned} \tag{B.20}$$

Averaging

$$\left\langle u_{\parallel}(N\Delta t)+\frac{b}{\gamma+k}\right\rangle=\frac{b}{\gamma+k}+u_{\parallel}(0)e^{-(\gamma+k)T} \quad , \tag{B.21}$$

which allows us to conclude that when we consider a non-biased average parallel velocity becomes zero a stationary state:

$$\left\langle u_{\parallel}(N\Delta t)\right\rangle=u_{\parallel}(0)e^{-(\gamma+k)T}\overset{T\to\infty}{\to}0 \quad . \tag{B.22}$$

B.2 Average Squared Parallel Velocity

The average squared parallel velocity $\langle |v_\parallel|^2 \rangle$ can be calculated by squaring expression (B.20), but first, we make substitutions $\chi = (1 - \gamma\Delta t)$ and $\alpha = \hat{p}_i \cdot \hat{p}_{i+1}$ for simplicity

$$\begin{aligned} v_\parallel^2(N\Delta t) &= \left[u_\parallel(n\Delta t) + \frac{b}{\gamma + k} \right]^2 \\ &= \chi^{2N} v_\parallel^2(0) \prod_{i=0}^{N-1} (\hat{p}_i \cdot \hat{p}_{i+1})^2 \\ &\quad + \sum_{i=1}^{N} \sum_{n=1}^{N} \chi^{2N-i-n} \left(\int_{(i-1)\Delta t}^{i\Delta t} \int_{(n-1)\Delta t}^{n\Delta t} (\xi_\parallel(s) + b)(\xi_\parallel(s') + b) ds\, ds' \right) \\ &\quad \times \prod_{j=i-1}^{N-1} (\hat{p}_j \cdot \hat{p}_{j+1}) \prod_{l=n-1}^{N-1} (\hat{p}_l \cdot \hat{p}_{l+1}) \\ &\quad + 2\chi^N v_\parallel(0) \prod_{q=0}^{N-1} (\hat{p}_q \cdot \hat{p}_{q+1}) \sum_{i=1}^{N} \chi^{N-i} \left(\int_{(i-1)\Delta t}^{i\Delta t} (\xi_\parallel(s) + b) ds \right) \prod_{j=i-1}^{N-1} (\hat{p}_j \cdot \hat{p}_{j+1}) \quad . \end{aligned} \tag{B.23}$$

averaging it, we get

$$\begin{aligned} \langle v_\parallel^2(N\Delta t) \rangle &= \Big\langle \chi^{2N} v_\parallel^2(0) \prod_{i=0}^{N-1} (\hat{p}_i \cdot \hat{p}_{i+1})^2 \\ &\quad + \sum_{i=1}^{N} \sum_{n=1}^{N} \chi^{2N-i-n} \left(\int_{(i-1)\Delta t}^{i\Delta t} \int_{(n-1)\Delta t}^{n\Delta t} (\xi_\parallel(s) + b)(\xi_\parallel(s') + b) ds\, ds' \right) \\ &\quad \times \prod_{j=i-1}^{N-1} (\hat{p}_j \cdot \hat{p}_{j+1}) \prod_{l=n-1}^{N-1} (\hat{p}_l \cdot \hat{p}_{l+1}) \\ &\quad + 2\chi^N v_\parallel(0) \prod_{q=0}^{N-1} (\hat{p}_q \cdot \hat{p}_{q+1}) \sum_{i=1}^{N} \chi^{N-i} \left(\int_{(i-1)\Delta t}^{i\Delta t} (\xi_\parallel(s) + b) ds \right) \prod_{j=i-1}^{N-1} (\hat{p}_j \cdot \hat{p}_{j+1}) \Big\rangle \quad , \end{aligned}$$

now we proceed by expanding the terms inside the integrals

$$\begin{aligned}\langle v_\parallel^2(N\Delta t)\rangle &= \Big\langle \chi^{2N} v_\parallel^2(0) \prod_{i=0}^{N-1} (\hat{p}_i \cdot \hat{p}_{i+1})^2 \\ &+ \sum_{i=1}^{N}\sum_{n=1}^{N} \chi^{2N-i-n} \left(\int_{(i-1)\Delta t}^{i\Delta t} \int_{(n-1)\Delta t}^{n\Delta t} (\xi_\parallel(s)\xi_\parallel(s') + b^2) ds\, ds' \right) \\ &\times \prod_{j=i-1}^{N-1} (\hat{p}_j \cdot \hat{p}_{j+1}) \prod_{l=n-1}^{N-1} (\hat{p}_l \cdot \hat{p}_{l+1}) \\ &+ 2\chi^N v_\parallel(0) \prod_{q=0}^{N-1} (\hat{p}_q \cdot \hat{p}_{q+1}) \sum_{i=1}^{N} \chi^{N-i} \left(\int_{(i-1)\Delta t}^{i\Delta t} (\xi_\parallel(s) + b) ds \right) \prod_{j=i-1}^{N-1} (\hat{p}_j \cdot \hat{p}_{j+1}) \Big\rangle \quad ,\end{aligned}$$

and then taking their averages. Here we know that the averages of the random stochastic variables become zero for they have zero average. The average of a product of a stochastic variable with itself is also zero if their respective time intervals are different i.e. $\langle \xi_\parallel(t)\xi_\parallel(t')\rangle = g\delta(t-t')$, if $t \neq t'$, then $\xi_\parallel(t)\xi_\parallel(t')\rangle = 0$. Then

$$\begin{aligned}\langle v_\parallel^2(N\Delta t)\rangle &= \chi^{2N} v_\parallel^2(0) \alpha^{2(N-1)} \\ &+ \sum_{i=1}^{N}\sum_{n=1}^{N} \chi^{2N-i-n} \left(\int_{(i-1)\Delta t}^{i\Delta t} \int_{(n-1)\Delta t}^{n\Delta t} (g\delta(s-s') + b^2) ds\, ds' \right) \\ &\times \Big\langle \prod_{j=i-1}^{N-1} (\hat{p}_j \cdot \hat{p}_{j+1}) \prod_{l=n-1}^{N-1} (\hat{p}_l \cdot \hat{p}_{l+1}) \Big\rangle \\ &+ 2\Big\langle v_\parallel(0)\, b\, \Delta t\, \chi^N \prod_{q=0}^{N-1} (\hat{p}_q \cdot \hat{p}_{q+1}) \sum_{i=1}^{N} \chi^{N-i} \prod_{j=i-1}^{N-1} (\hat{p}_j \cdot \hat{p}_{j+1}) \Big\rangle \quad .\end{aligned}$$

The equation then becomes

$$\begin{aligned}\langle v_{\parallel}^2(N\Delta t)\rangle &= \chi^{2N} v_{\parallel}^2(0)\alpha^{2(N-1)} \\ &+b^2(\Delta t)^2 \sum_{i=1}^{N}\sum_{n=1}^{N} \chi^{2N-i-n}\Big\langle \prod_{j=i-1}^{N-1}(\hat{p}_j\cdot\hat{p}_{j+1}) \prod_{l=n-1}^{N-1}(\hat{p}_l\cdot\hat{p}_{l+1})\Big\rangle \\ &+\sum_{i=1}^{N}\sum_{n=1}^{N} \chi^{2N-i-n}\left(\int_{(i-1)\Delta t}^{i\Delta t} g\,\delta_{i,n}\,ds\right)\Big\langle \prod_{j=i-1}^{N-1}(\hat{p}_j\cdot\hat{p}_{j+1}) \prod_{l=n-1}^{N-1}(\hat{p}_l\cdot\hat{p}_{l+1})\Big\rangle \\ &+2\Big\langle v_{\parallel}(0)\,b\,\Delta t\,\chi^N \sum_{i=1}^{N}\prod_{q=0}^{N-1}\prod_{j=i-1}^{N-1}\chi^{N-i}(\hat{p}_q\cdot\hat{p}_{q+1})(\hat{p}_j\cdot\hat{p}_{j+1})\Big\rangle \quad .\end{aligned}$$

After evaluating the integrals and taking the averages of all the terms in equation B.24, we get

$$\begin{aligned}\langle v_{\parallel}^2(N\Delta t)\rangle &= \chi^{2N} v_{\parallel}^2(0)\alpha^{2(N-1)} \\ &+b^2(\Delta t)^2 \sum_{i=1}^{N}\sum_{n=1}^{N} \chi^{2N-i-n}\Big\langle \prod_{j=i-1}^{N-1}(\hat{p}_j\cdot\hat{p}_{j+1}) \prod_{l=n-1}^{N-1}(\hat{p}_l\cdot\hat{p}_{l+1})\Big\rangle \\ &+g\Delta t \sum_{i=1}^{N}\chi^{2(N-i)}\Big\langle \prod_{j=i-1}^{N-1}(\hat{p}_j\cdot\hat{p}_{j+1})^2\Big\rangle \\ &+2\Big\langle v_{\parallel}(0)\,b\,\Delta t\,\chi^N \sum_{i=1}^{N}\prod_{q=0}^{N-1}\prod_{j=i-1}^{N-1}\chi^{N-i}(\hat{p}_q\cdot\hat{p}_{q+1})(\hat{p}_j\cdot\hat{p}_{j+1})\Big\rangle \quad ,\end{aligned}$$

for simplicity, we will solve each term in the expression (B.24) separately

$$V_1 = \chi^{2N} v_{\parallel}^2(0)\alpha^{2(N-1)} \tag{B.24}$$

$$V_2 = b^2(\Delta t)^2 \sum_{i=1}^{N}\sum_{n=1}^{N} \chi^{2N-i-n}\Big\langle \prod_{j=i-1}^{N-1}(\hat{p}_j\cdot\hat{p}_{j+1}) \prod_{l=n-1}^{N-1}(\hat{p}_l\cdot\hat{p}_{l+1})\Big\rangle \tag{B.25}$$

$$V_3 = g\Delta t \sum_{i=1}^{N}\chi^{2(N-i)}\Big\langle \prod_{j=i-1}^{N-1}(\hat{p}_j\cdot\hat{p}_{j+1})^2\Big\rangle \tag{B.26}$$

$$V_4 = 2\Big\langle v_{\parallel}(0)\,b\,\Delta t\,\chi^N \sum_{i=1}^{N}\prod_{q=0}^{N-1}\prod_{j=i-1}^{N-1}\chi^{N-i}(\hat{p}_q\cdot\hat{p}_{q+1})(\hat{p}_j\cdot\hat{p}_{j+1})\Big\rangle \quad . \tag{B.27}$$

The first term is straightforward, we just have to assume that $N \to \infty$ and use an exponential approximation

$$\begin{aligned} V_1 &= \chi^{2N} v_\parallel^2(0)\alpha^{2(N-1)} \\ &= v_\parallel^2(0)e^{-2(\gamma+k)T} \quad , \end{aligned} \tag{B.28}$$

where we considered that

$$\begin{aligned} \chi^{2N}\alpha^{2(N-1)} &= (1-\gamma\Delta t)^{2N}(1-k\Delta t)^{2(N-1)} \\ &\approx \left(1-\gamma\frac{T}{N}\right)^{2(N-1)}\left(1-k\frac{T}{N}\right)^{2(N-1)} && \text{(B.29)} \\ &\overset{N\to\infty}{\approx} e^{-2(\gamma+k)N\Delta t} && \text{(B.30)} \\ &\overset{N\to\infty}{\approx} e^{-2(\gamma+k)T} \quad . && \text{(B.31)} \end{aligned}$$

The second term is not so simple,

$$\begin{aligned} V_2 &= b^2(\Delta t)^2 \sum_{i=1}^{N}\sum_{n=1}^{N}\chi^{2N-i-n}\Big\langle \prod_{j=i-1}^{N-1}(\hat{p}_j\cdot\hat{p}_{j+1})\prod_{l=n-1}^{N-1}(\hat{p}_l\cdot\hat{p}_{l+1})\Big\rangle \\ &= b^2(\Delta t)^2 \sum_{i=1}^{N}\sum_{n=1}^{N}\chi^{2N-i-n}\alpha^{N-i}\alpha^{N-n} \end{aligned} \tag{B.32}$$

To solve it, we will invert the order of the powers of the summation and use the geometrical series identity (B.9)

$$\begin{aligned} V_2 &= b^2(\Delta t)^2 \sum_{i=0}^{N-1}\sum_{n=0}^{N-1}\chi^{i+n}\alpha^{i+n} \\ &= b^2(\Delta t)^2 \sum_{i=0}^{N-1}\chi^i\alpha^i \sum_{n=0}^{N-1}\chi^n\alpha^n \\ &= b^2(\Delta t)^2 \left(\frac{1-(\chi\alpha)^N}{1-\chi\alpha}\right)\left(\frac{1-(\chi\alpha)^N}{1-\chi\alpha}\right) \\ &= b^2(\Delta t)^2 \left(\frac{1-(\chi\alpha)^N}{1-\chi\alpha}\right)^2 \quad . \end{aligned} \tag{B.33}$$

Now we have again to use the approximation (B.11) such that we obtain

$$
\begin{aligned}
V_2 &= b^2(\Delta t)^2 \left(\frac{1-(\chi\alpha)^N}{1-\chi\alpha} \right)^2 \\
&\approx b^2(\Delta t)^2 \left(\frac{1-(\chi\alpha)^N}{1-(1-(\gamma+k)\Delta t)} \right)^2 \\
&\approx b^2(\Delta t)^2 \left(\frac{1-(\chi\alpha)^N}{(\gamma+k)\Delta t} \right)^2 \\
&\approx b^2 \left(\frac{1-e^{-(\gamma+k)T}}{\gamma+k} \right)^2 \quad . \qquad \text{(B.34)}
\end{aligned}
$$

The third one is

$$
\begin{aligned}
V_3 &= g\Delta t \sum_{i=1}^{N} \chi^{2(N-i)} \Big\langle \prod_{j=i-1}^{N-1} (\hat{p}_j \cdot \hat{p}_{j+1})^2 \Big\rangle \\
&= g\Delta t \sum_{i=1}^{N} \chi^{2(N-i)} \alpha^{2(N-i)} \\
&= g\Delta t \left(\frac{1-(\chi\alpha)^{2N}}{1-(\chi\alpha)^2} \right) \\
&= g \left(\frac{1-e^{-2(\gamma+k)T}}{2(\gamma+k)} \right) \quad . \qquad \text{(B.35)}
\end{aligned}
$$

And for the last term we have

$$
\begin{aligned}
V_4 &= 2\Big\langle v_{\parallel}(0)\, b\, \Delta t\, \chi^N \sum_{i=1}^{N} \prod_{q=0}^{N-1} \prod_{j=i-1}^{N-1} \chi^{N-i} (\hat{p}_q \cdot \hat{p}_{q+1})(\hat{p}_j \cdot \hat{p}_{j+1}) \Big\rangle \\
&= 2v_{\parallel}(0)\, b\, \Delta t\, \chi^N \sum_{i=1}^{N} \prod_{q=0}^{N-1} \prod_{j=i-1}^{N-1} \chi^{N-i} \alpha^N \alpha^{N-i+1} \\
&= 2v_{\parallel}(0)\, b\, \Delta t\, \chi^N \alpha^N \sum_{i=1}^{N} \chi^{N-i} \alpha^{N-i+1} \\
&= 2v_{\parallel}(0)\, b\, \Delta t\, \chi^N \alpha^N \left(\frac{1-(\chi\alpha)^N}{1-\chi\alpha} \right) \\
&= 2v_{\parallel}(0)\, b\, \Delta t\, e^{-(\gamma+k)T} \left(\frac{1-e^{-(\gamma+k)T}}{(\gamma+k)\Delta t} \right) \\
&= 2v_{\parallel}(0)\, b\, e^{-(\gamma+k)T} \left(\frac{1-e^{-(\gamma+k)T}}{(\gamma+k)} \right) \\
&= 2v_{\parallel}(0)\, b \left(\frac{e^{-(\gamma+k)T} - e^{-2(\gamma+k)T}}{(\gamma+k)} \right)
\end{aligned}
\tag{B.36}
$$

Now, returning to expression $(B.24) = V_1 + V_2 + V_3 + V_4$, we get

$$
\begin{aligned}
\langle v_{\parallel}^2(N\Delta t) \rangle &= v_{\parallel}^2(0) e^{-2(\gamma+k)T} + b^2 \left(\frac{1-e^{-(\gamma+k)T}}{\gamma+k} \right)^2 + g \left(\frac{1-e^{-2(\gamma+k)T}}{2(\gamma+k)} \right) \\
&\quad + 2bv_{\parallel}(0) \left(\frac{e^{-(\gamma+k)T} - e^{-2(\gamma+k)T}}{\gamma+k} \right) \qquad \text{(B.37)} \\
&= e^{-(\gamma+k)T} \left[-\frac{2b^2}{(\gamma+k)^2} + \frac{2bv_{\parallel}(0)}{\gamma+k} \right] \\
&\quad + e^{-2(\gamma+k)T} \left[v_{\parallel}^2(0) + \frac{b^2}{(\gamma+k)^2} - \frac{g}{2(\gamma+k)} - \frac{2bv_{\parallel}(0)}{\gamma+k} \right] + \frac{g}{2(\gamma+k)} + \frac{b^2}{(\gamma+k)^2} \quad , \qquad \text{(B.38)}
\end{aligned}
$$

finally

$$\begin{aligned}\langle v_{\parallel}^2(N\Delta t)\rangle &= e^{-(\gamma+k)T}\left[-\frac{2b^2}{(\gamma+k)^2}+\frac{2bv_{\parallel}(0)}{\gamma+k}\right] \\ &\quad +e^{-2(\gamma+k)T}\left[v_{\parallel}^2(0)+\frac{b^2}{(\gamma+k)^2}-\frac{g}{2(\gamma+k)}-\frac{2bv_{\parallel}(0)}{\gamma+k}\right]+\frac{g}{2(\gamma+k)}+\frac{b^2}{(\gamma+k)^2} \quad .\end{aligned} \tag{B.39}$$

Because for the biased anisotropic Ornstein-Uhlenbeck model, the average parallel velocity is not zero, the parallel velocity second momentum is

$$\begin{aligned}\langle v_{\parallel}^2\rangle - \langle v_{\parallel}\rangle^2 &= e^{-(\gamma+k)T}\left[-\frac{2b^2}{(\gamma+k)^2}+\frac{2bv_{\parallel}(0)}{\gamma+k}\right] \\ &\quad +e^{-2(\gamma+k)T}\left[v_{\parallel}^2(0)+\frac{b^2}{(\gamma+k)^2}-\frac{g}{2(\gamma+k)}-\frac{2bv_{\parallel}(0)}{\gamma+k}\right]+\frac{g}{2(\gamma+k)}+\frac{b^2}{(\gamma+k)^2} \\ &\quad -\frac{b^2}{(\gamma+k)^2}+\left(v_{\parallel}^2(0)+\frac{b^2}{(\gamma+k)^2}-\frac{2bv_{\parallel}(0)}{(\gamma+k)}\right)e^{-2(\gamma+k)T} \\ &\quad -\frac{2b}{(\gamma+k)}e^{-(\gamma+k)T}\left(v_{\parallel}-\frac{b}{(\gamma+k)}\right) \\ &= \frac{g}{2(\gamma+k)}\left(1-e^{-2(\gamma+k)T}\right) \quad ,\end{aligned} \tag{B.40}$$

which means that the dispersion in the velocity distribution is only an effect of the Wiener variable $\xi_{\parallel}$ with variance g, the same dispersion as we obtained in the **AOU** model. The bias variable b, only shifts the parallel distribution from $v_{\parallel}=0$ to $v_{\parallel}=\frac{b}{(\gamma+k)}$. Which would be the same result if we calculated the variance of the non-biased velocity $u_{\parallel}$.

Now, assuming that the system starts at the stationary state, where $v_{\parallel}(0)=\frac{b}{\gamma+k}$ and

$$v_{\parallel}^2(0) = \frac{g}{2(\gamma+k)}+\frac{b^2}{(\gamma+k)^2} \quad , \tag{B.41}$$

we obtain the same result if we considered the limits to $T\to\infty$

$$\langle v_{\parallel}^2(T)\rangle \overset{T\to\infty}{\equiv} \langle v_{\parallel}^2\rangle_{\text{stationary}} \tag{B.42}$$

$$= \frac{g}{2(\gamma+k)}+\frac{b^2}{(\gamma+k)^2} \quad , \tag{B.43}$$

we obtain the stationary average squared velocity (when the system relaxed, reaching a stationary state).

Appendix C

Mean Square Displacement

Here we assume that the parallel velocity can be written as

$$\vec{v}_{\parallel}(\Delta T) = \frac{\vec{r}_{\parallel}\left((n+1)\Delta t\right) - \vec{r}_{\parallel}(n\Delta t)}{\Delta t} \quad , \tag{C.1}$$

then, using equation B.5 from appendix B, we isolate the position terms of the displacement equation to obtain

$$\begin{aligned}
\Delta\vec{r}(n\Delta t) &= v_{\parallel}(n\Delta t)\ \Delta t\ \hat{p}_n \\
&= \Delta t\ \left[u_{\parallel}(n\Delta t) + \frac{b}{\gamma + k}\right]\hat{p}_n \\
&= \Delta t\ (1-\gamma\Delta t)^n \prod_{i=0}^{n-1}(\hat{p}_i \cdot \hat{p}_{i+1})\left[u_{\parallel}(0) + \frac{b}{\gamma + k}\right]\hat{p}_n \\
&\quad + b\Delta t^2\Big[(1-\gamma\Delta t)^{n-1}\prod_{i=0}^{n-1}(\hat{p}_i \cdot \hat{p}_{i+1}) + (1-\gamma\Delta t)^{n-2}\prod_{i=1}^{n-1}(\hat{p}_i \cdot \hat{p}_{i+1}) + \cdots + (\hat{p}_{n-1} \cdot \hat{p}_n)\Big]\hat{p}_n \\
&\quad + \Delta t\ (1-\gamma\Delta t)^{n-1}\prod_{i=0}^{n-1}(\hat{p}_i \cdot \hat{p}_{i+1})\int_0^{\Delta t}\xi_{\parallel}(s)ds\,\hat{p}_n \\
&\quad + \Delta t\ (1-\gamma\Delta t)^{n-2}\prod_{i=1}^{n-1}(\hat{p}_i \cdot \hat{p}_{i+1})\int_{\Delta t}^{2\Delta t}\xi_{\parallel}(s)ds\,\hat{p}_n \\
&\quad \cdots \\
&\quad + \Delta t\ \int_{n\Delta t}^{(n+1)\Delta t}[(n+1)\Delta t - s]\xi_{\parallel}(s)ds\,\hat{p}_n \quad ,
\end{aligned} \tag{C.2}$$

where $\Delta\vec{r}(n\Delta t) = \vec{r_{\parallel}}\left((n+1)\Delta t\right) - \vec{r}_{\parallel}(n\Delta t)$, or in a more synthesized notation

$$\begin{aligned}
\Delta\vec{r}(n\Delta t) &= v_{\parallel}(n\Delta t)\ \Delta t\ \hat{p}_n \\
&= \Delta t\ \left[u_{\parallel}(n\Delta t) + \frac{b}{\gamma+k}\right]\hat{p}_n \\
&= \Delta t\ (1-\gamma\Delta t)^n \prod_{i=0}^{n-1}(\hat{p}_i\cdot\hat{p}_{i+1})\left[u_{\parallel}(0) + \frac{b}{\gamma+k}\right]\hat{p}_n \\
&\quad + b\Delta t^2 \sum_{j=0}^{n-1}(1-\gamma\Delta t)^{n-1-j}\prod_{i=j}^{n-1}(\hat{p}_i\cdot\hat{p}_{i+1})\hat{p}_n \\
&\quad + \Delta t\ \sum_{j=0}^{n-1}(1-\gamma\Delta t)^{n-1-j}\prod_{i=j}^{n-1}(\hat{p}_i\cdot\hat{p}_{i+1})\int_{j\Delta t}^{(j+1)\Delta t}\xi_{\parallel}(s)ds\,\hat{p}_n \\
&\quad + \Delta t\ \int_{n\Delta t}^{(n+1)\Delta t}[(n+1)\Delta t - s]\xi_{\parallel}(s)ds\,\hat{p}_n
\end{aligned} \tag{C.3}$$

To find a total parallel displacement formula, we sum each parallel displacement, from $n=0$ to $n=N$ to obtain

$$\begin{aligned}
\vec{r_{\parallel}}\left((N+1)\Delta t\right) - \vec{r}_{\parallel}(0) &= \Delta t\ \left[u_{\parallel}(0) + \frac{b}{\gamma+k}\right]\sum_{n=0}^{N}(1-\gamma\Delta t)^n\prod_{i=0}^{n-1}(\hat{p}_i\cdot\hat{p}_{i+1})\hat{p}_n \\
&\quad + b\Delta t^2\sum_{n=0}^{N}\sum_{j=0}^{n-1}(1-\gamma\Delta t)^{n-1-j}\prod_{i=j}^{n-1}(\hat{p}_i\cdot\hat{p}_{i+1})\hat{p}_n \\
&\quad + \Delta t\ \sum_{n=0}^{N}\sum_{j=0}^{n-1}(1-\gamma\Delta t)^{n-1-j}\prod_{i=j}^{n-1}(\hat{p}_i\cdot\hat{p}_{i+1})\int_{j\Delta t}^{(j+1)\Delta t}\xi_{\parallel}(s)ds\,\hat{p}_n \\
&\quad + \Delta t\ \sum_{n=0}^{N}\int_{n\Delta t}^{(n+1)\Delta t}[(n+1)\Delta t - s]\xi_{\parallel}(s)ds\,\hat{p}_n \quad ,
\end{aligned} \tag{C.4}$$

then we expand all the term between parenthesis

$$\begin{aligned}
\vec{r_{\parallel}}\left((N+1)\Delta t\right) &= \vec{r}_{\parallel}(0) + u_{\parallel}(0)\Delta t \sum_{n=0}^{N}(1-\gamma\Delta t)^n \prod_{j=0}^{n-1}(\hat{p}_j \cdot \hat{p}_{j+1})\hat{p}_n && \text{(C.5)}\\
&+\frac{b}{\gamma+k}\,\Delta t \sum_{n=0}^{N}(1-\gamma\Delta t)^n \prod_{j=0}^{n-1}(\hat{p}_j \cdot \hat{p}_{j+1})\hat{p}_n && \text{(C.6)}\\
&+b\Delta t^2 \sum_{n=0}^{N}\sum_{i=0}^{n-1}(1-\gamma\Delta t)^{n-1-i} \prod_{j=i}^{n-1}(\hat{p}_j \cdot \hat{p}_{j+1})\hat{p}_n && \text{(C.7)}\\
&+\Delta t \sum_{n=0}^{N}\sum_{i=0}^{n-1}(1-\gamma\Delta t)^{n-1-i} \prod_{j=i}^{n-1}(\hat{p}_j \cdot \hat{p}_{j+1}) \int_{i\Delta t}^{(i+1)\Delta t} \xi_{\parallel}(s)ds\ \hat{p}_n && \text{(C.8)}\\
&+\Delta t \sum_{n=0}^{N} \int_{n\Delta t}^{(n+1)\Delta t} [(n+1)\Delta t - s]\xi_{\parallel}(s)ds\,\hat{p}_n \quad , && \text{(C.9)}
\end{aligned}$$

to find the general equation for the parallel displacement of a particle that moves according to our biased anisotropic Ornstein-Uhlenbeck model. For the total displacement, we must add the perpendicular displacement to equations (C.5-C.9):

$$\vec{r}_{\perp}\big((N+1)\Delta t\big) = \vec{r}_{\perp}(0) + \sum_{n=0}^{N} \int_{n\Delta t}^{(n+1)\Delta t} \xi_{\perp}(s)\, ds\, \hat{n}_n \quad . \tag{C.10}$$

We then have to square the total displacement and take its average, to obtain the MSD, but first, we define each term in the total displacement equation as:

$$\begin{aligned}
\vec{A1} &= u_{\parallel}(0)\Delta t \sum_{n=0}^{N}(1-\gamma\Delta t)^n \prod_{j=0}^{n-1}(\hat{p}_j \cdot \hat{p}_{j+1})\hat{p}_n\\
&+\Delta t \sum_{n=0}^{N}\sum_{i=0}^{n-1}(1-\gamma\Delta t)^{n-1-i} \prod_{j=i}^{n-1}(\hat{p}_j \cdot \hat{p}_{j+1}) \int_{i\Delta t}^{(i+1)\Delta t} \xi_{\parallel}(s)ds\ \hat{p}_n\\
&+\Delta t \sum_{n=0}^{N} \int_{n\Delta t}^{(n+1)\Delta t} [(n+1)\Delta t - s]\xi_{\parallel}(s)ds\,\hat{p}_n\\
&+\vec{r}_{\perp}(0) + \sum_{n=0}^{N} \int_{n\Delta t}^{(n+1)\Delta t} \xi_{\perp}(s)\, ds\, \hat{n}_n \quad , && \text{(C.11)}
\end{aligned}$$

$$\vec{A2} = \frac{b}{\gamma+k}\,\Delta t \sum_{n=0}^{N}(1-\gamma\Delta t)^n \prod_{j=0}^{n-1}(\hat{p}_j \cdot \hat{p}_{j+1})\hat{p}_n \quad \text{and} \tag{C.12}$$

$$\vec{A3} = b\Delta t^2 \sum_{n=0}^{N} \sum_{i=0}^{n-1} (1-\gamma\Delta t)^{n-1-i} \prod_{j=i}^{n-1} (\hat{p}_j \cdot \hat{p}_{j+1}) \hat{p}_n \quad . \tag{C.13}$$

Then we proceed to the squaring, followed by the averages over the noises:

$$\langle |\vec{r_\parallel}\left((N+1)\Delta t\right) - \vec{r_\parallel}(0)|^2 \rangle = \langle |A1|^2 \rangle + \langle |A2|^2 \rangle + \langle |A3|^2 \rangle + 2\langle \vec{A1} \cdot \vec{A2} \rangle + 2\langle \vec{A1} \cdot \vec{A3} \rangle + 2\langle \vec{A2} \cdot \vec{A3} \rangle \tag{C.14}$$

We calculate each term of the biased **AOU** particle's position:

$$\langle |A1|^2 \rangle = MSD_{unbiased} \quad , \tag{C.15}$$

which was obtained by de Almeida et. al. in [de Almeida et al., 2022]. The other products arise due the introduction of the bias constant b, thus have not yet been calculated, for $\langle A2^2 \rangle$ we have

$$\begin{aligned}
\langle |A2|^2 \rangle &= \left\langle \left(\frac{b}{\gamma+k}\, \Delta t \sum_{n=0}^{N} (1-\gamma\Delta t)^n \prod_{j=0}^{n-1} (\hat{p}_j \cdot \hat{p}_{j+1}) \hat{p}_n \right) \cdot \left(\frac{b}{\gamma+k}\, \Delta t \sum_{n=0}^{N} (1-\gamma\Delta t)^n \prod_{j=0}^{n-1} (\hat{p}_j \cdot \hat{p}_{j+1}) \hat{p}_n \right) \right\rangle \\
&= \left(\frac{b}{\gamma+k} \right)^2 \Delta t^2 \sum_{n=0}^{N} \sum_{m=0}^{N} (1-\gamma\Delta t)^{n+m} \left\langle \prod_{j=0}^{n-1} (\hat{p}_j \cdot \hat{p}_{j+1}) \prod_{k=0}^{m-1} (\hat{p}_k \cdot \hat{p}_{k+1})\, (\hat{p}_n \cdot \hat{p}_m) \right\rangle \\
&= \left(\frac{b}{\gamma+k} \right)^2 \Delta t^2 \sum_{n=0}^{N} (1-\gamma\Delta t)^{2n} \left\langle \left(\prod_{j=0}^{n-1} (\hat{p}_j \cdot \hat{p}_{j+1}) \right)^2 \right\rangle \qquad \text{(C.16)} \\
&\quad + 2 \left(\frac{b}{\gamma+k} \right)^2 \Delta t^2 \sum_{n=0}^{N-1} \sum_{m=n+1}^{N} (1-\gamma\Delta t)^{n+m} \left\langle \prod_{j=0}^{n-1} (\hat{p}_j \cdot \hat{p}_{j+1}) \prod_{k=0}^{m-1} (\hat{p}_k \cdot \hat{p}_{k+1})\, (\hat{p}_n \cdot \hat{p}_m) \right\rangle , \qquad \text{(C.17)}
\end{aligned}$$

where we separate the calculations even further:

$$
\begin{aligned}
(C.16) \quad &= \left(\frac{b}{\gamma+k}\right)^2 \Delta t^2 \sum_{n=0}^{N} (1-\gamma\Delta t)^{2n} \left\langle \left(\prod_{j=0}^{n-1} (\hat{p}_j \cdot \hat{p}_{j+1}) \right)^2 \right\rangle \\
&= \left(\frac{b}{\gamma+k}\right)^2 \Delta t^2 \sum_{n=0}^{N} (1-\gamma\Delta t)^{2n} (1-k\Delta t)^{2n} \\
&= \left(\frac{b}{\gamma+k}\right)^2 \Delta t^2 \sum_{n=0}^{N} (1-2(\gamma+k)\Delta t)^{n} \\
&= \left(\frac{b}{\gamma+k}\right)^2 \Delta t^2 \frac{1-(1-2(\gamma+k)\ \Delta t))^{n+1}}{2(\gamma+k)\Delta t} \\
&= \left(\frac{b}{\gamma+k}\right)^2 \Delta t \frac{1-(1-2(\gamma+k)\Delta t)^{n+1}}{2(\gamma+k)} \\
&\quad \to 0 \text{ if } \Delta t \to 0 \quad \text{and} \qquad (C.18)
\end{aligned}
$$

$$
\begin{aligned}
(C.17) &= 2\left(\frac{b}{\gamma+k}\right)^2 \Delta t^2 \sum_{n=0}^{N-1}\sum_{m=n+1}^{N}(1-\gamma\Delta t)^{n+m}\langle\prod_{j=0}^{n-1}(\hat{p}_j\cdot\hat{p}_{j+1})\prod_{k=0}^{m-1}(\hat{p}_k\cdot\hat{p}_{k+1})\,(\hat{p}_n\cdot\hat{p}_m)\rangle \\
&= 2\left(\frac{b}{\gamma+k}\right)^2 \Delta t^2 \sum_{n=0}^{N-1}\sum_{m=n+1}^{N}(1-\gamma\Delta t)^{n+m}(1-k\Delta t)^{m+n}(1-k\Delta t)^{|m-n|} \\
&= 2\left(\frac{b}{\gamma+k}\right)^2 \Delta t^2 \sum_{n=0}^{N-1}\sum_{m=n+1}^{N}(1-\gamma\Delta t)^{n+m}(1-k\Delta t)^{2m} \\
&= 2\left(\frac{b}{\gamma+k}\right)^2 \Delta t^2 \sum_{n=0}^{N-1}(1-\gamma\Delta t)^{n}\sum_{m=n+1}^{N}(1-\gamma\Delta t)^{m}(1-k\Delta t)^{2m} \\
&= 2\left(\frac{b}{\gamma+k}\right)^2 \Delta t^2 \sum_{n=0}^{N-1}(1-\gamma\Delta t)^{n}\frac{(1-(\gamma+2k)\Delta t)^{n+1}-(1-(\gamma+2k)\Delta t)^{N}}{(\gamma+2k)\Delta t} \\
&= 2\left(\frac{b}{\gamma+k}\right)^2 \Delta t^2 \sum_{n=0}^{N-1}\frac{(1-2(\gamma+k)\Delta t)^{n}}{(\gamma+2k)\Delta t} \\
&\quad -2\left(\frac{b}{\gamma+k}\right)^2 \Delta t^2 \sum_{n=0}^{N-1}(1-(\gamma+2k)\Delta t)^{N}\frac{(1-\gamma\Delta t)^{n}}{(\gamma+2k)\Delta t} \\
&= 2\left(\frac{b}{\gamma+k}\right)^2 \frac{1-(1-2(\gamma+k)\Delta t)^{N}}{(\gamma+2k)2(\gamma+k)} \\
&\quad -2\left(\frac{b}{\gamma+k}\right)^2 (1-\frac{1-(1-\gamma\Delta t)^{N}}{(\gamma+2k)\gamma} \\
&= 2\left(\frac{b}{\gamma+k}\right)^2 \frac{1-(1-2(\gamma+k)\Delta t)^{N}}{(\gamma+2k)2(\gamma+k)} \\
&\quad -2\left(\frac{b}{\gamma+k}\right)^2 (1-(\gamma+2k)\Delta t)^{N}\frac{1-(1-\gamma\Delta t)^{N}}{(\gamma+2k)\gamma} \\
&= 2\left(\frac{b}{\gamma+k}\right)^2 \frac{1-e^{-2(\gamma+k)\Delta T}}{(\gamma+2k)2(\gamma+k)} \\
&\quad -2\left(\frac{b}{\gamma+k}\right)^2 e^{-(\gamma+2k)\Delta T}\frac{1-e^{-\gamma\Delta T}}{(\gamma+2k)\gamma} \\
&= 2\left(\frac{b}{\gamma+k}\right)^2 \frac{1-e^{-2(\gamma+k)\Delta T}}{(\gamma+2k)2(\gamma+k)} \\
&\quad -2\left(\frac{b}{\gamma+k}\right)^2 \frac{e^{-(\gamma+2k)\Delta T}-e^{-2(\gamma+k)\Delta T}}{(\gamma+2k)\gamma} \quad . \qquad (C.19)
\end{aligned}
$$

Summing results (C.18) and (C.19) we obtain $\langle|A2|^2\rangle$

$$\langle |A2|^2 \rangle = -\frac{2}{\gamma}\left(\frac{b}{\gamma+k}\right)^2\left(\frac{1-e^{-2(\gamma+k)\Delta T}}{2(\gamma+k)} - \frac{1-e^{-(\gamma+2k)\Delta T}}{(\gamma+2k)}\right) \quad . \tag{C.20}$$

Now, we calculate $\langle |A3|^2 \rangle$:

$$\begin{aligned}
\langle |A3|^2 \rangle &= \left\langle \left(b\Delta t^2 \sum_{n=0}^{N}\sum_{i=0}^{n-1}(1-\gamma\Delta t)^{n-1-i}\prod_{j=i}^{n-1}(\hat{p}_j\cdot\hat{p}_{j+1})\hat{p}_n \right)\cdot\left(b\Delta t^2 \sum_{n=0}^{N}\sum_{i=0}^{n-1}(1-\gamma\Delta t)^{n-1-i}\prod_{j=i}^{n-1}(\hat{p}_j\cdot\hat{p}_{j+1})\hat{p}_n \right)\right\rangle \\
&= b^2\Delta t^4\left\langle \sum_{n=0}^{N}\sum_{m=0}^{N}\sum_{i=0}^{n-1}\sum_{k=0}^{m-1}(1-\gamma\Delta t)^{n+m-2-i-k}\prod_{j=i}^{n-1}(\hat{p}_j\cdot\hat{p}_{j+1})\prod_{\ell=k}^{m-1}(\hat{p}_\ell\cdot\hat{p}_{\ell+1})\,(\hat{p}_n\cdot\hat{p}_m)\right\rangle \\
&= b^2\Delta t^4\left\langle \sum_{n=0}^{N}\sum_{m=0}^{N}\sum_{i=0}^{n-1}\sum_{k=0}^{m-1}(1-\gamma\Delta t)^{n+m-2-i-k}(1-k\Delta t)^{n-i}(1-k\Delta t)^{m-k}(1-k\Delta t)^{|m-n|}\right\rangle \\
&= 2b^2\Delta t^4\left\langle \sum_{n=0}^{N-1}\sum_{m=n+1}^{N}\sum_{i=0}^{n-1}\sum_{k=0}^{m-1}(1-\gamma\Delta t)^{n+m-2-i-k}(1-k\Delta t)^{n-i}(1-k\Delta t)^{m-k}(1-k\Delta t)^{m-n}\right\rangle \\
&= 2b^2\Delta t^4\sum_{n=0}^{N-1}\sum_{m=n+1}^{N}(1-k\Delta t)^{m-n}\sum_{i=0}^{n-1}(1-(\gamma+k)\Delta t)^{n-1-i}\sum_{k=0}^{m-1}(1-(\gamma+k)\Delta t)^{m-1-k} \\
&= 2b^2\Delta t^4\sum_{n=0}^{N-1}\sum_{m=n+1}^{N}(1-k\Delta t)^{m-n}\left[\frac{1-(1-(\gamma+k)\Delta t)^n}{(\gamma+k)\Delta t}\right]\times\left[\frac{1-(1-(\gamma+k)\Delta t)^m}{(\gamma+k)\Delta t}\right] \\
&= \frac{2b^2\Delta t^2}{(\gamma+k)^2}\sum_{n=0}^{N-1}\sum_{m=n+1}^{N}(1-k\Delta t)^{m-n} && \text{(C.21)} \\
&\quad -2\frac{2b^2\Delta t^2}{(\gamma+k)^2}\sum_{n=0}^{N-1}\sum_{m=n+1}^{N}(1-k\Delta t)^{m-n}(1-(\gamma+k)\Delta t)^n && \text{(C.22)} \\
&\quad -\frac{2b^2\Delta t^2}{(\gamma+k)^2}\sum_{n=0}^{N-1}\sum_{m=n+1}^{N}(1-k\Delta t)^{m-n}(1-(\gamma+k)\Delta t)^m && \text{(C.23)} \\
&\quad +2\frac{2b^2\Delta t^2}{(\gamma+k)^2}\sum_{n=0}^{N-1}\sum_{m=n+1}^{N}(1-k\Delta t)^{m-n}(1-(\gamma+k)\Delta t)^{n+m} \quad . && \text{(C.24)}
\end{aligned}$$

Calculating each parcel separately we have:

$$\begin{aligned}
(C.21) &= \frac{2b^2\Delta t^2}{(\gamma+k)^2}\sum_{n=0}^{N-1}\sum_{m=n+1}^{N}(1-k\Delta t)^{m-n} \\
&= \frac{2b^2\Delta t^2}{(\gamma+k)^2}\sum_{n=0}^{N-1}\frac{(1-k\Delta t)-(1-k\Delta t)^{N-n}}{k\Delta t} \\
&= \frac{2b^2\Delta t}{k(\gamma+k)^2}\left[\sum_{n=0}^{N-1}1-\sum_{n=0}^{N-1}(1-k\Delta t)^{N-n}\right] \\
&= \frac{2b^2}{k(\gamma+k)^2}\left(\Delta T-\frac{1-e^{-k\Delta T}}{k}\right) && \text{(C.25)}
\end{aligned}$$

$$
\begin{aligned}
(C.22) &= -\frac{2b^2\Delta t^2}{(\gamma+k)^2}\sum_{n=0}^{N-1}\sum_{m=n+1}^{N}(1-\gamma\Delta t)^n(1-k\Delta t)^m \\
&= -\frac{2b^2\Delta t^2}{(\gamma+k)^2}\sum_{n=0}^{N-1}(1-\gamma\Delta t)^n\frac{(1-k\Delta t)^{n+1}-(1-k\Delta t)^{N+1}}{k\Delta t} \\
&= -\frac{2b^2\Delta t}{k(\gamma+k)^2}\left[\sum_{n=0}^{N-1}(1-(\gamma+k)\Delta t)^n-\sum_{n=0}^{N-1}(1-k\Delta t)^{N+1}(1-\gamma\Delta t)^n\right] \\
&= -\frac{2b^2}{k(\gamma+k)^2}\left(\frac{1-e^{-(\gamma+k)\Delta T}}{(\gamma+k)}-\frac{e^{-k\Delta T}(1-e^{-\gamma\Delta T})}{\gamma}\right) \qquad \text{(C.26)}
\end{aligned}
$$

$$
\begin{aligned}
(C.23) &= -\frac{2b^2\Delta t^2}{(\gamma+k)^2}\sum_{n=0}^{N-1}(1-k\Delta t)^{-n}\sum_{m=n+1}^{N}(1-(\gamma+2k)\Delta t)^m \\
&= -\frac{2b^2\Delta t^2}{(\gamma+k)^2}\sum_{n=0}^{N-1}(1-k\Delta t)^{-n}\left[\frac{(1-(\gamma+2k)\Delta t)^{n+1}}{(\gamma+2k)\Delta t}-\frac{(1-(\gamma+2k)\Delta t)^N}{(\gamma+2k)\Delta t}\right] \\
&= -\frac{2b^2\Delta t}{(\gamma+k)^2(\gamma+2k)}\left[\sum_{n=0}^{N-1}(1-(\gamma+k)\Delta t)^n-(1-(\gamma+k)\Delta t)^N\sum_{n=0}^{N-1}(1-k\Delta t)^{N-n}\right] \\
&= -\frac{2b^2}{(\gamma+k)^2(\gamma+2k)}\left[\frac{1-e^{(\gamma+k)\Delta T}}{(\gamma+k)}-\frac{e^{(\gamma+k)\Delta T}(1-e^{-k\Delta T})}{k}\right] \qquad \text{(C.27)}
\end{aligned}
$$

$$
\begin{aligned}
(C.24) &= \frac{2b^2\Delta t^2}{(\gamma+k)^2}\sum_{n=0}^{N-1}(1-\gamma\Delta t)^n\sum_{m=n+1}^{N}(1-(\gamma+2k)\Delta t)^m \\
&= \frac{2b^2\Delta t^2}{(\gamma+k)^2}\sum_{n=0}^{N-1}(1-\gamma\Delta t)^n\left[\frac{(1-(\gamma+2k)\Delta t)^{n+1}}{(\gamma+2k)\Delta t}-\frac{(1-(\gamma+2k)\Delta t)^N}{(\gamma+2k)\Delta t}\right] \\
&= \frac{2b^2\Delta t}{(\gamma+k)^2(\gamma+2k)}\left[\sum_{n=0}^{N-1}(1-2(\gamma+k)\Delta t)^n-(1-(\gamma+2k)\Delta t)^N\sum_{n=0}^{N-1}(1-\gamma\Delta t)^n\right] \\
&= \frac{2b^2}{(\gamma+k)^2(\gamma+2k)}\left[\frac{1-e^{-2(\gamma+k)\Delta T}}{2(\gamma+k)}-\frac{e^{-(\gamma+2k)\Delta T}(1-e^{-\gamma\Delta T})}{\gamma}\right] \qquad \text{(C.28)}
\end{aligned}
$$

Summing (C.25), (C.26),(C.27), and (C.28) we find $\langle|A3|^2\rangle$:

$$\begin{aligned}\langle|A3|^2\rangle &= \frac{2b^2}{k(\gamma+k)^2}\left(\Delta T-\frac{1-e^{-k\Delta T}}{k}\right)\\ &-\frac{2b^2}{k(\gamma+k)^2}\left(\frac{1-e^{-(\gamma+k)\Delta T}}{(\gamma+k)}-\frac{e^{-k\Delta T}(1-e^{-\gamma\Delta T})}{\gamma}\right)\\ &-\frac{2b^2}{(\gamma+k)^2(\gamma+2k)}\left(\frac{1-e^{-(\gamma+k)\Delta T}}{(\gamma+k)}-\frac{e^{-(\gamma+k)\Delta T}(1-e^{-k\Delta T})}{k}\right)\\ &+\frac{2b^2}{(\gamma+k)^2(\gamma+2k)}\left(\frac{1-e^{-2(\gamma+k)\Delta T}}{2(\gamma+k)}-\frac{e^{-(\gamma+2k)\Delta T}(1-e^{-\gamma\Delta T})}{\gamma}\right)\end{aligned} \tag{C.29}$$

Now we proceed in finding the crossed multiplication terms, here we observe that the average over the initial speed $u_{\|}(0)=0$, hence the only crossed term that survives the average is $\langle\vec{A2}\cdot\vec{A3}\rangle$. As follows:

$$
\begin{aligned}
\langle \vec{A2}\cdot\vec{A3}\rangle &= \frac{b^2\Delta t^3}{\gamma+k}\left\langle \sum_{n=0}^{N}\sum_{m=0}^{N}\sum_{i=0}^{m-1}(1-\gamma\Delta t)^n(1-\gamma\Delta t)^{m-1-i}\prod_{j=0}^{n-1}(\hat{p}_j\cdot\hat{p}_{j+1})\prod_{k=i}^{m-1}(\hat{p}_k\cdot\hat{p}_{k+1})(\hat{p}_n\cdot\hat{p}_m)\right\rangle \\
&= \frac{b^2\Delta t^3}{\gamma+k}\sum_{n=0}^{N}\sum_{m=0}^{N}\sum_{i=0}^{m-1}(1-\gamma\Delta t)^n(1-\gamma\Delta t)^{m-1-i}(1-k\Delta t)^n(1-k\Delta t)^{m-i}(1-k\Delta t)^{|m-n|} \\
&= \frac{b^2\Delta t^3}{\gamma+k}\sum_{n=0}^{N}\sum_{m=0}^{N}(1-\gamma\Delta t)^n(1-k\Delta t)^n(1-k\Delta t)^{|m-n|}\sum_{i=0}^{m-1}(1-(\gamma+k)\Delta t)^{m-i} \\
&= \frac{b^2\Delta t^2}{\gamma+k}\sum_{n=0}^{N}\sum_{m=0}^{N}(1-\gamma\Delta t)^n(1-k\Delta t)^n(1-k\Delta t)^{|m-n|}\frac{1-(1-(\gamma+k)\Delta t)^m}{(\gamma+k)} \\
&= \frac{b^2\Delta t^2}{(\gamma+k)^2}\sum_{n=0}^{N}\sum_{m=0}^{N}(1-\gamma\Delta t)^n(1-k\Delta t)^n(1-k\Delta t)^{|m-n|} \\
&\quad -\frac{b^2\Delta t^2}{(\gamma+k)^2}\sum_{n=0}^{N}\sum_{m=0}^{N}(1-\gamma\Delta t)^{n+m}(1-k\Delta t)^{n+m}(1-k\Delta t)^{|m-n|} \\
&= \frac{2b^2\Delta t^2}{(\gamma+k)^2}\sum_{n=0}^{N-1}\sum_{m=n+1}^{N}(1-\gamma\Delta t)^n(1-k\Delta t)^m \\
&\quad -\frac{2b^2\Delta t^2}{(\gamma+k)^2}\sum_{n=0}^{N-1}\sum_{m=n+1}^{N}(1-\gamma\Delta t)^{n+m}(1-k\Delta t)^{2m} \\
&= \frac{2b^2\Delta t}{k(\gamma+k)^2}\sum_{n=0}^{N-1}(1-\gamma\Delta t)^n\left((1-k\Delta t)^{n+1}-(1-k\Delta t)^N\right) \\
&\quad -\frac{2b^2\Delta t}{(\gamma+2k)(\gamma+k)^2}\sum_{n=0}^{N-1}(1-\gamma\Delta t)^n\left((1-(\gamma+2k)\Delta t)^{n+1}-(1-(\gamma+2k)\Delta t)^N\right) \\
&= \frac{2b^2}{k(\gamma+k)^3}\left(1-(1-(\gamma+k)\Delta t)^N\right) \\
&\quad -\frac{2b^2}{k\gamma(\gamma+k)^2}(1-k\Delta t)^N\left(1-(1-\gamma\Delta t)^N\right) \\
&\quad -\frac{2b^2}{2(\gamma+2k)(\gamma+k)^3}\left(1-(1-2(\gamma+k)\Delta t)^N\right) \\
&\quad +\frac{2b^2\Delta t}{\gamma(\gamma+2k)(\gamma+k)^2}(1-(\gamma+2k)\Delta t)^N\left(1-(1-\gamma\Delta t)^N\right) \\
&= \frac{2b^2}{k(\gamma+k)^3}(1-e^{-(\gamma+k)\Delta T}) \\
&\quad -\frac{2b^2}{k\gamma(\gamma+k)^2}e^{-k\Delta T}(1-e^{-\gamma\Delta T}) \\
&\quad -\frac{2b^2}{2(\gamma+2k)(\gamma+k)^3}(1-e^{-2(\gamma+k)\Delta T}) \\
&\quad +\frac{2b^2}{\gamma(\gamma+2k)(\gamma+k)^2}e^{-(\gamma+2k)\Delta T}(1-e^{-\gamma\Delta T})
\end{aligned}
\tag{C.30}
$$

Now we can write MSD_{biased}:

$$\begin{aligned}
MSD_{biased} &= MSD_{unbiased} \\
&\frac{2}{\gamma}\left(\frac{b}{\gamma+k}\right)^2\left(\frac{1-e^{-(\gamma+2k)\Delta T}}{(\gamma+2k)}-\frac{1-e^{-2(\gamma+k)\Delta T}}{2(\gamma+k)}\right) \\
&+\frac{2b^2}{k(\gamma+k)^2}\left(\Delta T-\frac{1-e^{-k\Delta T}}{k}\right) \\
&-\frac{2b^2}{k(\gamma+k)^2}\left(\frac{1-e^{-(\gamma+k)\Delta T}}{(\gamma+k)}-\frac{e^{-k\Delta T}(1-e^{-\gamma\Delta T})}{\gamma}\right) \\
&-\frac{2b^2}{(\gamma+k)^2(\gamma+2k)}\left(\frac{1-e^{-(\gamma+k)\Delta T}}{(\gamma+k)}-\frac{e^{-(\gamma+k)\Delta T}(1-e^{-k\Delta T})}{k}\right) \\
&+\frac{2b^2}{(\gamma+k)^2(\gamma+2k)}\left(\frac{1-e^{-2(\gamma+k)\Delta T}}{2(\gamma+k)}-\frac{e^{(-\gamma+2k)\Delta T}(1-e^{-\gamma\Delta T})}{\gamma}\right) \\
&+\frac{2b^2}{k(\gamma+k)^3}(1-e^{-(\gamma+k)\Delta T}) \\
&-\frac{2b^2}{k\gamma(\gamma+k)^2}e^{-k\Delta T}(1-e^{-\gamma\Delta T}) \\
&-\frac{2b^2}{2(\gamma+2k)(\gamma+k)^3}(1-e^{-2(\gamma+k)\Delta T}) \\
&+\frac{2b^2}{\gamma(\gamma+2k)(\gamma+k)^2}e^{-(\gamma+2k)\Delta T}(1-e^{-\gamma\Delta T})
\end{aligned} \tag{C.31}$$

To simplify the equation above, we then define some terms

$$M_1 = \frac{1-e^{-(\gamma+2k)\Delta T}}{\gamma+2k} \quad , \tag{C.32}$$

$$M_2 = \frac{1-e^{-2(\gamma+k)\Delta T}}{2(\gamma+k)} \quad , \tag{C.33}$$

$$M_3 = \frac{1-e^{-(\gamma+k)\Delta T}}{(\gamma+k)} \quad , \tag{C.34}$$

$$M_4 = \frac{1-e^{-k\Delta T}}{k} \quad , \tag{C.35}$$

$$M_5 = \frac{1-e^{-\gamma\Delta T}}{\gamma} \quad . \tag{C.36}$$

And rewrite the biased mean square displacement as

$$
\begin{aligned}
MSD_{biased} &= MSD_{unbiased} \\
&+\frac{2b^2}{\gamma(\gamma+k)^2}\left[M_1 - M_2\right] \\
&+\frac{2b^2}{k(\gamma+k)^2}\Big[\Delta T - M_4 - \cancel{M_3} + \cancel{M_5\left(1-kM_4\right)} + \cancel{M_3} - \cancel{M_5\left(1-kM_4\right)}\Big] \\
&+\frac{2b^2}{(\gamma+k)^2(\gamma+2k)}\Big[-M_3 + M_4\left(1-(\gamma+k)M_3\right) + \cancel{M_2} \\
&-\cancel{M_5\left(1-(\gamma+2k)M_1\right)} - \cancel{M_2} + \cancel{M_5\left(1-(\gamma+2k)M_1\right)}\Big] \\
&= MSD_{unbiased} \\
&+\frac{2b^2}{\gamma(\gamma+k)^2}\left[M_1 - M_2\right] \\
&+\frac{2b^2}{k(\gamma+k)^2}\Big[\Delta T - M_4\Big] \\
&+\frac{2b^2}{(\gamma+k)^2(\gamma+2k)}\Big[-M_3 + M_4\left(1-(\gamma+k)M_3\right)\Big] \\
&= MSD_{unbiased} \\
&+\frac{2b^2}{\gamma(\gamma+k)^2}\left[\frac{1-e^{-(\gamma+2k)\Delta T}}{\gamma+2k} - \frac{1-e^{-2(\gamma+k)\Delta T}}{2(\gamma+k)}\right] \\
&+\frac{2b^2}{k(\gamma+k)^2}\left[\Delta T - \frac{1-e^{-k\Delta T}}{k}\right] \\
&+\frac{2b^2}{(\gamma+k)^2(\gamma+2k)}\left[-\frac{1-e^{-(\gamma+k)\Delta T}}{\gamma+k} + \left(\frac{1-e^{-k\Delta T}}{k}\right)e^{-(\gamma+k)\Delta T}\right]
\end{aligned}
\tag{C.37}
$$

Writing the whole biased mean square displacement we then obtain

$$
\begin{aligned}
MSD_{biased} &= \frac{g}{(\gamma+k)(\gamma+2k)}\left[\Delta T - \frac{1}{(\gamma+2k)}(1-e^{-(\gamma+2k)\Delta T})\right] + 2qk\Delta T \\
&+\frac{2b^2}{\gamma(\gamma+k)^2}\left[\frac{1-e^{-(\gamma+2k)\Delta T}}{\gamma+2k} - \frac{1-e^{-2(\gamma+k)\Delta T}}{2(\gamma+k)}\right] \\
&+\frac{2b^2}{k(\gamma+k)^2}\left[\Delta T - \frac{1-e^{-k\Delta T}}{k}\right] \\
&+\frac{2b^2}{(\gamma+k)^2(\gamma+2k)}\left[-\frac{1-e^{-(\gamma+k)\Delta T}}{\gamma+k} + \frac{e^{-(\gamma+k)\Delta T}}{k} - \frac{e^{-(\gamma+2k)\Delta T}}{k}\right]
\end{aligned}
\tag{C.38}
$$

finally, we group the $e^{-(\gamma+2k)\Delta T}$ terms together. It can be done by adding the null term

$\frac{2b^2}{(\gamma+k)^2(\gamma+2k)}\left(\frac{1}{k}-\frac{1}{k}\right)$ to the equation, which in turn, results

$$\begin{aligned} MSD_{biased} &= \frac{g}{(\gamma+k)(\gamma+2k)}\left[\Delta T-\frac{1}{(\gamma+2k)}(1-e^{-(\gamma+2k)\Delta T})\right]+2qk\Delta T \\ &-\frac{2b^2}{\gamma(\gamma+k)^2}\left[\frac{1-e^{-2(\gamma+k)\Delta T}}{2(\gamma+k)}\right] \\ &+\frac{2b^2}{\gamma k(\gamma+k)}\left[\frac{1-e^{-(\gamma+2k)\Delta T}}{\gamma+2k}\right] \\ &+\frac{2b^2}{k(\gamma+k)^2}\left[\Delta T-\frac{1-e^{-k\Delta T}}{k}\right] \\ &-\frac{2b^2}{(\gamma+k)^2(\gamma+2k)}\left[\frac{1-e^{-(\gamma+k)\Delta T}}{\gamma+k}+\frac{1-e^{-(\gamma+k)\Delta T}}{k}\right] \quad , \end{aligned} \tag{C.39}$$

now, simplifying, we finally get

$$\begin{aligned} MSD_{biased} &= \frac{g}{(\gamma+k)(\gamma+2k)}\left[\Delta T-\frac{1}{(\gamma+2k)}(1-e^{-(\gamma+2k)\Delta T})\right]+2qk\Delta T \\ &-\frac{2b^2}{\gamma(\gamma+k)^2}\left[\frac{1-e^{-2(\gamma+k)\Delta T}}{2(\gamma+k)}\right] \\ &+\frac{2b^2}{\gamma k(\gamma+k)}\left[\frac{1-e^{-(\gamma+2k)\Delta T}}{\gamma+2k}\right] \\ &+\frac{2b^2}{k(\gamma+k)^2}\left[\Delta T-\frac{1-e^{-k\Delta T}}{k}\right] \\ &-\frac{2b^2}{k(\gamma+k)^2}\left[\frac{1-e^{-(\gamma+k)\Delta T}}{\gamma+k}\right] \quad . \end{aligned} \tag{C.40}$$

To verify the results of the analytical calculations, we plotted the mean square displacement of a simulation of a single cell moving according to our model biased model

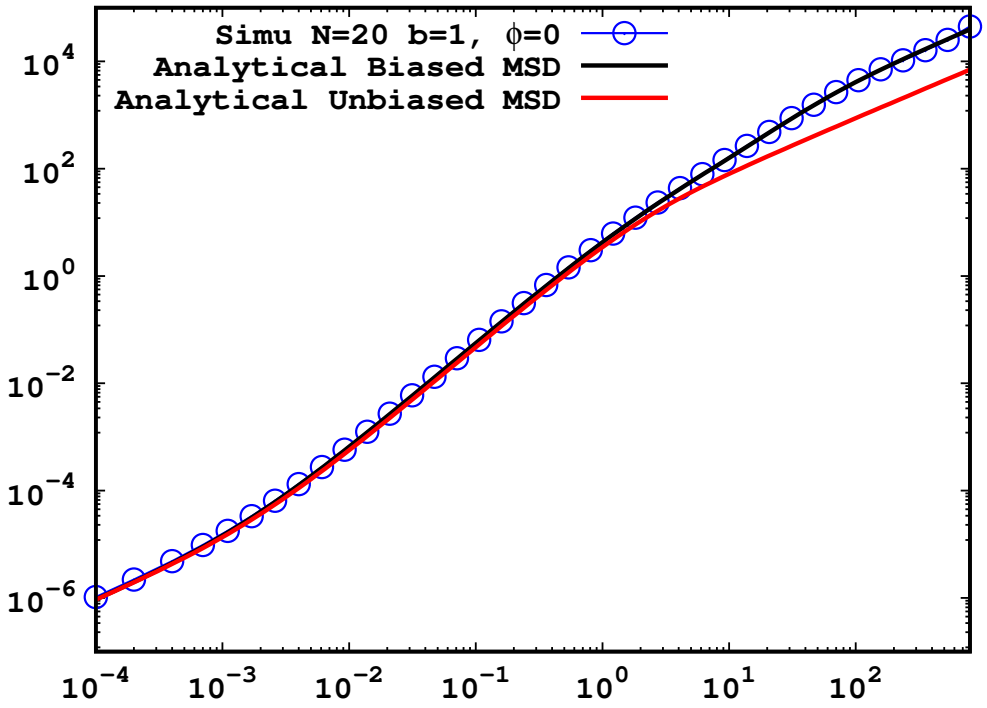

Figure C.1: Log-log plot of the Mean Square Displacement versus ΔT of 20 non-interacting particles with parameters $k = 0.04405$, $q = 0.1$, $g = 10$, $\gamma = 1$ and $b = 1$. The solid lines correspond to the analytical calculations corresponding to (C.40)

Since we have verified the analytical calculations with the results from a simulations, the next logical step should be to compare these results with other simulations and real world cell migrations experiments, but first it is necessary to establish a relationship between the parameters found in our model and real world phenomena and its consequences. The easiest way to do it, is to find the set of parameters (g, q, k, γ, b) as a function of the macroscopic parameters D and P, already used in stochastic literature as the diffusion coefficient and the persistence parameter respectively and also S defined in [de Almeida et al., 2022] as the fraction of time in which the crawler stays in the initial diffusive dynamic.

In a scenario without any complications, the procedure to identify the relationship between the microscopic parameters $((g, q, k, \gamma, b))$ and the macroscopic ones, would be assume a correspondence between the biased mean square displacement and an effective unbiased mean square displacement given as

$$MSD_{effective} = \frac{2DP}{1-S}\left(\frac{\Delta T}{P} - (1-S)\left(1 - e^{-\Delta T/P}\right)\right) \tag{C.41}$$

in such a way that

$$MSD_{biased}(g, q, k, \gamma, b, \Delta T) = MSD_{effective} \quad \text{and} \tag{C.42}$$

then obtain the relation between the macroscopic and the microscopic variable.

It was already done in [de Almeida et al., 2022], for a non biased self moving particle (b=0), it was found that

$$P = \frac{1}{(\gamma + 2k)} \quad , \tag{C.43}$$

$$D = \frac{g}{2(\gamma + k)(\gamma + 2k)} \quad \text{and} \tag{C.44}$$

$$S = \frac{2qk(\gamma + k)(\gamma + 2k)}{g + 2qk(\gamma + k)(\gamma + 2k)} \quad . \tag{C.45}$$

In the case of the biased model however, the mean square displacement resulted in the sum of exponential terms with different exponents thus, the procedure cited above results in a transcendental equation. Considering all this, we may at least find the limit cases for $\Delta T \to 0$ and $\Delta T \to \infty$.

To begin, we consider the case where $\Delta T \to 0$, which prompts us to expand the exponential terms of both effective MSD and the biased MSD and compare the results

$$\begin{aligned} MSD_{effective} &\overset{\Delta T \to 0}{=} \frac{2DP}{1-S}\left(\frac{\Delta T}{P} - (1-S)\left(1 - \left[1 - \frac{\Delta T}{P} + \mathcal{O}(\Delta T^2)\right]\right)\right) \\ &\approx \frac{2DPS}{1-S}\left(\frac{\Delta T}{P}\right) \\ &\approx \frac{2DS}{1-S}\Delta T \quad \text{now} \end{aligned} \tag{C.46}$$

we do the same for the biased MSD

$$\begin{aligned} MSD_{biased} \overset{\Delta T\to 0}{\approx} & \frac{g}{(\gamma+k)(\gamma+2k)}\left[\Delta T - \frac{1}{(\gamma+2k)}(1-1+(\gamma+2k)\Delta T)\right] + 2qk\Delta T \\ & -\frac{2b^2}{\gamma(\gamma+k)^2}\left[\frac{1-1+2(\gamma+k)\Delta T}{2(\gamma+k)}\right] \\ & +\frac{2b^2}{\gamma k(\gamma+k)}\left[\frac{1-1+(\gamma+2k)\Delta T}{\gamma+2k}\right] \\ & +\frac{2b^2}{k(\gamma+k)^2}\left[\Delta T - \frac{1-1+k\Delta T}{k}\right] \\ & -\frac{2b^2}{k(\gamma+k)^2}\left[\frac{1-1+(\gamma+k)\Delta T}{\gamma+k}\right] \\ \approx \quad & 2qk\Delta T + 2b^2\Delta T\left(\cancel{\frac{1}{\gamma k(\gamma+k)} - \frac{1}{\gamma(\gamma+k)^2} - \frac{1}{k(\gamma+k)^2}}\right) \\ \approx \quad & 2qk\Delta T \quad . \end{aligned} \tag{C.47}$$

The result implies that, for small times, we have

$$\frac{2DS}{1-S}\Delta T \overset{\Delta T\to 0}{\approx} 2qk\Delta T \tag{C.48}$$

For $\Delta T \to \infty$, we know that exponentials with negative exponents go to zero, which implies for an effective MSD

$$\begin{aligned} MSD_{effective} \overset{\Delta T\to\infty}{\approx} & \frac{2DP}{1-S}\left(\frac{\Delta T}{P} - (1-S)\right) \\ \approx \quad & \frac{2D\Delta T}{1-S} \quad , \end{aligned} \tag{C.49}$$

doing the same procedure of zeroing negative exponentials of ΔT, for the biased MSD, gets

us

$$\begin{aligned} MSD_{biased} \overset{\Delta T\to\infty}{\approx} & \frac{g}{(\gamma+k)(\gamma+2k)}\left[\Delta T-\frac{1}{(\gamma+2k)}\right]+2qk\Delta T \\ & -\frac{2b^2}{\gamma(\gamma+k)^2}\left[\frac{1}{2(\gamma+k)}\right] \\ & +\frac{2b^2}{\gamma k(\gamma+k)}\left[\frac{1}{\gamma+2k}\right] \\ & +\frac{2b^2}{k(\gamma+k)^2}\left[\Delta T-\frac{1}{k}\right] \\ & -\frac{2b^2}{k(\gamma+k)^2}\left[\frac{1}{\gamma+k}\right] \\ \approx & \frac{g\Delta T}{(\gamma+k)(\gamma+2k)}+2qk\Delta T+\frac{2b^2\Delta T}{k(\gamma+k)^2} \quad . \end{aligned} \tag{C.50}$$

With this, we find for $\Delta T \to \infty$ that

$$\frac{2D}{1-S}\Delta T \overset{\Delta T\to\infty}{=} \left[\frac{g}{(\gamma+k)(\gamma+2k)}+\frac{2b^2}{k(\gamma+k)^2}+2qk\right]\Delta T \tag{C.51}$$

We may also analyse the case where $k=0$, which implicates in a self-propelling particle that does not change its polarization orientation neither exhibits a perpendicular to polarization diffusion, thus, staying permanently in a 1D trajectory. At first sight, it may seem as a problem for we have in our biased MSD equation, three terms divided by k, they are

$$\frac{2b^2}{k(\gamma+k)^2}\left[\Delta T-\frac{1-e^{-k\Delta T}}{k}\right] \quad , \tag{C.52}$$

$$\frac{2b^2}{\gamma k(\gamma+k)}\left[\frac{1-e^{-(\gamma+2k)\Delta T}}{\gamma+2k}\right] \quad \text{and} \tag{C.53}$$

$$-\frac{2b^2}{k(\gamma+k)^2}\left[\frac{1-e^{-(\gamma+k)\Delta T}}{\gamma+k}\right] \quad . \tag{C.54}$$

The first term, when k goes to zero, has an exponential expansion proportional to k^2, which cancels out with the factor k^2 by which the expression is divided, producing an equation proportional to ΔT^2 and thus, generating ballistic dynamics.

$$\begin{aligned} \frac{2b^2}{k(\gamma+k)^2}\left[\Delta T-\frac{1-e^{-k\Delta T}}{k}\right] \overset{k\to 0}{\approx} & \frac{2b^2}{k(\gamma+k)^2}\left[\Delta T-\frac{1-\left(1-k\Delta T+\frac{k^2\Delta T^2}{2}\right)}{k}\right] \\ \approx & \frac{2b^2}{k(\gamma+k)^2}\left[\Delta T-\frac{k\Delta T}{k}+\frac{k^2\Delta T^2}{2k}\right] \\ \approx & \frac{b^2\Delta T^2}{(\gamma+k)^2} \end{aligned} \tag{C.55}$$

To show that we have non infinite terms, we may sum the last two and find the result

$$\begin{aligned}
\frac{2b^2\left(1-e^{-(\gamma+2k)\Delta T}\right)}{\gamma k(\gamma+k)(\gamma+2k)}-\frac{2b^2\left(1-e^{-(\gamma+k)\Delta T}\right)}{k(\gamma+k)^3} &\overset{k\to 0}{\approx} \frac{2b^2\left(1-e^{-\gamma\Delta T}\right)}{\gamma k(\gamma+k)(\gamma+2k)}-\frac{2b^2\left(1-e^{-\gamma\Delta T}\right)}{k(\gamma+k)^3} \\
&\approx \left(1-e^{-\gamma\Delta T}\right)\left(\frac{2b^2}{\gamma k(\gamma+k)(\gamma+2k)}-\frac{2b^2}{k(\gamma+k)^3}\right) \\
&\approx \frac{2b^2k}{\gamma(\gamma+2k)(\gamma+k)^3}\left(1-e^{-\gamma\Delta T}\right) \quad , \qquad \text{(C.56)}
\end{aligned}$$

which in fact results in a equation that is multiplied by k and not divided, so it must go to zero when $k \to 0$.

Appendix D

Velocity Auto-Correlation Function

The parallel-to-polarization velocity auto-correlation function is a function that shows the velocity correlation between two different instants of time separated by a time interval ΔT. Thus we consider a time $T = n\Delta t$ and another instant of time $T + \Delta T = (n + m)\Delta t$, where Δt is a infinitesimal time interval. The velocity auto-correlation function can then be written as

$$\begin{aligned} VACF(\Delta T) &= \langle \vec{v}_{\parallel}(T) \cdot \vec{v}_{\parallel}(T + \Delta T) \rangle \\ &= \langle v_{\parallel}(T)\hat{p}(t) \cdot \hat{p}(T + \Delta T)v_{\parallel}(T + \Delta T) \rangle \quad , \end{aligned} \tag{D.1}$$

where T represents a determined instant of time and ΔT, an arbitrary time interval. In terms of infinitesimal time intervals Δt, we may write $T = n\Delta t$ and $\Delta T = m\Delta t$ with $n, m \in \mathbb{N}$. Now we have to consider the parallel velocities in times T and $T + \Delta T$, from equation B.5

$$\begin{aligned} \vec{v}_{\parallel}(n\Delta t) &= v_{\parallel}(0)(1 - \gamma\Delta t)^n \prod_{j=0}^{n-1} (\hat{p}_j \cdot \hat{p}_{j+1})\hat{p}_n \\ &\quad + \sum_{i=0}^{n-1} (1 - \gamma\Delta t)^{n-1-i} \prod_{j=i}^{n-1} (\hat{p}_j \cdot \hat{p}_{j+1}) \int_{i\Delta t}^{(i+1)\Delta t} \big(\xi_{\parallel}(s) + b\big)\, ds\, \hat{p}_n \quad \text{and} \end{aligned} \tag{D.2}$$

$$\begin{aligned} \vec{v}_{\parallel}\left((n + m)\Delta t\right) &= v_{\parallel}(0)(1 - \gamma\Delta t)^{n+m} \prod_{j=0}^{n+m-1} (\hat{p}_j \cdot \hat{p}_{j+1})\hat{p}_{n+m} \\ &\quad + \sum_{i=0}^{n+m-1} (1 - \gamma\Delta t)^{n+m-1-i} \prod_{j=i}^{n-1} (\hat{p}_j \cdot \hat{p}_{j+1}) \int_{i\Delta t}^{(i+1)\Delta t} \big(\xi_{\parallel}(s) + b\big)\, ds\, \hat{p}_{n+m} \end{aligned} \tag{D.3}$$

Next, we calculate the product between both velocities and take their average over realizations, which is denoted by the brackets $\langle\,\rangle$. The product becomes

$$\begin{aligned}
\vec{v}_\parallel(T)\cdot\vec{v}_\parallel(T+\Delta T) &= v_\parallel^2(0)(1-\gamma\Delta t)^{2n+m}\prod_{j=0}^{n-1}(\hat{p}_j\cdot\hat{p}_{j+1})\prod_{j=0}^{n+m-1}(\hat{p}_j\cdot\hat{p}_{j+1})(\hat{p}_n\cdot\hat{p}_{n+m}) \\
&+v_\parallel(0)\sum_{l=0}^{n+m-1}(1-\gamma\Delta t)^{2n+m-1-l}\prod_{j=0}^{n+m-1}(\hat{p}_j\cdot\hat{p}_{j+1})\prod_{j=l}^{n-1}(\hat{p}_j\cdot\hat{p}_{j+1})(\hat{p}_n\cdot\hat{p}_{n+m})\int_{l\Delta t}^{(l+1)\Delta t}(\xi_\parallel(s)+b)ds \\
&+v_\parallel(0)\sum_{i=0}^{n-1}(1-\gamma\Delta t)^{2n+m-1-i}\prod_{j=0}^{n+m-1}(\hat{p}_j\cdot\hat{p}_{j+1})\prod_{j=i}^{n-1}(\hat{p}_j\cdot\hat{p}_{j+1})(\hat{p}_n\cdot\hat{p}_{n+m})\int_{i\Delta t}^{(i+1)\Delta t}(\xi_\parallel(s)+b)ds \\
&+\sum_{i=0}^{n-1}\sum_{l=0}^{n+m-1}(1-\gamma\Delta t)^{2n+m-2-i-l}\prod_{j=l}^{n+m-1}(\hat{p}_j\cdot\hat{p}_{j+1})\prod_{j=i}^{n-1}(\hat{p}_j\cdot\hat{p}_{j+1})\int_{l\Delta t}^{(l+1)\Delta t}\int_{i\Delta t}^{(i+1)\Delta t}\xi_\parallel(s')\xi_\parallel(s)ds\,ds' \\
&+\sum_{i=0}^{n-1}\sum_{l=0}^{n+m-1}(1-\gamma\Delta t)^{2n+m-2-i-l}\prod_{j=l}^{n+m-1}(\hat{p}_j\cdot\hat{p}_{j+1})\prod_{j=i}^{n-1}(\hat{p}_j\cdot\hat{p}_{j+1})\int_{l\Delta t}^{(l+1)\Delta t}\int_{i\Delta t}^{(i+1)\Delta t}b^2ds\,ds' \quad ,
\end{aligned}$$

we know that $\hat{p}_i\cdot\hat{p}_{i+1}=cos(\Delta\theta)$ for an arbitrary integer i, we also know from appendix F that $\hat{p}_{i+n}\cdot\hat{p}_i=cos(n\,\Delta\theta)$ and $\langle\hat{p}_{i+n}\cdot\hat{p}_i\rangle=\langle cos(n\,\Delta\theta)\rangle$ which can be approximated to $\langle cos(n\,\Delta\theta)\rangle\approx(1-k\Delta t)^n$, a conclusion reached from equation (F.15). In other words, the sequence of inner products of polarization vectors $\langle\prod_{j=n}^{m}(\hat{p}_j\cdot\hat{p}_{j+1})\rangle=\langle\hat{p}_n\cdot\hat{p}_m\rangle=(1-k\Delta t)^{|m-n|}$.

We also know that the averages of the random variables $\langle\xi_\parallel(s)\rangle=0$ because of their symmetrical Gaussian distribution around zero. For the products between two distinct Wiener variables, we know $\langle\xi_\parallel(s)\xi_\parallel(s')\rangle=g\,\delta(s-s')$ which become $\langle\xi_\parallel(s)\xi_\parallel(s')\rangle=g\,\delta_{i,l}$ when considering that the variables s and s' depend on the summation indexes i and l. Following these, we denote $\langle\vec{v}_\parallel(T)\cdot\vec{v}_\parallel(T+\Delta T)\rangle$ as $VACF(\Delta T)$ and proceed to obtain

$$\begin{aligned}
VACF(\Delta T) &= v_\parallel^2(0)(1-\gamma\Delta t)^{2n+m}(1-k\Delta t)^{2n+m-2}(1-k\Delta t)^{n+m-n} \\
&+v_\parallel(0)\sum_{l=0}^{n+m-1}(1-\gamma\Delta t)^{2n+m-1-l}(1-k\Delta t)^{2n+m-2-l}(1-k\Delta t)^{n+m-n}\int_{l\Delta t}^{(l+1)\Delta t}b\,ds \\
&+v_\parallel(0)\sum_{i=0}^{n-1}(1-\gamma\Delta t)^{2n+m-1-i}(1-k\Delta t)^{2n+m-2-i}(1-k\Delta t)^{n+m-n}\int_{i\Delta t}^{(i+1)\Delta t}b\,ds \\
&+\sum_{i=0}^{n-1}\sum_{l=0}^{n+m-1}(1-\gamma\Delta t)^{2n+m-2-i-l}(1-k\Delta t)^{2n+m-2-i-l}(1-k\Delta t)^{n+m-n}\int_{l\Delta t}^{(l+1)\Delta t}\int_{i\Delta t}^{(i+1)\Delta t}g\delta(s-s')ds\,ds' \\
&+\sum_{i=0}^{n-1}\sum_{l=0}^{n+m-1}(1-\gamma\Delta t)^{2n+m-2-i-l}(1-k\Delta t)^{2n+m-2-i-l}(1-k\Delta t)^{n+m-n}\int_{l\Delta t}^{(l+1)\Delta t}\int_{i\Delta t}^{(i+1)\Delta t}b^2ds\,ds' \quad ,
\end{aligned} \tag{D.4}$$

now, with an equation without stochastic variables, the integrals' solutions become trivial

$$\begin{aligned} VACF(\Delta T) &= v_{\parallel}^2(0)(1-\gamma\Delta t)^{2n+m}(1-k\Delta t)^{2n+m-2}(1-k\Delta t)^{n+m-n} \\ &+b\Delta t\, v_{\parallel}(0)\sum_{l=0}^{n+m-1}(1-\gamma\Delta t)^{2n+m-1-l}(1-k\Delta t)^{2n+m-2-l}(1-k\Delta t)^{n+m-n} \\ &+b\Delta t\, v_{\parallel}(0)\sum_{i=0}^{n-1}(1-\gamma\Delta t)^{2n+m-1-i}(1-k\Delta t)^{2n+m-2-i}(1-k\Delta t)^{n+m-n} \\ &+\sum_{i=0}^{n-1}\sum_{l=0}^{n+m-1}(1-\gamma\Delta t)^{2n+m-2-i-l}(1-k\Delta t)^{2n+m-2-i-l}(1-k\Delta t)^{n+m-n}\int_{i\Delta t}^{(i+1)\Delta t} g\delta_{i,l}ds \\ &+b^2\Delta t^2\sum_{i=0}^{n-1}\sum_{l=0}^{n+m-1}(1-\gamma\Delta t)^{2n+m-2-i-l}(1-k\Delta t)^{2n+m-2-i-l}(1-k\Delta t)^{n+m-n} \quad \text{then} \end{aligned} \tag{D.5}$$

solving the only remaining integral over g, we have

$$VACF(\Delta T) = v_{\parallel}^2(0)(1-\gamma\Delta t)^{2n+m}(1-k\Delta t)^{2n+m-2}(1-k\Delta t)^{n+m-n} \tag{D.6}$$

$$+b\Delta t\, v_{\parallel}(0)\sum_{l=0}^{n+m-1}(1-\gamma\Delta t)^{2n+m-1-l}(1-k\Delta t)^{2n+m-2-l}(1-k\Delta t)^{n+m-n} \tag{D.7}$$

$$+b\Delta t\, v_{\parallel}(0)\sum_{i=0}^{n-1}(1-\gamma\Delta t)^{2n+m-1-i}(1-k\Delta t)^{2n+m-2-i}(1-k\Delta t)^{n+m-n} \tag{D.8}$$

$$+g\Delta t\sum_{i=0}^{n-1}(1-\gamma\Delta t)^{2n+m-2-2i}(1-k\Delta t)^{2n+m-2-2i}(1-k\Delta t)^{n+m-n} \tag{D.9}$$

$$+b^2\Delta t^2\sum_{i=0}^{n-1}\sum_{l=0}^{n+m-1}(1-\gamma\Delta t)^{2n+m-2-i-l}(1-k\Delta t)^{2n+m-2-i-l}(1-k\Delta t)^{n+m-n}\quad , \tag{D.10}$$

to proceed, we must use the identities

$$\sum_{i=a}^{b}(1-x\,\Delta t)^i = \frac{(1-x\,\Delta t)^a-(1-x\,\Delta t)^b}{1-(1-x\,\Delta t)} \quad \text{and} \tag{D.11}$$

$$(1-x\Delta t)^N \overset{N\to\infty;\Delta t\to 0}{=} e^{-x\,N\,\Delta t} \tag{D.12}$$

where x is an arbitrary constant and a, b and N are arbitrary integers. We also divide the the velocity auto-correlation function into separate terms for more clarity in the calculations.

$$\begin{aligned} (D.6) &= v_{\parallel}^2(0)(1-\gamma\Delta t)^{2n+m}(1-k\Delta t)^{2n+m-2}(1-k\Delta t)^{n+m-n} \\ &= v_{\parallel}^2(0)e^{-\gamma(2n+m)\Delta t}(1-k\Delta t)^{2n+2m-2} \\ &= v_{\parallel}^2(0)e^{-\gamma(2n+m)\Delta t}e^{-k(2n+2m-2)\Delta t}\quad , \end{aligned}$$

considering that $n\Delta t = T$ and $m\Delta t = \Delta T$ (we may rule out the exponential $e^{-2\Delta t}$, for 2 is much smaller than the other terms m and n), then

$$(D.6) = v_{\parallel}^2(0)e^{-2(\gamma+k)T}e^{-(\gamma+2k)\Delta T}\quad .$$

The following results are obtained in a similar way

$$\begin{aligned}(D.7) &= b\Delta t\, v_{\parallel}(0) \sum_{l=0}^{n+m-1} (1-\gamma\Delta t)^{2n+m-1-l}(1-k\Delta t)^{2n+m-2-l}(1-k\Delta t)^{n+m-n} \\ &= b\Delta t\, v_{\parallel}(0) \sum_{l=0}^{n+m-1} (1-\gamma\Delta t)^{2n+m-1-l}(1-k\Delta t)^{2n+2m-2-l} \quad ,\end{aligned}$$

here, we note that it is possible to rewrite a summation as follows

$$\sum_{i=0}^{n-1} x^{n-i} = \sum_{i=1}^{n} x^{i} \quad , \tag{D.13}$$

where x is an arbitrary variable, the only difference in the summations, being that the left side starts to sum from the bigger powers to the smaller ones and the right side does the opposite, applying the same concept for expression (D.7), we obtain

$$\begin{aligned}(D.7) &= b\Delta t\,(1-\gamma\Delta t)^{n}(1-k\Delta t)^{n+m-1} v_{\parallel}(0) \sum_{l=0}^{n+m-1} (1-\gamma\Delta t)^{n+m-1-l}(1-k\Delta t)^{n+m-1-l} \\ &= b\Delta t\,(1-\gamma\Delta t)^{n}(1-k\Delta t)^{n+m-1} v_{\parallel}(0) \sum_{l=1}^{n+m} (1-\gamma\Delta t)^{l}(1-k\Delta t)^{l} \\ &= b\Delta t\, e^{-\gamma\, n\Delta t} e^{-k(n+m-1)\Delta t} v_{\parallel}(0) \sum_{l=1}^{n+m} (1-\gamma\Delta t)^{l}(1-k\Delta t)^{l} \\ &= b\Delta t\, e^{-\gamma\, n\Delta t} e^{-k(n+m-1)\Delta t} v_{\parallel}(0) \frac{1-(1-\gamma\Delta t)^{n+m}(1-k\Delta t)^{n+m}}{1-(1-\gamma\Delta t)(1-k\Delta t)} \quad ,\end{aligned}$$

where we may consider that $(1-\gamma\Delta t)(1-k\Delta t) = 1-k\Delta t-\gamma\Delta t$ due to the fact that $\Delta t^2 << \Delta t$ (we rule out the term $\gamma\, k\Delta t^2$), we also assume that $(1-\gamma\Delta t)^1(1-k\Delta t)^1 = 1$, because $1 >> \Delta t$, thus obtaining

$$\begin{aligned}(D.7) &= b\Delta t\, e^{-\gamma\, n\Delta t} e^{-k(n+m-1)\Delta t} v_{\parallel}(0) \frac{1-e^{-(\gamma+k)(n+m)\Delta t}}{(\gamma+k)\Delta t} \\ &= \frac{b v_{\parallel}(0)}{\gamma+k}\, e^{-\gamma\, n\Delta t} e^{-k(n+m-1)\Delta t} \left(1-e^{-(\gamma+k)(n+m)\Delta t}\right) \\ &= \frac{b v_{\parallel}(0)}{\gamma+k}\, e^{-(\gamma+k)T} e^{-k\Delta T} \left(1-e^{-(\gamma+k)(T+\Delta T)}\right) \quad .\end{aligned} \tag{D.14}$$

We then proceed to obtain (D.8)

$$
\begin{aligned}
(D.8) &= b\Delta t\, v_{\parallel}(0) \sum_{i=0}^{n-1} (1-\gamma\Delta t)^{2n+m-1-i}(1-k\Delta t)^{2n+m-2-i}(1-k\Delta t)^{n+m-n} \\
&= b\Delta t\, (1-\gamma\Delta t)^{n+m}(1-k\Delta t)^{n+2m-1} v_{\parallel}(0) \sum_{i=0}^{n-1} (1-\gamma\Delta t)^{n-1-i}(1-k\Delta t)^{n-1-i} \\
&= b\Delta t\, e^{-\gamma(n+m)\Delta t} e^{-k(n+2m-1)\Delta t} v_{\parallel}(0) \sum_{i=1}^{n} (1-\gamma\Delta t)^{i}(1-k\Delta t)^{i} \\
&= b\Delta t\, e^{-\gamma(n+m)\Delta t} e^{-k(n+2m-1)\Delta t} v_{\parallel}(0) \frac{(1-\gamma\Delta t)(1-k\Delta t) - (1-\gamma\Delta t)^{n}(1-k\Delta t)^{n}}{1-(1-\gamma\Delta t)(1-k\Delta t)} \\
&= b\Delta t\, e^{-\gamma(n+m)\Delta t} e^{-k(n+2m-1)\Delta t} v_{\parallel}(0) \frac{1-e^{-(\gamma+k)\, n\, \Delta t}}{1-(1-(\gamma+k)\Delta t)} \\
&= b v_{\parallel}(0)\Delta t\, e^{-\gamma(T+\Delta T)} e^{-k(T+2\Delta T)} \frac{1-e^{-(\gamma+k)\, n\, \Delta t}}{(\gamma+k)\Delta t} \\
&= \frac{b v_{\parallel}(0)}{(\gamma+k)}\, e^{-\gamma(T+\Delta T)} e^{-k(T+2\Delta T)} \left(1-e^{-(\gamma+k)T}\right) \\
&= \frac{b v_{\parallel}(0)}{(\gamma+k)}\, e^{-(\gamma+k)T} e^{-(\gamma+2k)\Delta T} \left(1-e^{-(\gamma+k)T}\right) \quad ,
\end{aligned}
$$

which ends our calculations for (D.8), proceeding to the next we have

$$
\begin{aligned}
(D.9) &= g\Delta t \sum_{i=0}^{n-1}(1-\gamma\Delta t)^{2n+m-2-2i}(1-k\Delta t)^{2n+m-2-2i}(1-k\Delta t)^{n+m-n} \\
&= g\Delta t \sum_{i=0}^{n-1}(1-\gamma\Delta t)^{2n+m-2-2i}(1-k\Delta t)^{2n+2m-2-2i} \\
&= g\Delta t\,(1-\gamma\Delta t)^{m}(1-k\Delta t)^{2m}\sum_{i=0}^{n-1}(1-\gamma\Delta t)^{2n-2-2i}(1-k\Delta t)^{2n-2-2i} \\
&= g\Delta t\,e^{-(\gamma+2k)\,m\,\Delta t}\sum_{i=0}^{n-1}(1-\gamma\Delta t)^{2n-2-2i}(1-k\Delta t)^{2n-2-2i} \\
&= g\Delta t\,e^{-(\gamma+2k)\,m\,\Delta t}\sum_{i=1}^{n}(1-\gamma\Delta t)^{2i}(1-k\Delta t)^{2i} \\
&= g\Delta t\,e^{-(\gamma+2k)\Delta T}\frac{1-(1-\gamma\Delta t)^{2n}(1-k\Delta t)^{2n}}{1-(1-\gamma\Delta t)^{2}(1-k\Delta t)^{2}} \\
&= g\Delta t\,e^{-(\gamma+2k)\Delta T}\frac{1-e^{-2(\gamma+k)T}}{1-\big(1-2(\gamma+k)\Delta t\big)} \\
&= g\Delta t\,e^{-(\gamma+2k)\Delta T}\frac{1-e^{-2(\gamma+k)T}}{2(\gamma+k)\Delta t\big)} \\
&= \frac{g}{2(\gamma+k)}\,e^{-(\gamma+2k)\Delta T}\left(1-e^{-2(\gamma+k)T}\right) \quad .
\end{aligned}
$$

The last term is

$$
\begin{aligned}
D.10 &= b^2\Delta t^2\sum_{i=0}^{n-1}\sum_{l=0}^{n+m-1}(1-\gamma\Delta t)^{2n+m-2-i-l}(1-k\Delta t)^{2n+m-2-i-l}(1-k\Delta t)^{n+m-n} \\
&= b^2\Delta t^2\sum_{i=0}^{n-1}\sum_{l=0}^{n+m-1}(1-\gamma\Delta t)^{2n+m-2-i-l}(1-k\Delta t)^{2n+2m-2-i-l} \\
&= b^2\Delta t^2\,(1-k\Delta t)^{m}\sum_{i=0}^{n-1}(1-\gamma\Delta t)^{n-1-i}(1-k\Delta t)^{n-1-i}\sum_{l=0}^{n+m-1}(1-\gamma\Delta t)^{n+m-1-l}(1-k\Delta t)^{n+m-1-l} \\
&= b^2\Delta t^2\,(1-k\Delta t)^{m}\sum_{i=1}^{n}(1-\gamma\Delta t)^{i}(1-k\Delta t)^{i}\sum_{l=1}^{n+m}(1-\gamma\Delta t)^{l}(1-k\Delta t)^{l} \\
&= b^2\Delta t^2\,(1-k\Delta t)^{m}\frac{1-(1-\gamma\Delta t)^{n}(1-k\Delta t)^{n}}{1-(1-\gamma\Delta t)(1-k\Delta t)}\frac{1-(1-\gamma\Delta t)^{n+m}(1-k\Delta t)^{n+m}}{1-(1-\gamma\Delta t)(1-k\Delta t)} \\
&= b^2\Delta t^2\,e^{-k\Delta T}\frac{1-e^{-(\gamma+k)T}}{(\gamma+k)\Delta t}\frac{1-e^{-(\gamma+k)(T+\Delta T)}}{(\gamma+k)\Delta t} \\
&= \frac{b^2}{(\gamma+k)^2}e^{-k\Delta T}\left(1-e^{-(\gamma+k)T}\right)\left(1-e^{-(\gamma+k)(T+\Delta T)}\right) \quad .
\end{aligned}
$$

To find the total parallel-to-polarization velocity we must sum the obtained expressions for (D.6), (D.7), (D.8), (D.9), and (D.10)

$$\begin{aligned} VACF(\Delta T) &= \langle \vec{v}_{\parallel}(T) \cdot \vec{v}_{\parallel}(T+\Delta T) \rangle = (D.6) + (D.7) + (D.8) + (D.9) + (D.10) \\ &= v_{\parallel}^2(0) e^{-2(\gamma+k)T} e^{-(\gamma+2k)\Delta T} \\ &\quad + \frac{b v_{\parallel}(0)}{\gamma+k} e^{-(\gamma+k)T} e^{-k\Delta T} \left(1 - e^{-(\gamma+k)(T+\Delta T)}\right) \\ &\quad + \frac{b v_{\parallel}(0)}{(\gamma+k)} e^{-(\gamma+k)T} e^{-(\gamma+2k)\Delta T} \left(1 - e^{-(\gamma+k)T}\right) \\ &\quad + \frac{g}{2(\gamma+k)} e^{-(\gamma+2k)\Delta T} \left(1 - e^{-2(\gamma+k)T}\right) \\ &\quad + \frac{b^2}{(\gamma+k)^2} e^{-k\Delta T} \left(1 - e^{-(\gamma+k)T}\right) \left(1 - e^{-(\gamma+k)(T+\Delta T)}\right) \quad . \end{aligned}$$

To continue the solution, we have to assume that the system has reached a stationary state where $\langle v_{\parallel}(0) \rangle = \frac{b}{\gamma+k}$ and $\langle v_{\parallel}^2(0) \rangle = \frac{g}{2(\gamma+k)} + \frac{b^2}{(\gamma+k)^2}$, results obtained in appendix B. Substituting these terms into the above expression, we reach

$$\begin{aligned} VACF(\Delta T) &= \left(\frac{g}{2(\gamma+k)} + \frac{b^2}{(\gamma+k)^2} \right) e^{-2(\gamma+k)T} e^{-(\gamma+2k)\Delta T} \\ &\quad + \frac{b^2}{(\gamma+k)^2} e^{-(\gamma+k)T} e^{-k\Delta T} \left(1 - e^{-(\gamma+k)(T+\Delta T)}\right) \\ &\quad + \frac{b^2}{(\gamma+k)^2} e^{-(\gamma+k)T} e^{-(\gamma+2k)\Delta T} \left(1 - e^{-(\gamma+k)T}\right) \\ &\quad + \frac{g}{2(\gamma+k)} e^{-(\gamma+2k)\Delta T} \left(1 - e^{-2(\gamma+k)T}\right) \\ &\quad + \frac{b^2}{(\gamma+k)^2} e^{-k\Delta T} \left(1 - e^{-(\gamma+k)T}\right) \left(1 - e^{-(\gamma+k)(T+\Delta T)}\right) \quad , \end{aligned}$$

the substitution allows us to cancel a series of terms

$$\begin{aligned} VACF(\Delta T) &= \left(\cancel{\frac{g}{2(\gamma+k)}} + \cancel{\frac{b^2}{(\gamma+k)^2}} \right) e^{-2(\gamma+k)T} e^{-(\gamma+2k)\Delta T} \\ &\quad + \cancel{\frac{b^2}{(\gamma+k)^2} e^{-(\gamma+k)T} e^{-k\Delta T} \left(1 - e^{-(\gamma+k)(T+\Delta T)}\right)} \\ &\quad + \frac{b^2}{(\gamma+k)^2} e^{-(\gamma+k)T} e^{-(\gamma+2k)\Delta T} \left(1 - \cancel{e^{-(\gamma+k)T}}\right) \\ &\quad + \frac{g}{2(\gamma+k)} e^{-(\gamma+2k)\Delta T} \left(1 - \cancel{e^{-2(\gamma+k)T}}\right) \\ &\quad + \frac{b^2}{(\gamma+k)^2} e^{-k\Delta T} \left(1 - \cancel{e^{-(\gamma+k)T}}\right) \left(1 - e^{-(\gamma+k)(T+\Delta T)}\right) \quad , \end{aligned}$$

leaving us with

$$\begin{aligned} VACF(\Delta T) &= \cancel{\frac{b^2}{(\gamma+k)^2}\, e^{-(\gamma+k)T}\, e^{-(\gamma+2k)\Delta T}} \\ &\quad + \frac{g}{2(\gamma+k)}\, e^{-(\gamma+2k)\Delta T} \\ &\quad + \frac{b^2}{(\gamma+k)^2} e^{-k\Delta T} \left(1 - \cancel{e^{-(\gamma+k)(T+\Delta T)}}\right) \\ &= \frac{g}{2(\gamma+k)}\, e^{-(\gamma+2k)\Delta T} + \frac{b^2}{(\gamma+k)^2} e^{-k\Delta T} \quad , \end{aligned} \tag{D.15}$$

and that is the final analytical solution for the parallel-to-polarization velocity auto-correlation function

$$VACF(\Delta T) = \frac{g}{2(\gamma+k)}\, e^{-(\gamma+2k)\Delta T} + \frac{b^2}{(\gamma+k)^2} e^{-k\Delta T} \quad . \tag{D.16}$$

Note that when $\Delta T \to 0$, we obtain

$$VACF(\Delta T) \overset{\Delta T \to 0}{=} \frac{g}{2(\gamma+k)} + \frac{b^2}{(\gamma+k)^2} = \langle v_{\parallel}^2 \rangle \quad , \tag{D.17}$$

which is the expected result, because if the interval between the two velocities goes to zero, the velocity auto-correlation function simply becomes the average of the squared velocity $\langle \vec{v}_{\parallel}(T) \cdot \vec{v}_{\parallel}(T+\Delta T) \rangle \overset{\Delta T \to 0}{=} \langle \vec{v}_{\parallel}(T) \cdot \vec{v}_{\parallel}(T) \rangle = \langle v_{\parallel}^2(T) \rangle$. Also note that when $\Delta T \to \infty$ we obtain $VACF(\Delta T \to \infty) = 0$ due to to the zeroing of the exponential terms, which is another expected result, since the auto-correlation of a stochastic with times separated by an infinite interval should be also zero as the particle has forgotten its initial state velocity.

Appendix E

Mean Velocity Autocorrelation Function

From appendix C, equation (C.9), we know that a particle's general position for the biased anisotropic Ornstein-Uhlenbeck system may be written as

$$\begin{aligned}\vec{r}\,((N+1)\Delta t) &= \vec{r}(0) + \Delta t\; v_{\parallel}(0)\sum_{m=0}^{N}(1-\gamma\Delta t)^{n}\prod_{i=0}^{n-1}(\hat{p}_i\cdot\hat{p}_{i+1})\hat{p}_m \\ &+\Delta t\;\sum_{m=0}^{N}\sum_{j=0}^{n-1}(1-\gamma\Delta t)^{n-1-j}\prod_{i=j}^{n-1}(\hat{p}_i\cdot\hat{p}_{i+1})\int_{j\Delta t}^{(j+1)\Delta t}(\xi_{\parallel}(s)+b)ds\,\hat{p}_m \\ &+\Delta t\;\sum_{m=0}^{N}\int_{n\Delta t}^{(n+1)\Delta t}[(n+1)\Delta t - s]\xi_{\parallel}(s)ds\,\hat{p}_m \\ &+\sum_{m=0}^{N}\int_{n\Delta t}^{(n+1)\Delta t}\xi_{\perp}(s)ds\,\hat{n}_m\end{aligned}$$

we may use this result to obtain an average velocity that depends upon a time interval $\delta = \Delta N\,\Delta t$, being ΔN an arbitrary integer. Thus, we define an average velocity at time $T = N\Delta t\,;\; N \in \mathbb{N}$ as

$$\vec{v}(T,\delta) = \frac{\vec{r}(T+\delta)-\vec{r}(T)}{\delta} \quad , \tag{E.1}$$

with the definition of the average velocity, we now propose the measure of the mean velocity auto-correlation function (**MVACF**)

$$\begin{aligned}\text{MVACF}(\Delta T,\delta) &= \langle\vec{v}(T,\delta)\cdot\vec{v}(T+\Delta T,\delta)\rangle \\ &= \left\langle\frac{\vec{r}(T+\delta)-\vec{r}(T)}{\delta}\cdot\frac{\vec{r}(T+\Delta T+\delta)-\vec{r}(T+\Delta T)}{\delta}\right\rangle \quad ,\end{aligned} \tag{E.2}$$

where $\Delta T = M\Delta t$. To proceed with the calculations, we the need to discover the equations for $\vec{r}(T+\delta)-\vec{r}(T)$ and $\vec{r}(T+\Delta T+\delta)-\vec{r}(T+\Delta T)$, which is easily obtained by subtracting

the general position for the particle at two different times

$$\begin{aligned}
\vec{r}\,((N+\Delta N)\Delta t) - \vec{r}(N\Delta t) &= \vec{r}(0) + \Delta t\; v_{\parallel}(0) \sum_{m=0}^{N+\Delta N} (1-\gamma\Delta t)^n \prod_{i=0}^{n-1} (\hat{p}_i \cdot \hat{p}_{i+1}) \hat{p}_m \\
&+\Delta t \sum_{m=0}^{N+\Delta N} \sum_{j=0}^{n-1} (1-\gamma\Delta t)^{n-1-j} \prod_{i=j}^{n-1} (\hat{p}_i \cdot \hat{p}_{i+1}) \int_{j\Delta t}^{(j+1)\Delta t} (\xi_{\parallel}(s)+b) ds\, \hat{p}_m \\
&+\Delta t \sum_{m=0}^{N+\Delta N} \int_{n\Delta t}^{(n+1)\Delta t} [(n+1)\Delta t - s] \xi_{\parallel}(s) ds\, \hat{p}_m \\
&+ \sum_{m=0}^{N+\Delta N} \int_{n\Delta t}^{(n+1)\Delta t} \xi_{\perp}(s) ds\, \hat{n}_m \\
&-\vec{r}(0) - \Delta t\; v_{\parallel}(0) \sum_{q=0}^{N} (1-\gamma\Delta t)^n \prod_{i=0}^{n-1} (\hat{p}_i \cdot \hat{p}_{i+1}) \hat{p}_q \\
&-\Delta t \sum_{q=0}^{N} \sum_{j=0}^{n-1} (1-\gamma\Delta t)^{n-1-j} \prod_{i=j}^{n-1} (\hat{p}_i \cdot \hat{p}_{i+1}) \int_{j\Delta t}^{(j+1)\Delta t} (\xi_{\parallel}(s)+b) ds\, \hat{p}_q \\
&-\Delta t \sum_{q=0}^{N} \int_{n\Delta t}^{(n+1)\Delta t} [(n+1)\Delta t - s] \xi_{\parallel}(s) ds\, \hat{p}_q \\
&- \sum_{q=0}^{N} \int_{n\Delta t}^{(n+1)\Delta t} \xi_{\perp}(s) ds\, \hat{n}_q \quad ,
\end{aligned}$$

because the expressions are the same until a certain point, the equivalent parts cancel each other, leaving only the summation indexes that remain between the position of smaller times and the one at greater times, i.e.

$$\begin{aligned}
\Delta\vec{r}\big((N+\Delta N)\Delta t\big) &= \vec{r}\,((N+\Delta N)\Delta t) - \vec{r}(N\Delta t) \\
&= \Delta t\; v_{\parallel}(0) \sum_{m=N}^{N+\Delta N} (1-\gamma\Delta t)^m \prod_{i=0}^{m-1} (\hat{p}_i \cdot \hat{p}_{i+1}) \hat{p}_m && \text{(E.3)} \\
&+\Delta t \sum_{m=N}^{N+\Delta N} \sum_{j=0}^{m-1} (1-\gamma\Delta t)^{m-1-j} \prod_{i=j}^{m-1} (\hat{p}_i \cdot \hat{p}_{i+1}) \int_{j\Delta t}^{(j+1)\Delta t} (\xi_{\parallel}(s)+b) ds\, \hat{p}_m && \text{(E.4)} \\
&+\Delta t \sum_{m=N}^{N+\Delta N} \int_{m\Delta t}^{(m+1)\Delta t} [(m+1)\Delta t - s] \xi_{\parallel}(s) ds\, \hat{p}_m && \text{(E.5)} \\
&+ \sum_{m=N}^{N+\Delta N} \int_{m\Delta t}^{(m+1)\Delta t} \xi_{\perp}(s) ds\, \hat{n}_m \quad . && \text{(E.6)}
\end{aligned}$$

observe that the indexes present on the sum expressions, now start from $m = N$ and go to $m = N + \Delta N$, now we have a general expression for a position separated by an arbitrary time interval, to find its average velocity, it is only necessary to divide the expression by δ, however we will not do it for now. The second position interval we want is $\vec{r}(T + \Delta T + \delta) -$

$\vec{r}(T+\Delta T)$, easily obtained through the process stated earlier

$$\begin{aligned}
\Delta\vec{r}\big((N+M+\Delta N)\Delta t\big) &= \vec{r}\big((N+M+\Delta N)\Delta t\big) - \vec{r}\big((N+M)\Delta t\big) \\
&= \Delta t\, v_{\parallel}(0) \sum_{q=N+M}^{N+M+\Delta N} (1-\gamma\Delta t)^q \prod_{i=0}^{q-1} (\hat{p}_i \cdot \hat{p}_{i+1})\hat{p}_q && \text{(E.7)} \\
&\quad +\Delta t \sum_{q=N+M}^{N+M+\Delta N} \sum_{j=0}^{q-1} (1-\gamma\Delta t)^{q-1-j} \prod_{i=j}^{q-1} (\hat{p}_i \cdot \hat{p}_{i+1}) \int_{j\Delta t}^{(j+1)\Delta t} (\xi_{\parallel}(s)+b)ds\,\hat{p}_q && \text{(E.8)} \\
&\quad +\Delta t \sum_{q=N+M}^{N+M+\Delta N} \int_{q\Delta t}^{(q+1)\Delta t} [(q+1)\Delta t - s]\xi_{\parallel}(s)ds\,\hat{p}_q && \text{(E.9)} \\
&\quad + \sum_{q=N+M}^{N+M+\Delta N} \int_{q\Delta t}^{(q+1)\Delta t} \xi_{\perp}(s)ds\,\hat{n}_q \quad . && \text{(E.10)}
\end{aligned}$$

The only thing remaining to do to obtain the mean velocity auto-correlation is to multiply both expressions (E.3-E.6) and (E.7-E.10) and take their average. However, because both expressions are too big, we will name each part of it and obtain the multiplication of the terms separately $(E.3) \equiv \vec{A}_1$, $(E.4) \equiv \vec{A}_2$, $(E.5) \equiv \vec{A}_3$, $(E.6) \equiv \vec{A}_4$ and $(E.7) \equiv \vec{B}_1$, $(E.8) \equiv \vec{B}_2$, $(E.9) \equiv \vec{B}_3$, $(E.10) \equiv \vec{B}_4$. The multiplication of both expressions would result in 16 terms ($\vec{A}_i \cdot \vec{B}_j,\ i,j \in [1,4]$), however some of these terms go to zero, if the series multiplication has a power of Δt greater than the number of summations, then it goes to zero as $\Delta t \to 0$, this happens because at every summation, we get something of the form

$$\sum_{i=a}^{b}(1-x\Delta t)^i = \frac{(1-x\Delta t)^a - (1-x\Delta t)^{b+1}}{1-(1-x\Delta t)} = \frac{(1-x\Delta t)^a - (1-x\Delta t)^{b+1}}{x\Delta t} \quad , \qquad \text{(E.11)}$$

with x being an arbitrary value, observe that every summation of a term of the form $(1-x\Delta t)$, is equivalent to a power divided by $x\Delta t$, thus if the average of an arbitrary multiplication $\vec{A}_3 \cdot \vec{B}_3$, for instance, is multiplied by Δt to a higher power than it has summation terms, it becomes proportional to some positive power of Δt, which is much smaller than unit and can be ruled out, the only multiplication where this does not happen is $\vec{A}_1 \cdot \vec{B}_1$, $\vec{A}_1 \cdot \vec{B}_2$, $\vec{A}_2 \cdot \vec{B}_1$

and $\vec{A}_2 \cdot \vec{B}_2$. Starting with $\vec{A}_1 \cdot \vec{B}_1$, we have

$$\begin{aligned}
\left\langle \vec{A}_1 \cdot \vec{B}_1 \right\rangle &= \left\langle \Delta t\, v_\parallel(0) \sum_{m=N}^{N+\Delta N} (1-\gamma\Delta t)^m \prod_{i=0}^{m-1} (\hat{p}_i \cdot \hat{p}_{i+1}) \hat{p}_m \right. \\
&\quad \left. \cdot \Delta t\, v_\parallel(0) \sum_{q=N+M}^{N+M+\Delta N} (1-\gamma\Delta t)^q \prod_{i=0}^{q-1} (\hat{p}_i \cdot \hat{p}_{i+1}) \hat{p}_q \right\rangle \\
&= \Delta t^2 v_\parallel^2(0) \sum_{m=N}^{N+\Delta N} \sum_{q=N+M}^{N+M+\Delta N} (1-\gamma\Delta t)^{m+q} \left\langle \prod_{i=0}^{m-1} (\hat{p}_i \cdot \hat{p}_{i+1}) \prod_{j=0}^{q-1} (\hat{p}_j \cdot \hat{p}_{j+1}) (\hat{p}_m \cdot \hat{p}_q) \right\rangle \\
&= \Delta t^2 v_\parallel^2(0) \sum_{m=N}^{N+\Delta N} \sum_{q=N+M}^{N+M+\Delta N} (1-\gamma\Delta t)^{m+q} (1-k\Delta t)^{m-1} (1-k\Delta t)^{q-1} (1-k\Delta t)^{|q-m|} \quad ,
\end{aligned}$$

where $\left\langle \prod_{i=a}^{b} (\hat{p}_i \cdot \hat{p}_{i+1}) \right\rangle = (1-k\Delta t)^{|b-a|}$ and $\langle (\hat{p}_a \cdot \hat{p}_b) \rangle = (1-k\Delta t)^{|b-a|}$, the demonstration of these identities can be found in appendix F. Because $q > m \,\forall\, q, m$, we know that $|q-m| = q-m$, which takes us to

$$\begin{aligned}
\left\langle \vec{A}_1 \cdot \vec{B}_1 \right\rangle &= \Delta t^2 v_\parallel^2(0) \sum_{m=N}^{N+\Delta N} \sum_{q=N+M}^{N+M+\Delta N} (1-\gamma\Delta t)^{m+q} (1-k\Delta t)^{m-1} (1-k\Delta t)^{q-1} (1-k\Delta t)^{q-m} \\
&= \Delta t^2 v_\parallel^2(0) \sum_{m=N}^{N+\Delta N} \sum_{q=N+M}^{N+M+\Delta N} (1-\gamma\Delta t)^{m+q} (1-k\Delta t)^{2q-1} \\
&= \Delta t^2 v_\parallel^2(0) \sum_{m=N}^{N+\Delta N} (1-\gamma\Delta t)^m \sum_{q=N+M}^{N+M+\Delta N} (1-\gamma\Delta t)^q (1-k\Delta t)^{2q-1} \\
&= \Delta t^2 v_\parallel^2(0) \left(\frac{(1-\gamma\Delta t)^N - (1-\gamma\Delta t)^{N+\Delta N}}{1-(1-\gamma\Delta t)} \right) \\
&\quad \times \left(\frac{(1-\gamma\Delta t)^{N+M}(1-k\Delta t)^{2(N+M)} - (1-\gamma\Delta t)^{N+M+\Delta N}(1-k\Delta t)^{2(N+M+\Delta N)}}{1-(1-\gamma\Delta t)(1-k\Delta t)^2} \right) \\
&= \Delta t^2 v_\parallel^2(0) \left(\frac{e^{-\gamma N\Delta t} - e^{-\gamma(N+\Delta N)\Delta t}}{\gamma\Delta t} \right) e^{-(\gamma+2k)(N+M)\Delta t} \left(\frac{1-e^{-\gamma\Delta N\Delta t} e^{-2k\Delta N\Delta t}}{(\gamma+2k)\Delta t} \right) \\
&= v_\parallel^2(0) e^{-\gamma N\Delta t} \left(\frac{1-e^{-\gamma\Delta N\Delta t}}{\gamma} \right) e^{-(\gamma+2k)(N+M)\Delta t} \left(\frac{1-e^{-(\gamma+2k)\Delta N\Delta t}}{(\gamma+2k)} \right) \\
&= v_\parallel^2(0) e^{-\gamma T} \left(\frac{1-e^{-\gamma\delta}}{\gamma} \right) e^{-(\gamma+2k)(T+\Delta T)} \left(\frac{1-e^{-(\gamma+2k)\delta}}{(\gamma+2k)} \right) \\
&= \frac{v_\parallel^2(0)}{\gamma(\gamma+2k)} e^{-\gamma T} e^{-(\gamma+2k)(T+\Delta T)} \left(1-e^{-\gamma\delta}\right)\left(1-e^{-(\gamma+2k)\delta}\right) \quad ,
\end{aligned}$$

which ends our calculation for the first term, the second one $\left\langle \vec{A}_1 \cdot \vec{B}_2 \right\rangle$ is obtained through

similar procedures

$$\left\langle \vec{A}_1 \cdot \vec{B}_2 \right\rangle = \left\langle \Delta t \; v_{\parallel}(0) \sum_{m=N}^{N+\Delta N} (1-\gamma\Delta t)^m \prod_{i=0}^{m-1} (\hat{p}_i \cdot \hat{p}_{i+1}) \hat{p}_m \right.$$
$$\left. \cdot \Delta t \sum_{q=N+M}^{N+M+\Delta N} \sum_{j=0}^{q-1} (1-\gamma\Delta t)^{q-1-j} \prod_{i=j}^{q-1} (\hat{p}_i \cdot \hat{p}_{i+1}) \int_{j\Delta t}^{(j+1)\Delta t} (\xi_{\parallel}(s) + b) ds \, \hat{p}_q \right\rangle \quad ,$$

where $\langle \xi_{\parallel} \rangle = 0$, because it is a stochastic variable with distribution centered around zero, thus the only remaining term in the integral is $b\Delta t$

$$\begin{aligned}
\left\langle \vec{A}_1 \cdot \vec{B}_2 \right\rangle &= \left\langle b\Delta t^3 \; v_{\parallel}(0) \sum_{m=N}^{N+\Delta N} (1-\gamma\Delta t)^m \prod_{i=0}^{m-1} (\hat{p}_i \cdot \hat{p}_{i+1}) \hat{p}_m \right. \\
&\quad \left. \sum_{q=N+M}^{N+M+\Delta N} \sum_{j=0}^{q-1} (1-\gamma\Delta t)^{q-1-j} \prod_{i=j}^{q-1} (\hat{p}_i \cdot \hat{p}_{i+1}) \, \hat{p}_q \right\rangle \\
&= b\Delta t^3 \left\langle v_{\parallel}(0) \sum_{m=N}^{N+\Delta N} (1-\gamma\Delta t)^m \prod_{i=0}^{m-1} (\hat{p}_i \cdot \hat{p}_{i+1}) \sum_{q=N+M}^{N+M+\Delta N} \sum_{j=0}^{q-1} (1-\gamma\Delta t)^{q-1-j} \prod_{i=j}^{q-1} (\hat{p}_i \cdot \hat{p}_{i+1}) \, \hat{p}_m \cdot \hat{p}_q \right\rangle \\
&= b\Delta t^3 v_{\parallel}(0) \sum_{m=N}^{N+\Delta N} (1-\gamma\Delta t)^m (1-k\Delta t)^{m-1} \sum_{q=N+M}^{N+M+\Delta N} \sum_{j=0}^{q-1} (1-\gamma\Delta t)^{q-1-j} (1-k\Delta t)^{q-1-j+|q-m|} \\
&= b\Delta t^3 v_{\parallel}(0) \sum_{m=N}^{N+\Delta N} \sum_{q=N+M}^{N+M+\Delta N} \sum_{j=0}^{q-1} (1-\gamma\Delta t)^{q+m-1-j} (1-k\Delta t)^{q+m-2-j+|q-m|} \quad ,
\end{aligned}$$

because q is always bigger than m, then $|q-m| = q-m$, getting us

$$\begin{aligned}
\left\langle \vec{A}_1 \cdot \vec{B}_2 \right\rangle &= b\Delta t^3 v_{\parallel}(0) \sum_{m=N}^{N+\Delta N} \sum_{q=N+M}^{N+M+\Delta N} \sum_{j=0}^{q-1} (1-\gamma\Delta t)^{q+m-1-j}(1-k\Delta t)^{q+m-2-j+q-m} \\
&= b\Delta t^3 v_{\parallel}(0) \sum_{m=N}^{N+\Delta N} \sum_{q=N+M}^{N+M+\Delta N} \sum_{j=0}^{q-1} (1-\gamma\Delta t)^{q+m-1-j}(1-k\Delta t)^{2q-2-j} \\
&= b\Delta t^3 v_{\parallel}(0) \sum_{m=N}^{N+\Delta N} (1-\gamma\Delta t)^{m} \sum_{q=N+M}^{N+M+\Delta N} \sum_{j=0}^{q-1} (1-\gamma\Delta t)^{q+m-1-j}(1-k\Delta t)^{2q-2-j} \\
&= b\Delta t^3 v_{\parallel}(0) \sum_{m=N}^{N+\Delta N} (1-\gamma\Delta t)^{m} \sum_{q=N+M}^{N+M+\Delta N} \sum_{j=0}^{q-1} (1-\gamma\Delta t)^{q-1-j}(1-k\Delta t)^{2q-2-j} \\
&= b\Delta t^3 v_{\parallel}(0) \left(\frac{(1-\gamma\Delta t)^{N} - (1-\gamma\Delta t)^{N+\Delta N}}{1-(1-\gamma\Delta t)} \right) \sum_{q=N+M}^{N+M+\Delta N} \sum_{j=0}^{q-1} (1-\gamma\Delta t)^{q-1-j}(1-k\Delta t)^{2q-2-j} \\
&= b\Delta t^3 v_{\parallel}(0) \left(\frac{e^{-\gamma N\Delta t} - e^{-\gamma(N+\Delta N)\Delta t}}{\gamma\Delta t} \right) \sum_{q=N+M}^{N+M+\Delta N} (1-k\Delta t)^{q-1} \sum_{j=0}^{q-1} (1-\gamma\Delta t)^{q-1-j}(1-k\Delta t)^{q-1-j} \\
&= b\Delta t^3 v_{\parallel}(0) \left(\frac{e^{-\gamma N\Delta t} - e^{-\gamma(N+\Delta N)\Delta t}}{\gamma\Delta t} \right) \sum_{q=N+M}^{N+M+\Delta N} (1-k\Delta t)^{q-1} \sum_{j=1}^{q} (1-\gamma\Delta t)^{q}(1-k\Delta t)^{q} \\
&= b\Delta t^3 v_{\parallel}(0) \left(\frac{e^{-\gamma N\Delta t} - e^{-\gamma(N+\Delta N)\Delta t}}{\gamma\Delta t} \right) \sum_{q=N+M}^{N+M+\Delta N} (1-k\Delta t)^{q-1} \frac{1-(1-\gamma\Delta t)^{q}(1-k\Delta t)^{q}}{1-(1-\gamma\Delta t)(1-k\Delta t)} \\
&= b\Delta t^3 v_{\parallel}(0) e^{-\gamma T} \left(\frac{1-e^{-\gamma\delta}}{\gamma\Delta t} \right) \sum_{q=N+M}^{N+M+\Delta N} (1-k\Delta t)^{q-1} \frac{1-(1-\gamma\Delta t)^{q}(1-k\Delta t)^{q}}{(\gamma+k)\Delta t} \quad ,
\end{aligned}$$

here we used the fact that $\sum_{i=0}^{N-1} x^{N-i} = \sum_{i=1}^{N} x^i$ and that $(1-k\Delta t)(1-\gamma\Delta t) \stackrel{\Delta t\to 0}{=} 1-(\gamma+k)\Delta t$, because $\gamma k \Delta t^2 << \Delta t$, now we only have to obtain the sum over the summation index q

$$\begin{aligned}
\left\langle \vec{A}_1 \cdot \vec{B}_2 \right\rangle &= \frac{b\Delta t v_{\parallel}(0)}{\gamma(\gamma+k)} e^{-\gamma T} \left(1-e^{-\gamma\delta}\right) \left((1-k\Delta t)^{N+M} \left(\frac{1-(1-k\Delta t)^{\Delta N}}{1-(1-k\Delta t)} \right) \right. \\
&\quad \left. -(1-\gamma\Delta t)^{N+M}(1-k\Delta t)^{2(N+M)} \left(\frac{1-(1-\gamma\Delta t)^{\Delta N\Delta t}(1-k\Delta t)^{2\Delta N\Delta t}}{1-(1-\gamma\Delta t)(1-k\Delta t)^2} \right) \right) \\
&= \frac{b\Delta t v_{\parallel}(0)}{\gamma(\gamma+k)} e^{-\gamma T} \left(1-e^{-\gamma\delta}\right) \left(e^{-k(N+M)\Delta t} \left(\frac{1-e^{-k\Delta N\Delta t}}{k\Delta t} \right) - e^{-(\gamma+2k)(N+M)\Delta t} \left(\frac{1-e^{-(\gamma+2k)\Delta N\Delta t}}{(\gamma+2k)\Delta t} \right) \right) \\
&= \frac{b v_{\parallel}(0)}{\gamma(\gamma+k)} e^{-\gamma T} \left(1-e^{-\gamma\delta}\right) \left(e^{-k(T+\Delta T)} \left(\frac{1-e^{-k\delta}}{k} \right) - e^{-(\gamma+2k)(T+\Delta T)} \left(\frac{1-e^{-(\gamma+2k)\delta}}{(\gamma+2k)} \right) \right) \quad ,
\end{aligned}$$

which is the final form of $\left\langle \vec{A}_1 \cdot \vec{B}_2 \right\rangle$, next, we must obtain $\left\langle \vec{A}_2 \cdot \vec{B}_1 \right\rangle$

$$\left\langle \vec{A}_2 \cdot \vec{B}_1 \right\rangle = \left\langle \Delta t \sum_{m=N}^{N+\Delta N} \sum_{j=0}^{m-1} (1-\gamma\Delta t)^{m-1-j} \prod_{i=j}^{m-1} (\hat{p}_i \cdot \hat{p}_{i+1}) \int_{j\Delta t}^{(j+1)\Delta t} \left(\xi_{\parallel}(s) + b\right) ds\, \hat{p}_m \right.$$
$$\left. \cdot \Delta t v_{\parallel}(0) \sum_{q=N+M}^{N+M+\Delta N} (1-\gamma\Delta t)^q \prod_{l=0}^{q-1} (\hat{p}_l \cdot \hat{p}_{l+1}) \hat{p}_q \right\rangle \quad , \tag{E.12}$$

where $\langle \xi_{\parallel}(t) \rangle = 0$, given $\xi_{\parallel}$ is a Gaussian stochastic variable with a distribution centered around zero, thus, the integral in equation E.12 results in $b\Delta t$, and the equation becomes

$$\left\langle \vec{A}_2 \cdot \vec{B}_1 \right\rangle = \left\langle b\Delta t^3 \sum_{m=N}^{N+\Delta N} \sum_{j=0}^{m-1} (1-\gamma\Delta t)^{m-1-j} \prod_{i=j}^{m-1} (\hat{p}_i \cdot \hat{p}_{i+1})\, \hat{p}_m \right.$$
$$\left. \cdot v_{\parallel}(0) \sum_{q=N+M}^{N+M+\Delta N} (1-\gamma\Delta t)^q \prod_{l=0}^{q-1} (\hat{p}_l \cdot \hat{p}_{l+1}) \hat{p}_q \right\rangle \quad . \tag{E.13}$$

From appendix F, we know that the average of each successive projection equals $\langle \hat{p}_i \cdot \hat{p}_{i+1} \rangle = (1 - k\Delta t)$ and that two projections separated by more than one time-step can be decomposed into $\langle \hat{p}_i \cdot \hat{p}_j \rangle = \prod_{l=i}^{j} (\hat{p}_l \cdot \hat{p}_{l+1}) = (1-k\Delta t)^{|i-j|}$. This result implies that we are able to do the same for equation E.13

$$\left\langle \vec{A}_2 \cdot \vec{B}_1 \right\rangle = b\Delta t^3 \sum_{m=N}^{N+\Delta N} \sum_{j=0}^{m-1} (1-\gamma\Delta t)^{m-1-j} (1-k\Delta t)^{m-1-j}$$
$$v_{\parallel}(0) \sum_{q=N+M}^{N+M+\Delta N} (1-\gamma\Delta t)^q (1-k\Delta t)^{q-1} (1-k\Delta t)^{|q-m|} \quad . \tag{E.14}$$

Because $q > m$ is always true, $|q-m| = q-m$

$$\begin{aligned}
\left\langle \vec{A}_2 \cdot \vec{B}_1 \right\rangle &= b\Delta t^3 \sum_{m=N}^{N+\Delta N} \sum_{j=0}^{m-1} (1-\gamma\Delta t)^{m-1-j} (1-k\Delta t)^{m-1-j} \\
&\quad v_{\parallel}(0) \sum_{q=N+M}^{N+M+\Delta N} (1-\gamma\Delta t)^q (1-k\Delta t)^{q-1} (1-k\Delta t)^{q-m} \\
&= b v_{\parallel}(0) \Delta t^3 \sum_{m=N}^{N+\Delta N} \sum_{j=0}^{m-1} \sum_{q=N+M}^{N+M+\Delta N} (1-\gamma\Delta t)^{q+m-1-j} (1-k\Delta t)^{2q-1-j} \\
&= b v_{\parallel}(0) \Delta t^3 \left(\frac{e^{-(\gamma+2k)(T+\Delta T)} - e^{-(\gamma+2k)(T+\delta+\Delta T)}}{(\gamma+2k)\Delta t} \right) \\
&\quad \sum_{m=N}^{N+\Delta N} \sum_{j=0}^{m-1} (1-\gamma\Delta t)^{m-1-j} (1-k\Delta t)^{-1-j} \quad ,
\end{aligned} \tag{E.15}$$

where we used the fact that $\sum_{q=a}^{b} x^q = \frac{x^a - x^{b+1}}{1-x}$ for an arbitrary variable x and that $(1 - \gamma\Delta t)^a(1 - k\Delta t)^{2a} = e^{-(\gamma+2k)a\Delta t}$.

Proceeding to solve the summations with corresponding indexes m and j, we have

$$\begin{aligned}
\left\langle \vec{A}_2 \cdot \vec{B}_1 \right\rangle &= \frac{bv_\parallel(0)\Delta t^2}{(\gamma+2k)} e^{-(\gamma+2k)(T+\Delta T)} \left(1 - e^{-(\gamma+2k)\delta}\right) \\
&\quad \sum_{m=N}^{N+\Delta N} \sum_{j=0}^{m-1} (1-\gamma\Delta t)^{m-1-j}(1-k\Delta t)^{-1-j} \\
&= \frac{bv_\parallel(0)\Delta t^2}{(\gamma+2k)} e^{-(\gamma+2k)(T+\Delta T)} \left(1 - e^{-(\gamma+2k)\delta}\right) \\
&\quad \sum_{m=N}^{N+\Delta N} \frac{(1-k\Delta t)^{-m} - (1-\gamma\Delta t)^N}{1-(1-\gamma\Delta t)(1-k\Delta t)} \\
&= \frac{bv_\parallel(0)\Delta t^2}{(\gamma+2k)} e^{-(\gamma+2k)(T+\Delta T)} \left(1 - e^{-(\gamma+2k)\delta}\right) \\
&\quad \sum_{m=N}^{N+\Delta N} \frac{(1-k\Delta t)^{-m} - (1-\gamma\Delta t)^N}{(\gamma+k)\Delta t} \quad ,
\end{aligned}$$

in equation E.16 we know that $\sum_{j=0}^{j=m-1} a^{m-j}b^{-j} = \frac{b^{-m} - a^m}{1-ab}$ for arbitrary variables a and b. We also used the fact that $(1-k\Delta t)(1-\gamma\Delta t) = 1 - (\gamma+k)\Delta t + \gamma k \Delta t^2 \overset{\Delta t \to 0}{\approx} 1 - (\gamma+k)\Delta t$, which takes us to

$$\begin{aligned}
\left\langle \vec{A}_2 \cdot \vec{B}_1 \right\rangle &= -\frac{bv_\parallel(0)\Delta t}{(\gamma+2k)(\gamma+k)} e^{-(\gamma+2k)(T+\Delta T)} \left(1 - e^{-(\gamma+2k)\delta}\right) \\
&\quad \left(\frac{(1-k\Delta t)^{-N} - (1-k\Delta t)^{-N-\Delta N}}{1-(1-k\Delta t)} + \frac{(1-\gamma\Delta t)^N(1-\gamma\Delta t)^{N+\Delta N}}{1-(1-\gamma\Delta t)} \right) \\
&= -\frac{bv_\parallel(0)\Delta t}{(\gamma+2k)(\gamma+k)} e^{-(\gamma+2k)(T+\Delta T)} \left(1 - e^{-(\gamma+2k)\delta}\right) \left(\frac{e^{kT}(1-e^{k\delta})}{k\Delta t} + \frac{e^{-\gamma T}(1-e^{-\gamma\delta})}{\gamma\Delta t} \right) \\
&= -\frac{bv_\parallel(0)}{(\gamma+2k)(\gamma+k)} e^{-(\gamma+2k)(T+\Delta T)} \left(1 - e^{-(\gamma+2k)\delta}\right) \left(\frac{e^{kT}(1-e^{k\delta})}{k} + \frac{e^{-\gamma T}(1-e^{-\gamma\delta})}{\gamma} \right).
\end{aligned} \tag{E.16}$$

Now, the only remaining non zero average product is $\langle \vec{A}_2 \cdot \vec{B}_2 \rangle$

$$\begin{aligned}
\langle \vec{A}_2 \cdot \vec{B}_2 \rangle &= \left\langle \Delta t \sum_{m=N}^{N+\Delta N} \sum_{j=0}^{m-1} (1-\gamma\Delta t)^{m-1-j} \prod_{i=j}^{m-1} (\hat{p}_i \cdot \hat{p}_{i+1}) \int_{j\Delta t}^{(j+1)\Delta t} (\xi_\parallel(s) + b) ds\, \hat{p}_m \right. \\
&\quad \left. \cdot \Delta t \sum_{q=N+M}^{N+M+\Delta N} \sum_{j=0}^{q-1} (1-\gamma\Delta t)^{q-1-j} \prod_{i=j}^{q-1} (\hat{p}_i \cdot \hat{p}_{i+1}) \int_{j\Delta t}^{(j+1)\Delta t} (\xi_\parallel(s) + b) ds\, \hat{p}_q \right\rangle
\end{aligned}$$

for ease of calculus, we separate the calculation into two parts, one corresponding to the non-biased part of integral $\int_{j\Delta t}^{(j+1)\Delta t}(\xi_{\parallel}+b)ds$ and the other corresponding to the biased part (the non-biased part corresponds to the terms proportional to the Wiener variable $\xi_{\parallel}$, the biased part stands for the terms multiplied by the bias b). Starting from the non biased part, we have

$$\begin{aligned}\langle \vec{A}_{2\,\mathrm{nb}} \cdot \vec{B}_{2\,\mathrm{nb}} \rangle &= \Bigg\langle \Delta t \sum_{m=N}^{N+\Delta N} \sum_{j=0}^{m-1} (1-\gamma\Delta t)^{m-1-j} \prod_{i=j}^{m-1} (\hat{p}_i \cdot \hat{p}_{i+1}) \int_{j\Delta t}^{(j+1)\Delta t} \xi_{\parallel}(s) ds\, \hat{p}_m \\ &\quad \cdot \Delta t \sum_{q=N+M}^{N+M+\Delta N} \sum_{l=0}^{q-1} (1-\gamma\Delta t)^{q-1-l} \prod_{i=l}^{q-1} (\hat{p}_i \cdot \hat{p}_{i+1}) \int_{l\Delta t}^{(l+1)\Delta t} \xi_{\parallel}(s) ds\, \hat{p}_q \Bigg\rangle \quad .\end{aligned}$$

Because the integrals $\int_{j\Delta t}^{(j+1)\Delta t}\xi_{\parallel}(s)ds$ and $\int_{l\Delta t}^{(l+1)\Delta t}\xi_{\parallel}(s)ds$ have intersecting time intervals, their averaged product isn't equivalent to 0, we have

$$\begin{aligned}\int_{j\Delta t}^{(j+1)\Delta t} \xi_{\parallel}(s)ds \int_{l\Delta t}^{(l+1)\Delta t} \xi_{\parallel}(s')ds' &= \int_{l\Delta t}^{(l+1)\Delta t} \int_{j\Delta t}^{(j+1)\Delta t} \xi_{\parallel}(s)\xi_{\parallel}(s')dsds' \\ &= \int_{l\Delta t}^{(l+1)\Delta t} \int_{j\Delta t}^{(j+1)\Delta t} g\delta(s-s')dsds' \\ &= \delta_{l,j} \int_{l\Delta t}^{(l+1)\Delta t} g ds' \\ &= \delta_{l,j} g \Delta t \quad , \end{aligned} \tag{E.17}$$

where the only scenario that the integrals' intervals overlap is when $l = j$, thus the result in equation E.17.

Back to $\langle \vec{A}_{2\,\mathrm{nb}} \cdot \vec{B}_{2\,\mathrm{nb}} \rangle$, we have

$$\begin{aligned}
\langle \vec{A}_{2\,\mathrm{nb}} \cdot \vec{B}_{2\,\mathrm{nb}} \rangle &= \Bigg\langle g\Delta t^3 \sum_{m=N}^{N+\Delta N} \sum_{j=0}^{m-1} (1-\gamma\Delta t)^{m-1-j} \prod_{i=j}^{m-1} (\hat{p}_i \cdot \hat{p}_{i+1}) \hat{p}_m \\
&\quad \cdot \sum_{q=N+M}^{N+M+\Delta N} \sum_{l=0}^{q-1} (1-\gamma\Delta t)^{q-1-l} \prod_{i=l}^{q-1} (\hat{p}_i \cdot \hat{p}_{i+1}) \hat{p}_q \delta_{l,j} \Bigg\rangle \\
&= \Bigg\langle g\Delta t^3 \sum_{q=N+M}^{N+M+\Delta N} \sum_{m=N}^{N+\Delta N} \sum_{l=0}^{q-1} \sum_{j=0}^{m-1} (1-\gamma\Delta t)^{q+m-2-l-j} \prod_{i=j}^{m-1} (\hat{p}_i \cdot \hat{p}_{i+1}) \\
&\quad \prod_{i=l}^{q-1} (\hat{p}_i \cdot \hat{p}_{i+1}) \hat{p}_q \cdot \hat{p}_m \delta_{l,j} \Bigg\rangle \\
&= g\Delta t^3 \sum_{q=N+M}^{N+M+\Delta N} \sum_{m=N}^{N+\Delta N} \sum_{l=0}^{q-1} \sum_{j=0}^{m-1} (1-\gamma\Delta t)^{q+m-2-l-j} (1-k\Delta t)^{m-1-j} \\
&\quad (1-k\Delta t)^{q-1-l} (1-k\Delta t)^{|q-m|} \delta_{l,j} \\
&= g\Delta t^3 \sum_{q=N+M}^{N+M+\Delta N} \sum_{m=N}^{N+\Delta N} \sum_{j=0}^{m-1} (1-\gamma\Delta t)^{q+m-2-2j} (1-k\Delta t)^{m-1-j} \\
&\quad (1-k\Delta t)^{q-1-j} (1-k\Delta t)^{|q-m|} \quad , \qquad \text{(E.18)}
\end{aligned}$$

in the last step of (E.18), the Kronecker's $\delta_{l,j}$ forced $l = j$, and this only happens from $j, l = 0$ to $j, l = m-1$, the upper limit being $m-1$ because $m < q$. We also know that $|q-m| = q-m$, thus

$$\begin{aligned}
\langle \vec{A}_{2\,\mathrm{nb}} \cdot \vec{B}_{2\,\mathrm{nb}} \rangle &= g\Delta t^3 \sum_{q=N+M}^{N+M+\Delta N} \sum_{m=N}^{N+\Delta N} \sum_{j=0}^{m-1} (1-\gamma\Delta t)^{q+m-2-2j} (1-k\Delta t)^{m-1-j} \\
&\quad (1-k\Delta t)^{q-1-j} (1-k\Delta t)^{q-m} \\
&= g\Delta t^3 \sum_{q=N+M}^{N+M+\Delta N} \sum_{m=N}^{N+\Delta N} \sum_{j=0}^{m-1} (1-\gamma\Delta t)^{q+m-2-2j} (1-k\Delta t)^{2q-2-2j} \quad .
\end{aligned}$$

To solve equation E.19, we need to multiply it by $(1-\gamma\Delta t)^{m-m}(1-k\Delta t)^{2m-2m}$, which

produces

$$\begin{aligned}
\langle \vec{A}_{2\,\mathrm{nb}} \cdot \vec{B}_{2\,\mathrm{nb}} \rangle &= g\Delta t^3 \sum_{q=N+M}^{N+M+\Delta N} \sum_{m=N}^{N+\Delta N} (1-\gamma\Delta t)^{q-m}(1-k\Delta t)^{2q-2m} \sum_{j=0}^{m-1} (1-\gamma\Delta t)^{2(m-j)}(1-k\Delta t)^{2(m-j)} \\
&= g\Delta t^3 \sum_{q=N+M}^{N+M+\Delta N} \sum_{m=N}^{N+\Delta N} (1-\gamma\Delta t)^{q-m}(1-k\Delta t)^{2q-2m} \left(\frac{1-(1-\gamma\Delta t)^{2m}(1-k\Delta t)^{2m}}{1-(1-\gamma\Delta t)^2(1-k\Delta t)^2} \right) \\
&= g\Delta t^3 \sum_{q=N+M}^{N+M+\Delta N} \sum_{m=N}^{N+\Delta N} (1-\gamma\Delta t)^{q-m}(1-k\Delta t)^{2q-2m} \left(\frac{1-(1-(\gamma+k)\Delta t)^{2m}}{2(\gamma+k)\Delta t} \right) \\
&= \frac{g\Delta t^2}{2(\gamma+k)} \sum_{q=N+M}^{N+M+\Delta N} \sum_{m=N}^{N+\Delta N} (1-\gamma\Delta t)^{q}(1-k\Delta t)^{2q} \left[(1-(\gamma+2k)\Delta t)^{-2m} - (1-\gamma\Delta t)^{m} \right] \\
&= g\Delta t \left(-\frac{e^{(\gamma+2k)T} - e^{(\gamma+2k)(T+\delta)}}{(\gamma+2k)} - \frac{e^{-\gamma T} - e^{-\gamma(T+\delta)}}{\gamma} \right) \sum_{q=N+M}^{N+M+\Delta N} \frac{(1-\gamma\Delta t)^q(1-k\Delta t)^{2q}}{2(\gamma+k)} \\
&= -g\Delta t \left(\frac{e^{(\gamma+2k)T} - e^{(\gamma+2k)(T+\delta)}}{(\gamma+2k)} - \frac{e^{-\gamma T} - e^{-\gamma(T+\delta)}}{\gamma} \right) \left(\frac{e^{-(\gamma+2k)(T+\Delta T)} - e^{-(\gamma+2k)(T+\Delta T+\delta)}}{2(\gamma+k)(\gamma+2k)\Delta t} \right) \\
&= -g\Delta t \left(e^{(\gamma+2k)T} \frac{1-e^{(\gamma+2k)(\delta)}}{(\gamma+2k)} - e^{-\gamma T} \frac{1-e^{-\gamma(\delta)}}{\gamma} \right) \left(e^{-(\gamma+2k)(T+\Delta T)} \frac{1-e^{-(\gamma+2k)\delta}}{2(\gamma+k)(\gamma+2k)\Delta t} \right) \\
&= -\frac{g}{2(\gamma+k)} \frac{e^{-(\gamma+2k)\Delta T}\left(1-e^{-(\gamma+2k)\delta}\right)\left(1-e^{(\gamma+2k)\delta}\right)}{(\gamma+2k)^2} \\
&\quad -\frac{g}{2(\gamma+k)} \frac{e^{-2(\gamma+k)T}e^{-(\gamma+2k)\Delta T}(1-e^{-(\gamma+2k)\delta})(1-e^{-\gamma\delta})}{\gamma(\gamma+2k)} \quad . \qquad \text{(E.19)}
\end{aligned}$$

This finishes our calculations for the non biased part of $\langle \vec{A}_2 \cdot \vec{B}_2 \rangle$, as for the biased part we have

$$\begin{aligned}
\langle \vec{A}_{2\,\mathrm{b}} \cdot \vec{B}_{2\,\mathrm{b}} \rangle &= \left\langle b^2\Delta t^4 \sum_{m=N}^{N+\Delta N} \sum_{j=0}^{m-1} (1-\gamma\Delta t)^{m-1-j} \prod_{i=j}^{m-1} (\hat{p}_i \cdot \hat{p}_{i+1}) \hat{p}_m \right. \\
&\quad \left. \cdot \sum_{q=N+M}^{N+M+\Delta N} \sum_{l=0}^{q-1} (1-\gamma\Delta t)^{q-1-j} \prod_{i=l}^{q-1} (\hat{p}_i \cdot \hat{p}_{i+1}) \hat{p}_q \right\rangle \quad ,
\end{aligned}$$

here, we know that $\langle \hat{p_q} \cdot \hat{p_m} \rangle = (1-k\Delta t)^{|q-m|}$, where $q > m$ is always true, thus $|q-m| = q-m$, we may also know that $\left\langle \prod_{i=j}^{m-1} (\hat{p}_i \cdot \hat{p}_{i+1}) \right\rangle = (1-k\Delta t)^{m-1-j}$ from the previous calculations

and from appendix F, thus

$$\begin{aligned}
\langle \vec{A}_{2\mathrm{b}} \cdot \vec{B}_{2\mathrm{b}} \rangle &= b^2 \Delta t^4 \sum_{m=N}^{N+\Delta N} \sum_{j=0}^{m-1} (1-\gamma\Delta t)^{m-1-j} (1-k\Delta t)^{m-1-j} \\
&\quad \times \sum_{q=N+M}^{N+M+\Delta N} \sum_{l=0}^{q-1} (1-\gamma\Delta t)^{q-1-j} (1-k\Delta t)^{q-1-l} (1-k\Delta t)^{q-m} \\
&= b^2 \Delta t^4 \sum_{m=N}^{N+\Delta N} \sum_{j=0}^{m-1} (1-\gamma\Delta t)^{m-1-j} (1-k\Delta t)^{-1-j} \\
&\quad \times \sum_{q=N+M}^{N+M+\Delta N} \sum_{l=0}^{q-1} (1-\gamma\Delta t)^{q-1-j} (1-k\Delta t)^{2q-1-l} \quad . \qquad \text{(E.20)}
\end{aligned}$$

from now on, each summation (over the indices m and q) can be solved separately as the terms are each independent.

$$
\begin{aligned}
\langle \vec{A}_{2\mathrm{b}} \cdot \vec{B}_{2\mathrm{b}} \rangle &= b^2 \Delta t^4 \sum_{m=N}^{N+\Delta N} \sum_{j=0}^{m-1} (1-\gamma\Delta t)^{m-1-j} (1-k\Delta t)^{-1-j} \\
&\quad \times \sum_{q=N+M}^{N+M+\Delta N} \sum_{l=0}^{q-1} (1-\gamma\Delta t)^{q-1-j} (1-k\Delta t)^{2q-1-l} \\
&= b^2 \Delta t^4 \sum_{m=N}^{N+\Delta N} \sum_{j=0}^{m-1} (1-\gamma\Delta t)^{m-1-j} (1-k\Delta t)^{-1-j} \\
&\quad \times \sum_{q=N+M}^{N+M+\Delta N} (1-k\Delta t)^{q} \frac{1-(1-\gamma\Delta t)^q (1-k\Delta t)^q}{(\gamma+k)\Delta t} \\
&= \frac{b^2 \Delta t^3}{(\gamma+k)} \sum_{m=N}^{N+\Delta N} \sum_{j=0}^{m-1} (1-\gamma\Delta t)^{m-1-j} (1-k\Delta t)^{-1-j} \\
&\quad \times \left(\frac{(1-k\Delta t)^{N+M} - (1-k\Delta t)^{N+M+\Delta N}}{1-(1-k\Delta t)} - \frac{(1-(\gamma+2k))^{N+M} - (1-(\gamma+2k))^{N+M+\Delta N}}{1-(1-(\gamma+2k)\Delta t)} \right) \\
&= \frac{b^2 \Delta t^2}{(\gamma+k)} \sum_{m=N}^{N+\Delta N} \frac{(1-k\Delta t)^{-m} - (1-\gamma\Delta t)^m}{1-\big(1-(\gamma+k)\Delta t\big)} \\
&\quad \times \left(e^{-k(T+\Delta T)} \frac{1-e^{-k\delta}}{k} - e^{-(\gamma+2k)(T+\Delta T)} \frac{1-e^{-(\gamma+2k)\delta}}{(\gamma+2k)} \right) \\
&= \frac{b^2 \Delta t}{(\gamma+k)} \left(\frac{(1-k\Delta t)^{-N-\Delta N} - (1-k\Delta t)^{-N}}{1-(1-k\Delta t)} - \frac{(1-\gamma\Delta t)^{N} - (1-\gamma\Delta t)^{N+\Delta N}}{1-(1-\gamma\Delta t)} \right) \\
&\quad \times \left(e^{-k(T+\Delta T)} \frac{1-e^{-k\delta}}{k} - e^{-(\gamma+2k)(T+\Delta T)} \frac{1-e^{-(\gamma+2k)\delta}}{(\gamma+2k)} \right) \\
&= \frac{b^2}{(\gamma+k)} \left(-e^{kT} \frac{1-e^{k\delta}}{k\Delta t} - e^{-\gamma T} \frac{1-e^{-\gamma\delta}}{\gamma\Delta t} \right) \\
&\quad \times \left(e^{-k(T+\Delta T)} \frac{1-e^{-k\delta}}{k} - e^{-(\gamma+2k)(T+\Delta T)} \frac{1-e^{-(\gamma+2k)\delta}}{(\gamma+2k)} \right) \quad .
\end{aligned}
$$

Now, the only remaining step for us to obtain the **MVACF** analytical solution is to

sum all of the separate non-zero products and divide it by δ^2

$$
\begin{aligned}
\psi(\delta,\Delta T)\,\delta^2 &= \langle\vec{A}_1\cdot\vec{B}_1\rangle+\langle\vec{A}_1\cdot\vec{B}_2\rangle+\langle\vec{A}_2\cdot\vec{B}_1\rangle+\langle\vec{A}_{2\,nb}\cdot\vec{B}_{2\,nb}\rangle+\langle\vec{A}_{2\,b}\cdot\vec{B}_{2\,b}\rangle \\
&= v_\parallel^2(0)\frac{e^{-2(\gamma+k)T}e^{-(\gamma+2k)\Delta T}(1-e^{-\gamma\delta})(1-e^{-(\gamma+2k)\delta})}{\gamma(\gamma+2k)} \\
&\quad+\frac{b^2}{k(\gamma+2k)(\gamma+k)^2}e^{-(\gamma+k)T}e^{-(\gamma+2k)\Delta T}(1-e^{-(\gamma+2k)\delta})(1-e^{k\delta}) \\
&\quad+\frac{b^2}{\gamma(\gamma+2k)(\gamma+k)^2}e^{-2(\gamma+k)T}e^{-(\gamma+2k)\Delta T}(1-e^{-(\gamma+2k)\delta})(1-e^{-\gamma\delta}) \\
&\quad-\frac{b^2}{k^2(\gamma+k)^2}e^{-k\Delta T}(1-e^{-k\delta})(1-e^{k\delta}) \\
&\quad-\frac{b^2}{\gamma k(\gamma+k)^2}e^{-(\gamma+k)T}e^{-k\Delta T}(1-e^{-k\delta})(1-e^{-\gamma\delta}) \\
&\quad-\frac{bv_\parallel(0)}{\gamma(\gamma+k)(\gamma+2k)}e^{-2(\gamma+k)T}e^{-(\gamma+2k)\Delta T}(1-e^{-\gamma\delta})(1-e^{-(\gamma+2k)\delta}) \\
&\quad+\frac{bv_\parallel(0)}{\gamma k(\gamma+k)}e^{-(\gamma+k)T}e^{-k\Delta T}(1-e^{-\gamma\delta})(1-e^{-k\delta}) \\
&\quad-\frac{bv_\parallel(0)}{k(\gamma+2k)(\gamma+k)}e^{-(\gamma+k)T}e^{-(\gamma+2k)T}(1-e^{-(\gamma+2k)\delta})(1-e^{k\delta}) \\
&\quad-\frac{bv_\parallel(0)}{\gamma(\gamma+2k)(\gamma+k)}e^{-2(\gamma+k)T}e^{-(\gamma+2k)\Delta T}(1-e^{-(\gamma+2k)\delta})(1-e^{-\gamma\delta}) \\
&\quad-\frac{g}{2(\gamma+k)}\frac{e^{-(\gamma+2k)\Delta T}\left(1-e^{-(\gamma+2k)\delta}\right)\left(1-e^{(\gamma+2k)\delta}\right)}{(\gamma+2k)^2} \\
&\quad-\frac{g}{2(\gamma+k)}\frac{e^{-2(\gamma+k)T}e^{-(\gamma+2k)\Delta T}(1-e^{-(\gamma+2k)\delta})(1-e^{-\gamma\delta})}{\gamma(\gamma+2k)}
\end{aligned}
\tag{E.21}
$$

Now we substitute the $v_\parallel(0)$ and $v_\parallel^2(0)$ for their stationary values and cancel the op-

posite signaled terms

$$\begin{aligned}
\psi(\delta,\Delta T)\,\delta^2 \;=\; & \left(\frac{g}{2(\gamma+k)}+\frac{b^2}{(\gamma+k)^2}\right)\frac{e^{-2(\gamma+k)T}e^{-(\gamma+2k)\Delta T}(1-e^{-\gamma\delta})(1-e^{-(\gamma+2k)\delta})}{\gamma(\gamma+2k)} \\
& +\frac{b^2}{k(\gamma+2k)(\gamma+k)^2}e^{-(\gamma+k)T}e^{-(\gamma+2k)\Delta T}(1-e^{-(\gamma+2k)\delta})(1-e^{k\delta}) \\
& +\frac{b^2}{\gamma(\gamma+2k)(\gamma+k)^2}e^{-2(\gamma+k)T}e^{-(\gamma+2k)\Delta T}(1-e^{-(\gamma+2k)\delta})(1-e^{-\gamma\delta}) \\
& -\frac{b^2}{k^2(\gamma+k)^2}e^{-k\Delta T}(1-e^{-k\delta})(1-e^{k\delta}) \\
& -\frac{b^2}{\gamma k(\gamma+k)^2}e^{-(\gamma+k)T}e^{-k\Delta T}(1-e^{-k\delta})(1-e^{-\gamma\delta}) \\
& -\frac{b^2}{\gamma(\gamma+k)^2(\gamma+2k)}e^{-2(\gamma+k)T}e^{-(\gamma+2k)\Delta T}(1-e^{-\gamma\delta})(1-e^{-(\gamma+2k)\delta}) \\
& +\frac{b^2}{\gamma k(\gamma+k)^2}e^{-(\gamma+k)T}e^{-k\Delta T}(1-e^{-\gamma\delta})(1-e^{-k\delta}) \\
& -\frac{b^2}{k(\gamma+2k)(\gamma+k)^2}e^{-(\gamma+k)T}e^{-(\gamma+2k)T}(1-e^{-(\gamma+2k)\delta})(1-e^{k\delta}) \\
& -\frac{b^2}{\gamma(\gamma+2k)(\gamma+k)^2}e^{-2(\gamma+k)T}e^{-(\gamma+2k)\Delta T}(1-e^{-(\gamma+2k)\delta})(1-e^{-\gamma\delta}) \\
& -\frac{g}{2(\gamma+k)}\frac{e^{-(\gamma+2k)\Delta T}\left(1-e^{-(\gamma+2k)\delta}\right)\left(1-e^{(\gamma+2k)\delta}\right)}{(\gamma+2k)^2} \\
& -\frac{g}{2(\gamma+k)}\frac{e^{-2(\gamma+k)T}e^{-(\gamma+2k)\Delta T}(1-e^{-(\gamma+2k)\delta})(1-e^{-\gamma\delta})}{\gamma(\gamma+2k)} \quad , \qquad \text{(E.22)}
\end{aligned}$$

after canceling the terms with opposite signals, we end up with

$$\begin{aligned}
\psi(\delta,\Delta T) \;=\; & \frac{g}{2(\gamma+k)(\gamma+2k)^2\delta^2}e^{-(\gamma+2k)\Delta T}(1-e^{-(\gamma+2k)\delta})(e^{(\gamma+2k)\delta}-1) \\
& +\frac{b^2}{k^2(\gamma+k)^2\delta^2}e^{-(\gamma+2k)\Delta T}(1-e^{-k\delta})(e^{k\delta}-1) \quad , \qquad \text{(E.23)}
\end{aligned}$$

which can also be written as

$$\begin{aligned}
\psi(\delta,\Delta T) \;=\; & \frac{g}{(\gamma+k)(\gamma+2k)^2\delta^2}e^{-(\gamma+2k)\Delta T}\Big(cosh\big((\gamma+2k)\delta\big)-1\Big) \\
& +\frac{2b^2}{k^2(\gamma+k)^2\delta^2}e^{-(\gamma+2k)\Delta T}\Big(cosh\big(k\delta\big)-1\Big) \quad , \qquad \text{(E.24)}
\end{aligned}$$

this is the analytical solution for the **MVACF**. Notice that for $\delta \to 0$ (emulating an infinite precision **VACF** solution), we recover the **VACF** solution

$$\begin{aligned}
\psi(\delta, \Delta T) &\overset{\delta\to 0}{=} \frac{g}{2(\gamma+k)(\gamma+2k)^2\delta^2} e^{-(\gamma+2k)\Delta T}\Big(1-\big(1-(\gamma+2k)\delta\big)\Big)\Big(\big(1+(\gamma+2k)\delta\big)-1\Big) \\
&\quad + \frac{b^2}{k^2(\gamma+k)^2\delta^2} e^{-(\gamma+2k)\Delta T}\Big(1-\big(1-k\delta\big)\Big)\Big(\big(1+k\delta\big)-1\Big) \\
&\overset{\delta\to 0}{=} \frac{g}{2(\gamma+k)(\gamma+2k)^2\delta^2} e^{-(\gamma+2k)\Delta T}\Big((\gamma+2k)\delta\Big)\Big((\gamma+2k)\delta\Big) \\
&\quad + \frac{b^2}{k^2(\gamma+k)^2\delta^2} e^{-(\gamma+2k)\Delta T}\Big(k\delta\Big)^2 \\
&\overset{\delta\to 0}{=} \frac{g}{2(\gamma+k)} e^{-(\gamma+2k)\Delta T} + \frac{b^2}{(\gamma+k)^2} e^{-(\gamma+2k)\Delta T} = VACF(\Delta T) \quad . \qquad \text{(E.25)}
\end{aligned}$$

Appendix F

θ Dynamics

Here we introduce calculations for a particle with an internal degree of freedom represented by a polarization vector $\hat{p} = (cos(\theta), sin(\theta))$ subject to a chemical field that forces the particle to orient itself to the point of highest concentration. Mathematically speaking, we specify a polarization vector whose direction varies according to a stochastic differential equation with decay, forcing $\theta \to \theta_q$ with intensity ϕ and θ_q an arbitrary direction dictated by some chemical concentrations.

We assume, without loss of generality, that $\theta_q = 0$, creating a particle that migrates preferentially in the $\theta = 0$ direction. Also note that all calculations work for $\phi = 0$, which represents the case where there is no chemical field and takes us back to the biased anisotropic Ornstein-Uhlenbeck model.

Considering the differential equation for the angular position $\theta(t)$ as

$$\frac{d\theta}{dt} = -\phi\theta + \beta_\perp \quad , \tag{F.1}$$

where

$$\langle \beta_\perp(t)\beta_\perp(t')\rangle_{\beta_\perp} = 2k\delta(t-t') \quad . \tag{F.2}$$

We obtain a solution for $\theta(t)$ via an integrating factor or via the Green's function method

$$\begin{aligned}
\frac{d\theta}{dt}e^{\phi t} + \phi\theta e^{\phi t} &= \beta_\perp e^{\phi t} \\
\int_{t_0}^{t} \frac{d}{dt'}(\theta e^{\phi t'})dt' &= \int_{t_0}^{t} \beta_\perp e^{\phi t'} dt' \\
\theta(t)e^{\phi t} - \theta(t_0)e^{\phi t_0} &= \int_{t_0}^{t} \beta_\perp e^{\phi t'} dt' \\
\theta(t) &= \theta(t_0)e^{\phi(t_0-t)} + \int_{t_0}^{t} \beta_\perp e^{\phi(t'-t)} dt' \quad . \qquad \text{(F.3)}
\end{aligned}$$

After using this solution, we can then obtain other pertinent measures, like the averaged squared angle, where $\langle X \rangle_N$ represents the average of the variable X considering all possible realizations of the stochastic term $\beta_\perp$. But first we have to find $\Delta\theta = \theta(t) - \theta(0)$, assuming $t_0 = 0$ with no loss of generality

$$\theta(t) - \theta(0) = \theta(0)e^{-\phi t} - \theta(0) + \int_{t_0}^{t} \beta_\perp e^{-\phi(t-s)} ds \quad , \qquad \text{(F.4)}$$

with the result above (F.4) we can find its average and its average squared value

$$\langle \theta(t) \rangle = \langle \theta(t_0) \rangle e^{-\phi(t-t_0)} \quad \forall \quad t \in [t_0, \infty] \quad , \qquad \text{(F.5)}$$

meaning that the average direction for the polarization vector is 0 as we have chosen $\theta_q = 0$. The squared average for θ is

$$\begin{aligned}
\langle |\Delta\theta|^2 \rangle &= \left\langle \theta^2(0)(e^{-\phi t} - 1)^2 + \theta(0)(e^{-\phi t} - 1) \int_0^t \beta_\perp e^{-\phi(t-s)} ds + \int_0^t \int_0^t \beta_\perp(s)\beta_\perp(s') e^{-\phi(2t-s-s')} ds\, ds' \right\rangle \\
&= \left\langle \theta^2(0)(e^{-\phi t} - 1)^2 \right\rangle + \left\langle \theta(0)(e^{-\phi t} - 1) \int_0^t \beta_\perp e^{-\phi(t-s)} ds \right\rangle + \left\langle \int_0^t \int_0^t \beta_\perp(s)\beta_\perp(s') e^{-\phi(2t-s-s')} ds\, ds' \right\rangle \\
&= \left\langle \theta^2(0)(e^{-\phi t} - 1)^2 \right\rangle + 0 + \left\langle \int_0^t \int_0^t \beta_\perp(s)\beta_\perp(s') e^{-\phi(2t-s-s')} ds\, ds' \right\rangle \\
&= \theta^2(0)(e^{-2\phi t} + 1 - 2e^{-\phi t}) + \int_0^t \int_0^t 2k\delta(s-s') e^{-\phi(2t-s-s')} ds\, ds' \\
&= \theta^2(0)(e^{-2\phi t} + 1 - 2e^{-\phi t}) + 2k \int_0^t e^{-2\phi(t-s)} ds \\
&= \theta^2(0)(e^{-2\phi t} + 1 - 2e^{-\phi t}) + \frac{k}{\phi}(1 - e^{-2\phi t}) \quad .
\end{aligned}$$

If we assume that $t \to \infty$, then we obtain the asymptotic solution for $\langle|\Delta\theta|^2\rangle$, which is

$$\begin{aligned}\langle|\Delta\theta|^2\rangle_{\text{asymptotic}} &= \lim_{t\to\infty} \theta^2(0)(e^{-2\phi t} + 1 - 2e^{-\phi t}) + \frac{k}{\phi}(1 - e^{-2\phi t}) \\ &= \theta^2(0) + \frac{k}{\phi} \quad \text{and} \end{aligned} \tag{F.6}$$

if we assume $\phi \to 0$ before taking the limit of $t \to \infty$, we get

$$\begin{aligned}\langle|\Delta\theta|^2\rangle_{\text{asymptotic}} &= \lim_{\phi\to 0} \theta^2(0)(e^{-2\phi t} + 1 - 2e^{-\phi t}) + \frac{k}{\phi}(1 - e^{-2\phi t}) \\ &= \lim_{\phi\to 0} \theta^2(0)(1 - 2\phi t + 1 - 2 + 2\phi t) + \frac{k}{\phi}(1 - e^{-2\phi t}) \qquad \text{(F.7)} \\ &= \lim_{\phi\to 0} \frac{k}{\phi}(1 - e^{-2\phi t}) \qquad \text{(F.8)}\end{aligned}$$

now expanding the exponential term we obtain

$$\begin{aligned}\langle|\Delta\theta|^2\rangle_{\phi\to 0} &\approx \frac{k}{\phi}(1 - 1 - 2\phi t) \\ &= 2kt, \end{aligned} \tag{F.9}$$

implying that when $\phi = 0$, we have a simple diffusion in θ i.e. $\Delta\theta = \int_0^t \beta_\perp(s)\, ds$, taking us back to usual migration without chemotaxis.

Another important measure is the cosine of an angle variation $\Delta\theta_{i,j}$, where i and j are integers such that $t = i\Delta t$ and $t' = j\Delta t$ and also that $|i - j| \neq 1$. This calculation is important because the cosine represents the projection of a unit vector onto another, which occurs recursively in the anisotropic Ornstein-Uhlenbeck model [de Almeida et al., 2022] and the biased anisotropic Ornstein-Uhlenbeck model. We have the product denoted as

$$\begin{aligned}(\hat{p}_i \cdot \hat{p}_j) &= \cos(\Delta\theta_{i,j}) = \cos(\Delta\theta_{i,i+1} + \Delta\theta_{i+1,i+2} + \cdots + \Delta\theta_{j-2,j-1} + \Delta\theta_{j-1,j}) \\ &= \cos(\theta_{i,i+1})\cos(\theta_{i+1,i+2} + \cdots + \theta_{j-1,j}) - \sin(\theta_{i,i+1})\sin(\theta_{i+1,i+2} + \cdots + \theta_{j-1,j}) \quad .\end{aligned}$$

Assuming that $\Delta\theta_{i,i+1} << 1$ for any integer i, then we obtain the sine and cosine values of it

$$\cos(\Delta\theta_{i,i+1}) \approx 1 - \frac{(\Delta\theta_{i,i+1})^2}{2} \quad \text{and} \tag{F.10}$$

$$\sin(\Delta\theta_{i,i+1}) \approx (\Delta\theta_{i,i+1}) \quad . \tag{F.11}$$

Now expanding equation (F.10) through sines and cosines sums, we can find a general equation for $\cos(\Delta\theta_{i,j})$.

$$\begin{aligned}
\langle\cos(\Delta\theta_{i,j})\rangle &= (1-k\Delta t)\cos(\Delta\theta_{i+1,j}) + \phi\langle\theta_i\rangle\Delta t\sin(\Delta\theta_{i+1,j}) \\
&= (1-k\Delta t)^2\cos(\Delta\theta_{i+2,j}) + (1-k\Delta t)\phi\langle\theta_i\rangle\Delta t\sin(\Delta\theta_{i+2,j}) \\
&- (\phi\langle\theta_i\rangle\Delta t)^2\cos(\Delta\theta_{i+2,j}) + (1-k\Delta t)(\phi\langle\theta_i\rangle\Delta t)\sin(\Delta\theta_{i+2,j}) \\
&= (1-k\Delta t)^3\cos(\Delta\theta_{i+3,j}) + (1-k\Delta t)^2(\phi\langle\theta_i\rangle\Delta t)\sin(\Delta\theta_{i+3,j}) \\
&- (1-k\Delta t)(\phi\langle\theta_i\rangle\Delta t)^2\cos(\Delta\theta_{i+3,j}) + (1-k\Delta t)^2(\phi\langle\theta_i\rangle\Delta t)\sin(\Delta\theta_{i+3,j}) \\
&- (1-k\Delta t)(\phi\langle\theta_i\rangle\Delta t)^2\cos(\Delta\theta_{i+3,j}) + (\phi\langle\theta_i\rangle\Delta t)^3\sin(\Delta\theta_{i+3,j}) \\
&- (1-k\Delta t)(\phi\langle\theta_i\rangle\Delta t)^2\cos(\Delta\theta_{i+3,j}) + (1-k\Delta t)^2(\phi\langle\theta_i\rangle\Delta t)\sin(\Delta\theta_{i+3,j}) \quad ,
\end{aligned} \tag{F.12}$$

if we generalize the equation above (F.12), we get

$$\begin{aligned}
\cos(\Delta\theta_{i,j}) &= c_0(1-k\Delta t)^{|i-j|} + c_1(1-k\Delta t)^{|i-j|-1}(\phi\langle\theta_i\rangle\Delta t) + c_2(1-k\Delta t)^{|i-j|-2}(\phi\langle\theta_i\rangle\Delta t)^2 \\
&+ \cdots + c_{|i-j|-1}(1-k\Delta t)(\phi\langle\theta_i\rangle\Delta t)^{|i-j|-1} + c_{|i-j|}(\phi\langle\theta_i\rangle\Delta t)^{|i-j|} \\
&= c_0(1-k\Delta t)^{|i-j|} + \sum_{n=1}^{|i-j|} c_n(1-k\Delta t)^{|i-j|-n}(\phi\langle\theta_{i+n}\rangle\Delta t)^n \quad ,
\end{aligned} \tag{F.13}$$

where n is an integer between i and j and c_n is an arbitrary coefficient. Remembering that $\langle\theta_N\rangle = \langle\theta_{t_0}\rangle e^{-\phi N\Delta t}$, then

$$\langle \cos(\Delta\theta_{i,j}) \rangle \;=\; c_0(1-k\Delta t)^{|i-j|} + \sum_{n=1}^{|i-j|} c_n (1-k\Delta t)^{|i-j|-n} (\phi \langle \theta_{t_0} \rangle e^{-\phi(i+n)\Delta t} \Delta t)^n \quad , \text{(F.14)}$$

if $i, j \to \infty$ in such a way that $i\Delta t = T_i$ and $j\Delta t = T_j$ are finite values, we make the summation terms go to zero as $\phi\, \theta_{t0} e^{-\phi(i\Delta t)} \to 0$. This way, the cosine of $|i-j|$ successive variations in θ become

$$\langle \cos(\Delta\theta_{i,j}) \rangle \quad \overset{i,j\to\infty}{\approx} \quad c_0(1-k\Delta t)^{|i-j|} \quad ,$$

then, if all of the summation terms are zero with the exception of the first, we notice that $c_0 = 1$ by comparing equation F.15 with equation F.12 (the term with the highest power of $(1-k\Delta)$ has a coefficient 1 multiplying it). This result means that we can approximate the cosine of a variation in θ as the product of cosines of infinitesimal variations $\Delta\theta$. Here the assumption that $i, j \to \infty$ is the same as considering that the system is in a stationary state.